An experimental study of the development of gaseous ionization at ultra high frequencies

R.E. Long

An Experimental Study of the Development of Gaseous Ionization at Ultra High Frequencies

by

R. E. Long, B.Sc.

Being on account of the work carried out at the University of Durham during the period from September, 1959 to September, 1962

Thesis submitted to the University of Durham in support of an application for a degree of Doctor of Philosophy

ACKNOWLEDGMENTS

The author wishes to offer his sincere thanks to Dr. W.A. Prowse, his supervisor, for his patient guidance and encouragement during the course of this work: to Professor G.D. Rochester and the staff of the Physics Department, South Road, Durham for providing laboratory facilities: to Mr. M.F. Boyer and Mr. R.G. Earl for their numerous illuminating discussions: to Miss P.G. Crosby for her critism of the manuscript: to Miss P.M. Hall who patiently undertook the typing: and to the British Electrical and Allied Industries Research Association for their provision of a maintenance grant and their contribution towards the cost of the apparatus.

List of Principle Symbols

a effective radius of the electrodes

b radius of the holes in the emitting electrode

d gap width

D electron diffusion coefficient

E_{dc} unidirection or drift field in the interelectrode gap

E_{uhf} u.h.f. field in the interelectrode gap

f frequency of the modulating voltage

i_1 total electron current emitted by the filament

i_2 total current collected by the far electrode

i_{20} initial gap current: the current flowing to the collecting electrode in the absence of a u.h.f. field so that a drift field only acts

i_3 current collected by the internal collecting plate of the far electrode

see Fig. 2.1 on back cover

i_B back diffusion current: the current flowing from the interelectrode gap to the front face of the emitting electrode

j $\sqrt{-1}$

ℓ $\sqrt{\left[\lambda^2 - \frac{\psi}{D}\right]}$

n the electron density

t time

t_L mean lifetime of an electron in the interelectrode gap

t_T transit time: the mean time taken by an electron to cross the interelectrode gap

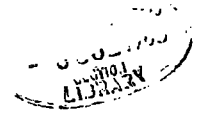

U $n_0 e^{\pm\lambda z}$

V_1 applied unidirectional voltage between the filament and the emitting electrode shell

V_2 applied unidirectional voltage across the inter-electrode gap

V_3 applied unidirectional voltage between the collecting plate and the collecting electrode shell

see Fig. 2.1 on back cover

V_{dc} the actual unidirectional voltage across the inter-electrode gap

V_p the polarization voltage: the voltage across the two films in series

V_{uhf} u.h.f. voltage across the interelectrode gap

w the number of secondary electrons produced at the cathode per an electron in the gap

α Townsend's first ionization coefficient: the number of ionizing collisions per an individual electron, per unit distance drifted

λ $\frac{\mu E_{dc}}{D}$

η ionizing efficiency: $\eta = \frac{\alpha}{E_{dc}}$ for discharges under pure unidirectional fields

ψ_1 ionization rate per an individual electron

ψ_2 recombination rate per an individual electron

ψ_3 attachment rate per an individual electron

ψ $\psi_1 - \psi_2 - \psi_3$ = the net ionization rate per an individual electron

τ_F relaxation time (of thin films)

μ electron mobility

ω $2\pi f$ = angular frequency of the modulating field

CONTENTS

CHAPTER 1

INTRODUCTION

Several attempts have been made to elucidate the mechanism of conduction in gases both before and after breakdown. For unidirectional fields, this mechanism has been widely investigated notably by Townsend and his school and later by Llewellyn Jones. They have demonstrated that collision ionization is an important phenomenon and a considerable number of experiments have been performed to measure ionization coefficients over a wide range of conditions. The significance of ionization has also been demonstrated for alternating fields but direct measurements have been of very limited extent. Few, if any, measurements have been made of ionization before breakdown for the case when electrons may move back and forth in the gas without colliding with the electrodes. The present experiment is designed to extend measurements of ionization into this region, and follows the experiments by which Townsend measured his coefficient, α, with unidirectional fields. The method is to measure the amplification of an electron stream crossing a region over which there is a high frequency field.

1.1 Conduction Processes

Electrons drifting through a gas collide with gas molecules and, as a consequence, move with a random movement superimposed upon their drift motion. Hence their flow is by diffusion as well as drift.

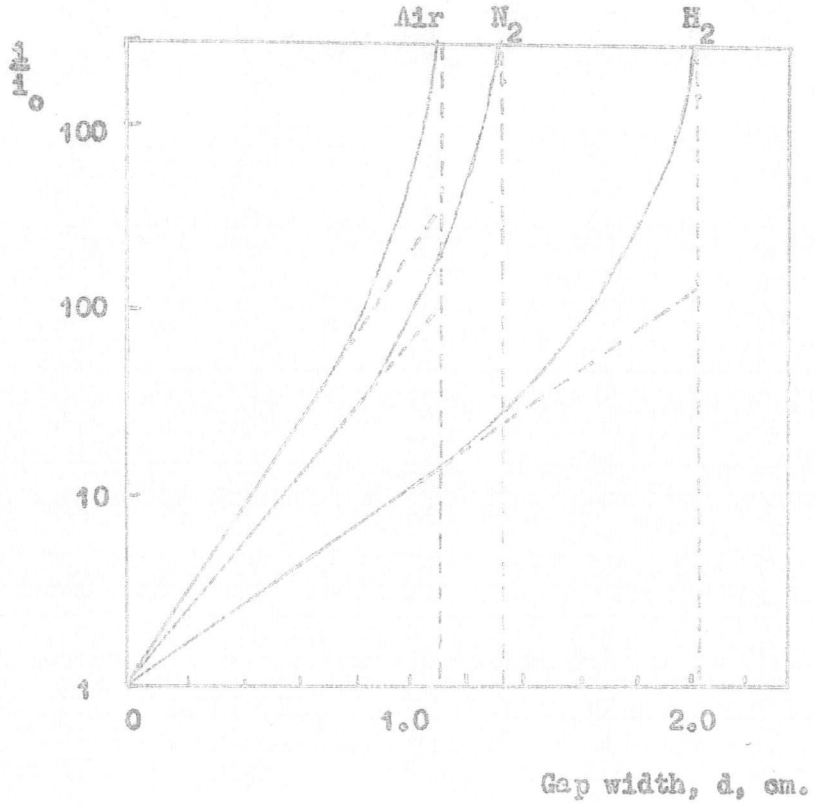

Fig. 1.1 Typical $\frac{i}{i_o}$ - d curves
(from Llewellyn Jones, 1951)

Further, these collisions leave the electrons with a range of energies (Druyvesteyn, 1930).

An electron whose random energy exceeds the ionization energy of an atom or molecule may, on collision, generate other electrons by collision ionization (Townsend, 1900, 1903, 1915).

e.g. $e + A \rightarrow e + A^{+} + e$ 1.1

Both the original and generated electron may then ionize other atoms or molecules and so on, to give an electron avalanche. Townsend showed that if a current, i_o, is injected at the cathode of a parallel plate gap, width, d, across which there is a drift field, E_{dc}, the current reaching the anode is

$$i = i_o \epsilon^{\int_o^d \alpha . dx} \qquad \ldots\ldots\ldots 1.2$$

where α is the number of ionizing collisions per cm drift, per an electron.

The value of α depends on the number of electrons with energy greater than the ionization energy and thus depends on the electron energy distribution which is a function of $\frac{E_{dc}}{p}$. A typical experimental plot of Amplification, $A = \frac{i}{i_o}$, against gap width for constant $\frac{E_{dc}}{p}$ (figure 1.1) shows initially the exponential rise of amplification with gap width resulting from collision ionization. At larger gap widths, this line departs from the simple exponential and has been interpreted by Townsend in terms of secondary processes by which positive ions and photons formed by electron-gas molecule collisions, cause emission of electrons on striking the cathode. This leads to

the equation:

$$A = \frac{i}{i_o} = \frac{\epsilon^{\alpha d}}{1 - \frac{w}{\alpha}\epsilon^{(\alpha d - 1)}} \qquad \ldots\ldots\ldots 1.3$$

where w is the number of secondary electrons produced at the cathode per an electron in the gap.

1.2 Balance of electron generation and removal processes

Electrons may be lost from a discharge by drifting to an electrode or diffusing to the boundary. In addition, they may be lost in the volume of the gas by recombination with positive ions or attachment to neutral molecules.

A discharge, in general, represents a balance between these loss processes and the generation processes (including both the internal generation processes described above and those due to an external agency e.g. photoemission or photoionization etc.). From a consideration of an elemental volume of the discharge, this balance may be expressed by the equation of continuity for electrons in a gas (Townsend, 1925),

$$\nabla^2(D.n) - \frac{\mu E_{dc}}{D} \cdot \frac{\partial n}{\partial z} + \psi n + x = \frac{\partial n}{\partial t} \qquad \ldots\ldots\ldots 1.4$$

where

n = electron density

D = diffusion coefficient of electrons

μ = mobility of electrons

E_{dc} = drift field directed along the z-axis

x = rate of generation of electrons by an external agency per unit volume.

and ψ represents the net rate of generation of electrons per an individual electron by collision ionization and is given by

$$\psi = \psi_1 - \psi_2 - \psi_3 \qquad \ldots\ldots\ldots 1.5$$

where, ψ_1 = ionization rate per an individual electron

ψ_2 = recombination rate per an individual electron

ψ_3 = attachment rate per an individual electron.

In equation 1.4, the terms represent respectively, the rate of loss of electrons by diffusion, the rate of loss by drift, the net rate of generation by collision ionization, the rate of volume generation by an external agency and the rate of change of electron density, which is zero when equilibrium has been established.

If the loss rate exceeds the internal generation rate (inclusive of secondary emission), then generation of electrons by an external agency is necessary for the discharge to be maintained. The electron current reaching the boundaries of such a discharge is then proportional to the injected current, the constant of proportionality being dependent on the ionization coefficient and thus on the applied field (e.g. equation 1.2 for unidirectional fields in parallel plate gaps).

If the total generation rate exceeds the loss rate, equilibrium can no longer be established between the current injected and that lost from the discharge. The equilibrium set up is then one between the internal generation and loss processes. The onset of this breakdown condition occurs at a definite voltage known as the breakdown voltage.

1.3 Breakdown in unidirectional fields

Here the structure of the discharge is an electron avalanche

originating at the cathode. Secondary emission provides a means of generating electrons to retain the avalanche independently of any external agency. Hence at breakdown the general condition that the system be self-maintaining is satisfied. This condition is thus given by equation 1.3 when,

$$1 - \frac{w}{\alpha} \epsilon^{(\alpha d - 1)} = 0 \qquad \ldots\ldots\ldots 1.6$$

and i becomes independent of i_o, the current emitted into the gap by an external agency.

Equation 1.6 is known as Townsend's criterion for breakdown in uniform unidirectional fields. From this it follows that breakdown for a given gap is dependent on w and α, which are both functions of $\frac{E_{dc}}{p}$. Thus the breakdown condition (equation 1.6) may be satisfied independently of the current flowing, provided no space charge effects occur. This has been tested experimentally by Llewellyn Jones and Parker, 1950, 1952, who showed that the maintaining potential of a self-maintaining discharge was independent of the current for low current densities but decreased at higher current densities when space charge effects became appreciable.

1.4 Breakdown in Alternating Fields

At low frequencies and low gas pressures, electrons are swept alternately to each electrode. Each half cycle may then be considered as a unidirectional discharge and has similar characteristics.

At higher frequencies the electrons can move to and fro in the gas without colliding with the electrodes. The predominant loss mechanism is then diffusion rather than drift. Thus the vibrating electrons diffuse through the gas until they come close enough to a boundary to

be swept to it by the field. Such are known as diffusion controlled or ultra high frequency (u.h.f.) discharges, and were recognised by Gill and Donaldson, 1931, as a decrease in the breakdown stress to about half the unidirectional or low frequency field value (first observed by Gutton and Gutton, 1928).

The present work is concerned with this latter type of discharge. Following Townsend, ionization studies under such conditions, are attempted using a small drift field to sweep out the electrons. Varnerin and Brown, 1950, have shown that in such discharges, where a small drift field is superimposed upon the u.h.f. field, the diffusion theory applied to pure u.h.f. discharges is applicable. This will therefore be discussed further.

The breakdown condition for diffusion controlled discharges has been widely studied, notably by Sanborn Brown and his collaborators who have worked out a detailed theory. The condition for breakdown is that on the average each electron must generate another electron by collision ionization before being lost from the gap by diffusion. This is the condition that the discharge be self-maintaining and stable. Herlin and Brown, 1948a, have expressed this condition in terms of the equation of continuity (equation 1.4) applicable to these conditions:-

$$D.\ \nabla^2.n + \psi n = 0 \qquad \ldots\ldots\ldots\ 1.7$$

The first term represents the rate of loss by diffusion and the second the rate of formation of electrons.

By solving this equation, the breakdown condition may be deduced as:-

$$\psi = \frac{D}{\Lambda^2} \qquad \ldots\ldots\ldots\ 1.8$$

Here Λ^2, the diffusion length for the gap, is a function of the shape and dimensions of the vessel containing the discharge.

From the condition for breakdown that one ionization collision occurs in the lifetime of each electron, the mean electron lifetime is from equation 1.8, $\frac{\Lambda^2}{D}$. It is of interest here to note that consideration of the random walk of an electron shows that the mean time to diffuse a distance, r, is proportional to $\frac{r^2}{D}$. This suggests that Λ is a measure of the mean distance an electron must diffuse to reach a boundary.

For the case of a cylindrical vessel, length d and radius a,

$$\frac{1}{\Lambda^2} = \left(\frac{\pi}{d}\right)^2 + \left(\frac{2.405}{a}\right)^2 \qquad \ldots\ldots\ldots \text{1.9}$$

where the first term represents loss to the ends and the second loss to the curved surface.

Equation 1.8 suggests that vessels of different shape, but of the same diffusion length, have the same breakdown field. This has been demonstrated by Herlin and Brown 1948b showing the validity of the diffusion theory.

As in the unidirectional field case the value of ψ depends on the electron energy distribution and thus on $\frac{E_{uhf}}{p}$, where E_{uhf} is the r.m.s. value of the u.h.f. field and p is the gas pressure. Since D is also a function of $\frac{E_{uhf}}{p}$, Prowse and Clark (1958) were able to show from the criterion for breakdown (equation 1.8) that the relation between $p\Lambda$ and $E_{uhf}\Lambda$ should be unique for any given gas. MacDonald and Brown, 1949, showed by dimensional analysis that these were proper variables for the

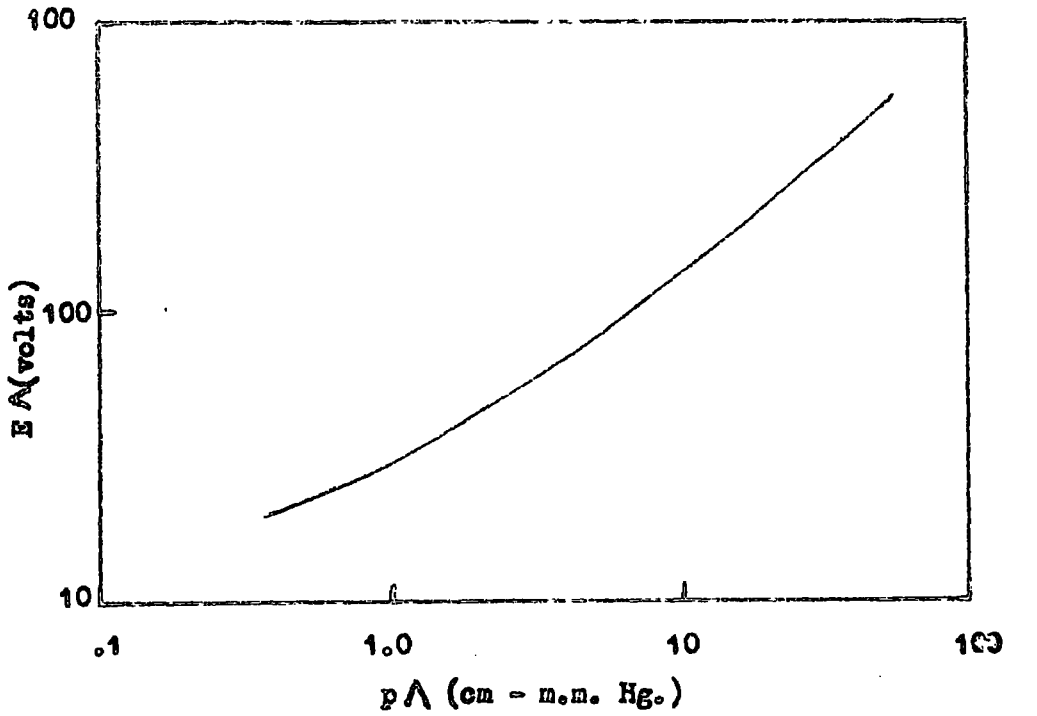

Fig. 1.2, EΛ - pΛ plot for hydrogen (Taken from Brown, 'Basic Data of Plasma Physics,' 1959)

discussion of u.h.f. breakdown.

The many measurements of u.h.f. breakdown fields in microwave cavities have been shown (Brown, 1956) to form unique $E\Lambda$, $p\Lambda$ plots for a given gas (e.g. Fig. 1.2 for hydrogen) and thus to be compatible with the diffusion theory. Prowse and Clark tested the theory at 5 Mc/s for cylindrical gap of varying dimensions and found unique $E_{uhf}\Lambda$-$p\Lambda$ plots for the u.h.f. region.

Thus it may be concluded that the diffusion control of the discharge in this region is well established.

Varnerin and Brown (1950) have shown that when a small unidirectional field, E_{dc}, is superimposed upon the u.h.f. field, the diffusion theory holds provided that Λ is replaced by a modified diffusion length, Λ_m, given by

$$\frac{1}{\Lambda_m^2} = \frac{1}{\Lambda^2} + \left(\frac{E_{dc}}{2D/\mu}\right)^2 \qquad \ldots\ldots\ldots 1.10$$

Employing Λ_m in the condition for breakdown they obtained values of the mean electron energy and the ratio of electron mobility, μ, to the diffusion coefficient, D, for diffusion controlled conditions.

1.5 Surface Phenomena

As shown in section 1.3, surfaces play an important part in discharges under unidirectional fields. Llewellyn Jones and Davies, 1951a and b, found a marked difference in the unidirectional breakdown stress for clean and oxide coated electrodes. This they interpreted as a change in secondary emission processes (De Boer, 1935).

A similar experiment (Llewellyn Jones and Morgan, 1951), with alternating fields showed that the u.h.f. breakdown stress was indepen-

dent of the cleanliness of the electrode surfaces. Hence they concluded that surfaces played a negligible part in u.h.f. breakdown.

Herlin and Brown, 1948a, showed that in diffusion controlled discharges, the diffusion length would have to be modified if secondary processes were important. The fact that experimental data, obtained by several workers, and for a range of variously shaped vessels, is compatible with a unique $E_{uhf}\Lambda, p\Lambda$ plot, suggests that no such modification is required and that secondary processes are negligible.

In general, surfaces have been found to have negligible effect on the breakdown stress for the diffusion controlled region. However, their effect when a small drift field is superimposed upon the u.h.f. field does not appear to have been investigated. In the latter part of this thesis some attempt is made to elucidate the effects of surface phenomena under such conditions.

1.6 Ionization in u.h.f. fields

Herlin and Brown, 1948a, suggested, as a consequence of equation 1.7, that $\frac{\Psi}{D}$ was the proper ionization coefficient in purely diffusion controlled systems. Considering the random walk of an electron, the time taken to diffuse unit distance is proportional to $\frac{1}{D}$, so that $\frac{\Psi}{D}$ is proportional to the number of ionizing collisions per unit distance the electron has diffused. It is thus analogous to Townsend's α, the number of ionizing collisions per unit distance an electron has drifted, which is applicable to drift controlled discharges. Herlin and Brown found it convenient to define a coefficient, $\xi = \frac{\Psi}{D} \cdot \frac{1}{E^2_{uhf}}$, to be analogous to the ionization efficiency defined by Townsend as $\eta = \frac{\alpha}{E_{dc}}$. Measurements of ξ were made

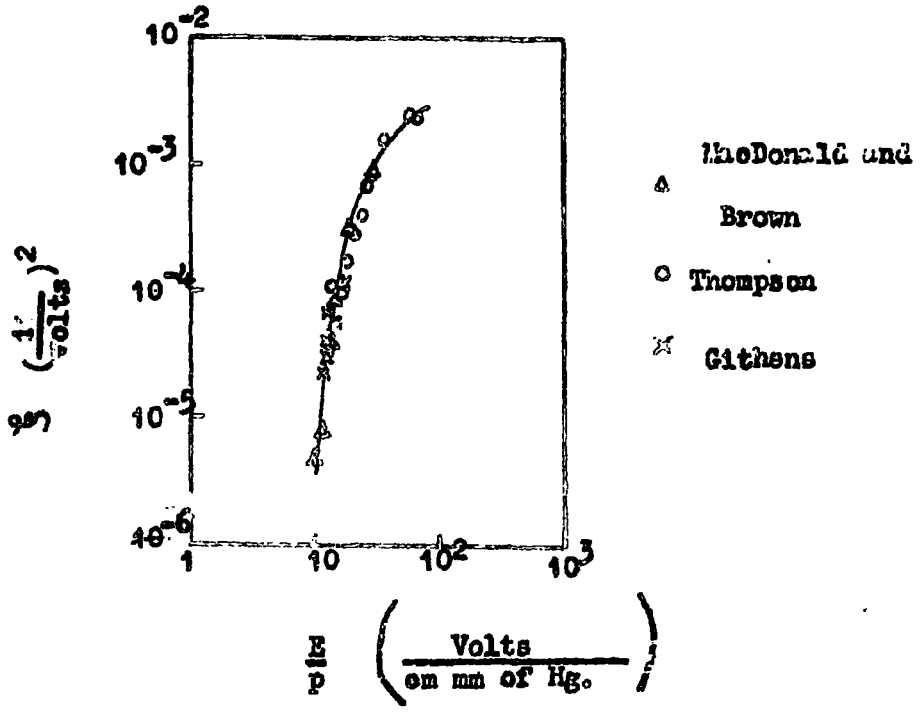

Fig. 1.3 Experimental $\frac{D}{\mu}$ curves of Thompson (1937), Githens (1941) and MacDonald and Brown (1949). The data covers a frequency range of 5 to 3000 Mc/s and a range of diffusion lengths from Λ = 0.0505 cm to Λ = 0.50 cm (taken from MacDonald and Brown (1949)

at breakdown using the criterion of equation 1.8 expressed as $\xi = \frac{1}{\Lambda^2 E_{uhf}^2}$. Figure 1.3 is a summary of results for hydrogen. Varnerin and Brown, 1950, extended this work to conditions where a small drift field was superimposed on the u.h.f. field.

These measurements of ionization have been confined to breakdown. No measurements had been made of ionization coefficients before breakdown, as had been done for unidirectional fields by Townsend in his measurements of α.

There Townsend was able to analyse the condition at breakdown from the increase of conduction by the gas as the drift field approached that for breakdown. Similarly measurements of conduct/ion with u.h.f. fields before breakdown are thought to provide a useful approach to the analysis of u.h.f. breakdown as well as to provide useful data on the conductivity of gases under such conditions. Such an experiment is that described in this thesis.

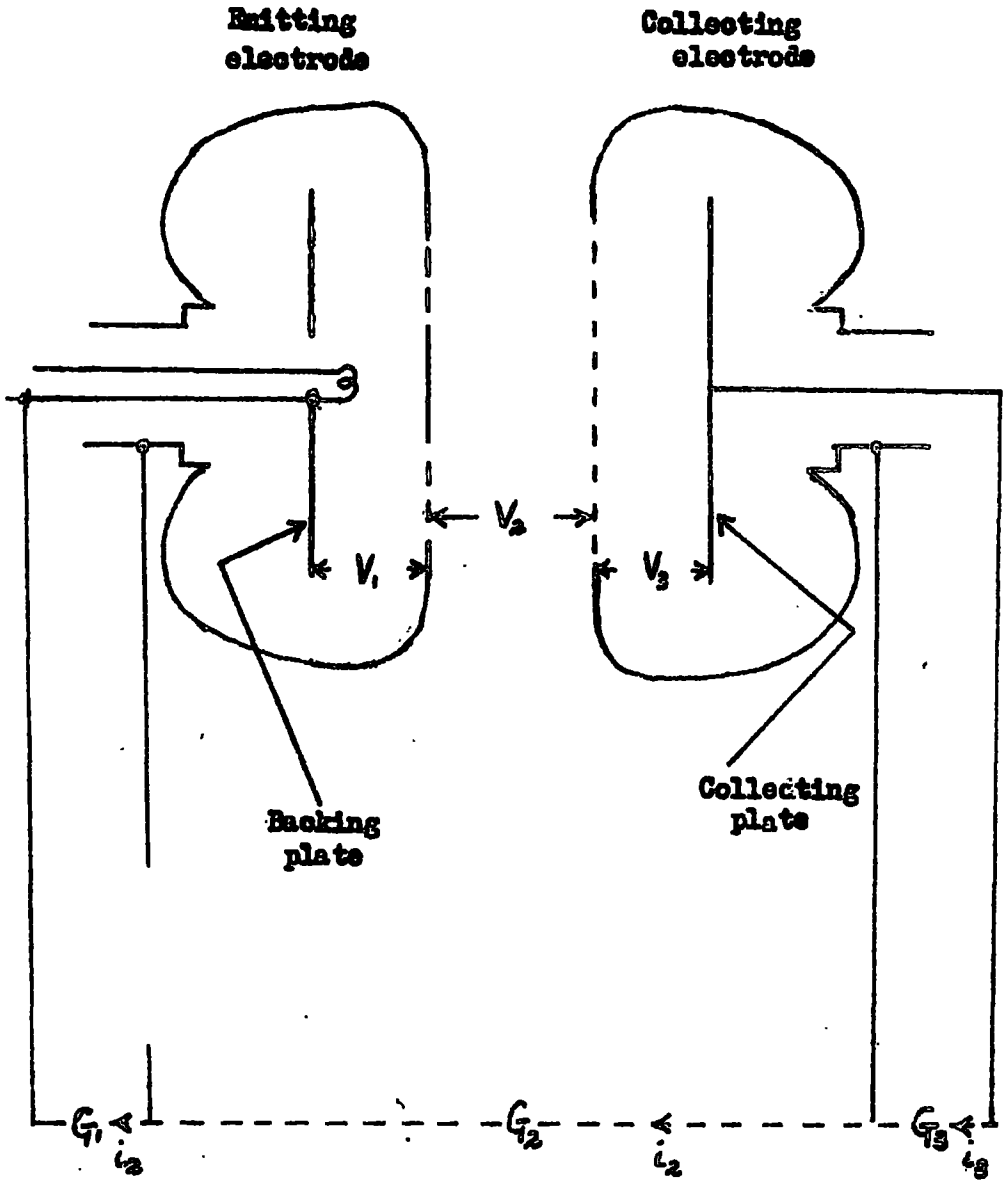

Fig. 2.1 Diagram of the Electrode and Current measuring system

This figure is also available on the back cover for reference

CHAPTER 2

THE PROBLEM, ITS PRACTICAL AND THEORETICAL ASPECTS

2.1 General Description of Apparatus

The apparatus was basically that developed by Nicholls (1960), with certain improvements and modifications which will be described in detail in the next chapter.

Figure 2.1 shows diagramatically the electrode assembly, which consists of two hollow, perforated, Rogowski-profiled electrodes. A stream of electrons derived from an oxide coated filament, is drawn to the back of the emitting electrode by a drift field provided by the unidirectional voltage, V_1, applied between the backing plate and the electrode shell. A fraction of these electrons is injected into the gap through holes in the electrode. These electrons are allowed to drift across the inter-electrode gap under a drift field, E_{dc}, provided by a voltage, V_2, applied across the gap.

A fraction of the electrons incident on the collecting electrode flow through the holes and are drawn to a collecting plate by a drift field resulting from a voltage, V_3, applied between the collecting electrode shell and the internal collecting plate.

The currents measured are (Figure 2.1):-

a) The total current emitted by the filament, i_1.

b) The current collected by the collecting electrode system, i_2.

and c) The current collected on the internal collecting plate of the far electrode, i_3.

The first two are measured by galvanometers G_1 and G_2, and i_3 (and also i_2 if required) by an electrometer method.

Provision is made for the application of a u.h.f. field between the electrodes, which is superimposed upon the small drift field, V_2.

2.2 The methods of measurement

In the absence of a u.h.f. field a stream of electrons flow across the interelectrode gap under drift field only. The current then received by the collecting electrode system will be referred to as the initial gap current, i_{20}.

When the u.h.f. field is applied, this electron flow will be modified so that the current to the collecting electrode system changes to a value, i_2. The effect of the u.h.f. field is then measured as the amplification of this electron stream, defined as:

$$A = \frac{i_2}{i_{20}} \qquad \ldots\ldots\ldots \quad 2.1$$

The mean time taken for an electron to cross the interelectrode gap will be referred to as the mean transit time, t_T. The measurement of transit times is attempted by use of a method similar to that of Bradbury and Nielson (1936). The electrons are sent across the gap in puffs and gated on the for side to provide a resonant system. For this purpose the electrodes bounding the ionization region are perforated and hollow to accommodate the electron generation and gating system.

2.3 The Theoretical Aspects

It may be shown that in the present apparatus, the electrons oscillate

about 100 times as they move across the gap. Thus the electrons are oscillating under u.h.f. conditions.

In pure u.h.f. conditions, i.e. in the absence of a drift field, diffusion has predominant control of electron lifetime so that an electron has an equal probability of flow to either electrode. Under these conditions no unidirectional current is expected so that ionization would have to be measured in terms of the u.h.f. current flow across the gap. This has, in principle, been used in tuned cavities to study the decay of plasmas (Brown and Biondi, 1949, and others). However, such measurements are not easy to perform nor is it easy to derive expressions for the ionization rate. To overcome these difficulties the application of a small drift field provides a unidirectional component in the system. Hence currents may be measured in terms of their unidirectional component. Further the drift field provides a concept of directional flow in the system which simplifies the physical picture of the mechanism and electron flow patterns in the gap. However, if the ionization observed is to be the result of energy communicated by the u.h.f. field rather than the drift field, it is necessary that this drift field be small.

If the Townsend approach to the process of amplification is to be followed, it is necessary to assume that drift is predominant in controlling the electron flow pattern. Then, as in the unidirectional field case, it is possible to define a coefficient, ζ, which corresponds to Townsend's α, and to derive the amplification of an electron stream crossing a gap of width d as $e^{\zeta d}$. Alternatively by a similar argument,

the amplification may be derived in terms of the mean transit time, t_T, and the ionization rate, ψ, as $\epsilon^{\psi t_T}$.

In diffusion controlled systems the amplification is controlled by the lifetime of electrons in the ionizing field rather than the distance travelled during their lifetime. Hence ψ rather than ζ is the proper variable for measurement of ionization. Further, in the present experiment, ζ is dependent on the drift field and is therefore not a unique function of the u.h.f. field. On the other hand the net ionization rate, ψ, may be expected to be dependent solely on the electron energy and thus predominantly on the u.h.f. field. Hence measurement of ψ is attempted in the present experiment.

As suggested by the Townsend-type relation, $A = \epsilon^{\psi t_T}$, it was originally thought that ψ could be calculated from simultaneous measurements of amplification and transit time. However a fuller theoretical treatment, prompted by preliminary measurements of amplification, suggests that diffusion is comparable to drift so that this simple equation is not applicable. In the present experiment the electron energy is supplied by the u.h.f. field rather than the drift field as in the unidirectional case considered by Townsend. Hence the ratio of diffusion coefficient to drift velocity is greater and diffusion may be expected to have greater control of electron flow. The present view is that both amplification and transit time experiments can individually give values of ψ provided some theory of electron flow in the gap is assumed. These experiments are therefore treated separately in what follows.

Nicholls (1960) has obtained preliminary measurements of amplifica-

tion with the present apparatus. In particular he has established that there is a rapid growth of ionization as breakdown is approached. The problem remaining is therefore to elucidate the mechanism which can explain these results in terms of drift, diffusion and ionization coefficients and thus obtain some accurate measurements of the ionization rate.

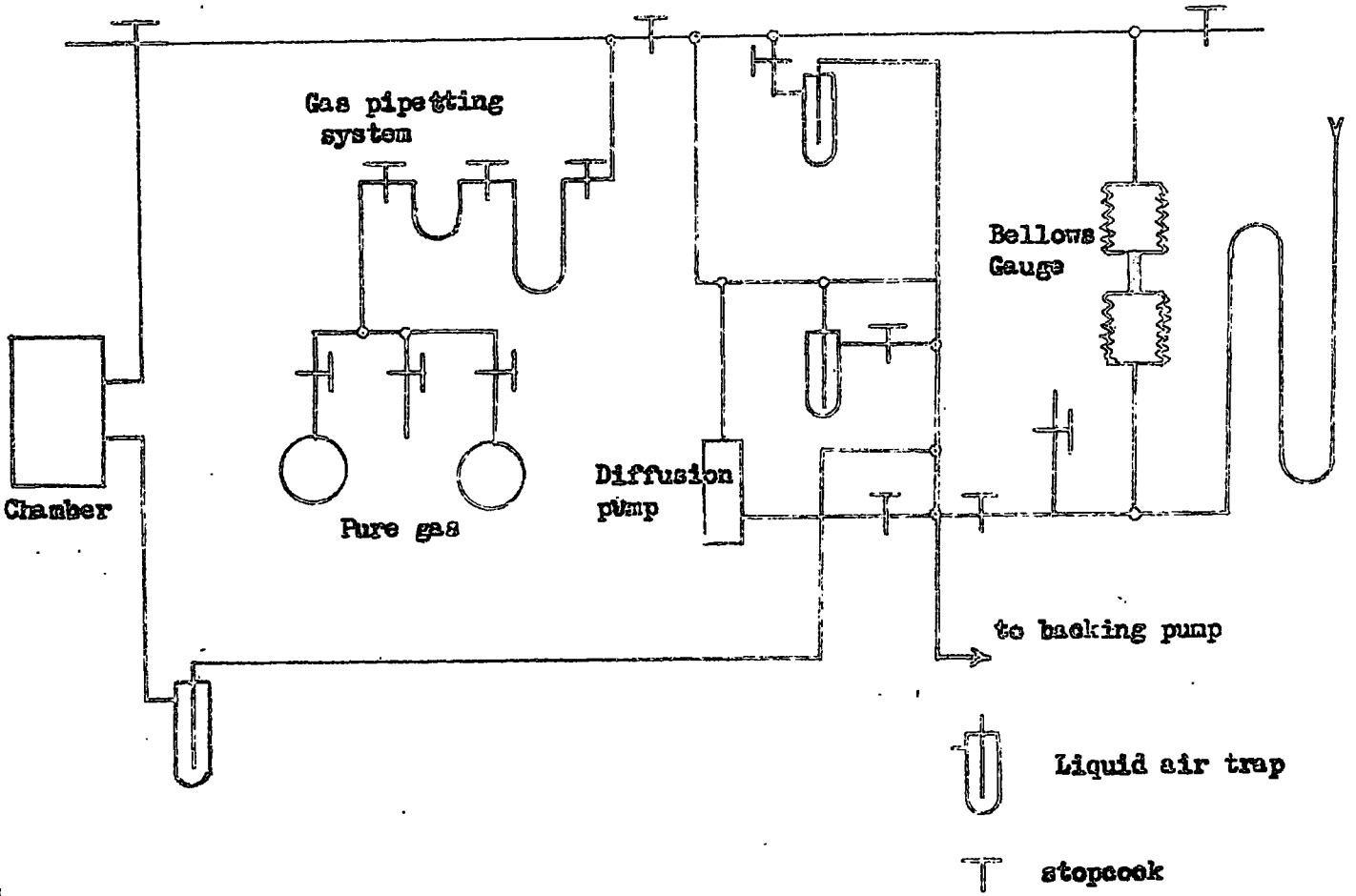

Fig. 3.1 The evacuation and gas pipetting system

CHAPTER 3

APPARATUS

3.1 Details of the Electrode System

The electrodes (brass) were those used by Nicholls, 1960. The perforations were confined to the flat face as indicated in figure 2.1. In the emitting electrode this face is .076 cm thick and is drilled with 35 holes of 0.038 cm diameter, countersunk on the inside to a depth of .038 cm. In the collecting electrode there are about 50 holes of twice the diameter to provide a greater transmission of electrons to the inner collecting plate. To prevent positive ions striking the filament no holes are drilled in the centre of the emitting electrode for an area of 0.6 cm diameter.

The electrode system is contained in a chamber connected to a vacuum and gas pipetting system. This enables air to be removed, by attaining a vacuum of better than 10^{-4} mm. Hg. and the chamber may then be filled with the required gas at a given pressure. Initially the vacuum system was that used by Nicholls and is shown in figure 3.1. Later a modified form was used (Figure 11.1, Chapter 11). The pressure of gas was measured using a differential bellows gauge calibrated against a mercury column. The range of pressure was between 3 and 10 mm. Hg. and the impurity content, estimated from observations on the ability of the system to retain a vacuum, was better than 1 part in 10^4. The system was outgased by leaving under vacuum for at least a week before measurements were made.

Approximately $\frac{1}{5}$th full size

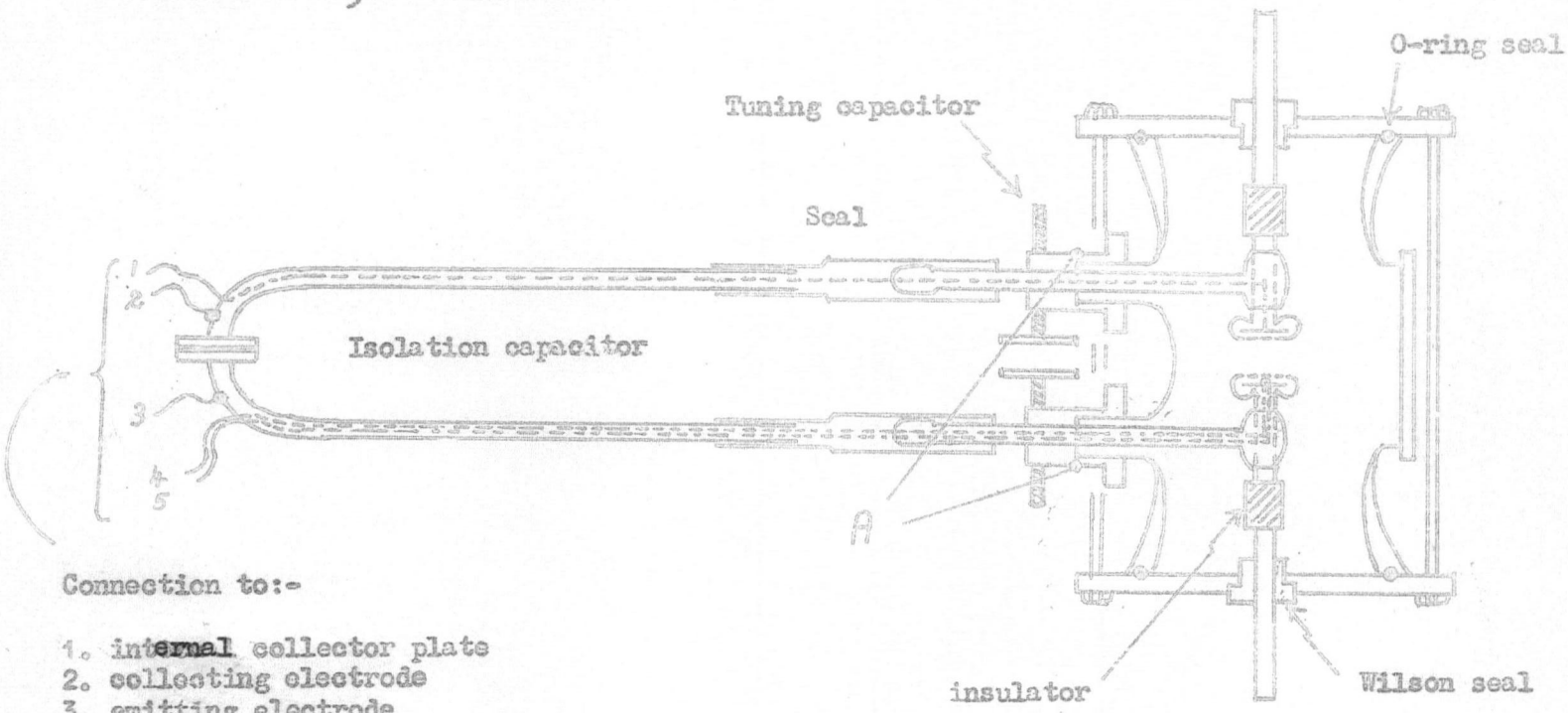

Connection to:-

1. internal collector plate
2. collecting electrode
3. emitting electrode
4 and 5. filament

Fig. 3.2 The chamber and the quarter wave transmission line

A u.h.f. field may be applied between the electrodes by attaching them to the open end of a tuned $\frac{\lambda}{4}$ transmission line (Figure 3.2). An oscillator, of frequency 106.8 Mc/s, was loosely coupled to the closed end of this line. The amplitude of the oscillationsand thus the voltage across the inter-electrode gap was adjusted by use of a Variac transformer which altered the h.t. voltage applied to the oscillator.

A diode voltmeter, capacitatively coupled across the line at points A of figure 3.2, was used to indicate voltages across the gap. It was not possible to connect a direct-reading voltmeter to the electrodes, but this is not essential so long as a means is available of calibrating a loose-coupled indicating meter in terms of gap voltage. For this calibration an ellipsoid fieldmeter was used.

3.2 The ellipsoid fieldmeter

This instrument consists of a Wood's metal bead hung on a quartz fibre midway between the electrodes. It may be shown (Maxwell, 1904), that the frequency of torsoinal oscillation, R_1, is dependent on the field in the gap, E, according to the relation,

$$E = K(n_1^2 - n_o^2)^{\frac{1}{2}} \qquad \ldots\ldots\ldots 3.1$$

where K is a constant and n_o is the natural frequency of oscillation i.e. that for which the field is zero.

This instrument has been used by Thornton and Thompson, 1932, for measurement of high unidirectional fields and by Bruce, 1947, for high alternating fields. The inaccuracies dealt with by Bruce, 1947, can be neglected when the instrument is directly calibrated. Nicholls, 1960, has shown that equation 3.1 holds for u.h.f. fields and that K is independent of frequency. Thus the instrument may be used as a change-over instrument between unidirectional and u.h.f. fields.

The frequency of the bead was measured with a stop-watch, using an electro-mechanical counter operated by a Morse key to count the oscillations. It was found necessary to limit the initial amplitude of the oscillation to some predescribed value and to time a constant number of oscillations in order to get compatible repeatable results. In this way a calibration accuracy of about 1% was obtainable.

The relation between the indication of the diode voltmeter, θ, and the actual voltage, V_{uhf}, across the electrodes was found to depend on the gap width, d. For a given gap width, θ was found to be proportional to V_{uhf}.

Nicholls suggests that this variation of voltmeter sensitivity is attributable to variation of the position of the voltmeter on the standing wave pattern allong the line. As the gap width is increased the capacitance across the end of the line is decreased. To compensate, the line is retuned by increasing the tuning capacitance on the other side of the voltmeter. This effectively moves the voltmeter allong the standing wave closer to the gap, with corresponding larger reading on

the voltmeter for a given gap voltage.

Following this suggestion a quantitative approach has been attempted.

It may be shown (Jackson, 1944) that for a line of characteristic impedance, Z_o, terminated with an impedance, Z_T, the voltage, V_y, at a distance, y, from the termination is related to the voltage, V_T, at the termination by

$$V_y = V_T \left(\cosh Py + \frac{Z_o}{Z_T} \cdot \sinh Py\right) \qquad \ldots\ldots\ldots 3.2$$

where P is the propagation constant.

Applying this to the present case, V_T is the voltage across the gap, $V_{uhf} = E_{uhf} \cdot d$, V_y is the voltage across the line at the point of coupling of the diode voltmeter and y is the distance from gap to voltmeter along the line. In the above calibration, the terminating impedance, Z_T, was that of the gap capacitance only, so that the voltmeter sensitivity, $\frac{\theta}{E_{uhf}}$, is related to the gap width, d, by (equation 3.2):

$$\frac{\theta}{E_{uhf}} = \frac{d \cdot \cos Py}{K} - \frac{Z_o \omega \epsilon_o A}{K} \cdot \sin Py \qquad \ldots\ldots\ldots 3.3$$

where A = area of the electrodes,

and K = voltage sensitivity of the diode voltmeter, defined by

$$V_y = K \cdot \theta.$$

Thus a plot of $\frac{\theta}{E_{uhf}}$ against d is expected to be a straight line with an intercept on the d-axis at

$$d = Z_o \omega \epsilon_o A \cdot \tan Py \qquad \ldots\ldots\ldots 3.4$$

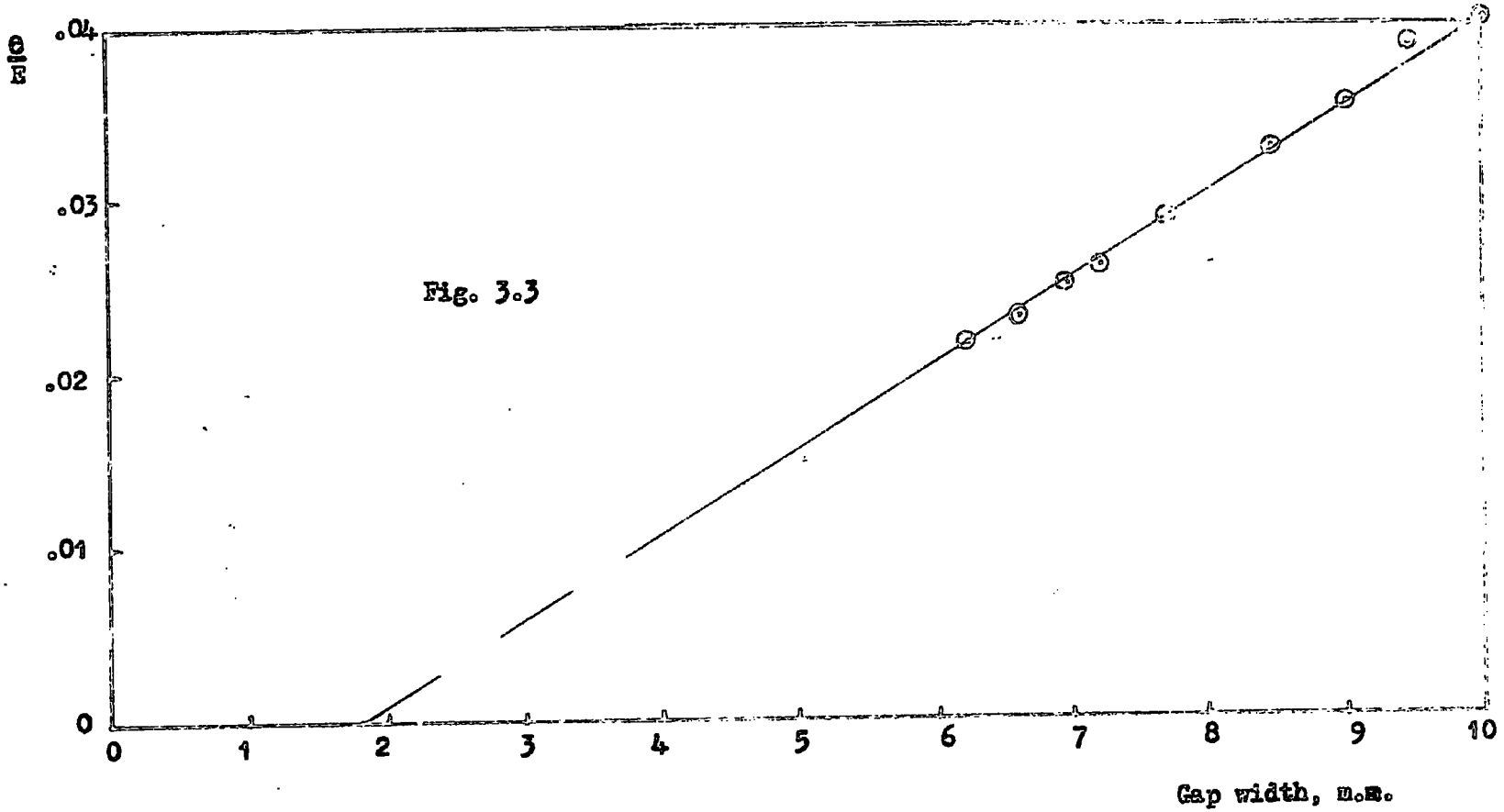

Fig. 3.3

An experimental plot for the instrument used is shown in figure 3.3 and has an intercept at d = 1.8 mm. An approximate value of Z_o may be obtained by treating the line as a pair of parallel cylinders, remote from other objects. This gives $Z_o = 300\Omega$, and allows the point of intercept to be calculated from equation 3.4 as d = 2 mm. approximately. This is close enough to the experimental value to afford support to the theory.

It should be noted that equation 3.2 shows that the sensitivity of the diode voltmeter depends on the gap impedance, Z_T. This, however, can only be obtained directly from the geometrical gap capacitance when the gap is empty. When the gas is conducting, the impedance of the discharge must be taken into account.

If it is assumed that the collision frequency, ν, of electrons in the gap is independent of electron velocity (approximately true for hydrogen) the conductivity of the discharge maybe considered to be (Margenau, 1946)

$$\frac{e^2 n}{m\omega} \cdot \frac{1}{1 + (\nu/\omega)^2} \cdot \left[\frac{\nu}{\omega} - j\right]$$

where, n = mean electron density in the gap,

e and m are the electronic charge and mass respectively

and ω = angular frequency of the applied u.h.f. field.

Calculationsfrom this, suggest that the admittance of the discharge is of the order of that of the gap capacitance for the highest electron densities used in the experiments to be described. Thus at

higher electron densities (higher amplifications) some deviation in the calibration of the diode voltmeter is to be expected. However, in the lower range of gap amplifications upon which the work to be described is concentrated, a calibration accuracy of 5% is to be expected.

3.3 The Current Measurement and Voltage Supply Systems (Figure 3.4)

The voltages V_1, V_2 and V_3 are provided by batteries B_1, B_2 and B_5 varied by potentiometers RV_1, RV_2 and RV_3 respectively. They are measured at the points indicated in figure 3.4. The sensitivity of these voltmeters was such that the variation in voltage which provided a change of 1% in the corresponding current was easily detectable. This enabled these voltages to be manually stabilised so that their variation would cause less than 1% variation in the currents flowing.

Currents are measured with galvanometers where possible, but i_3 and in certain cases i_2, were so small that an electrometer method was found necessary. A Wolf string electrometer in a null circuit was found satisfactory.

The electrometer was basically used to measure the voltage dropped by the current on passing through a large resistor. The resistor was chosen to make this voltage about 10 volts. Since these resistors, R_1 and R_2, are necessarily in series with the voltage sources V_2 and V_3 when measuring i_2 and i_3 respectively, the voltage applied to the electrodes will be reduced by the voltage dropped across the corresponding resistor. Further these voltages will then vary with current

Fig. 3.4

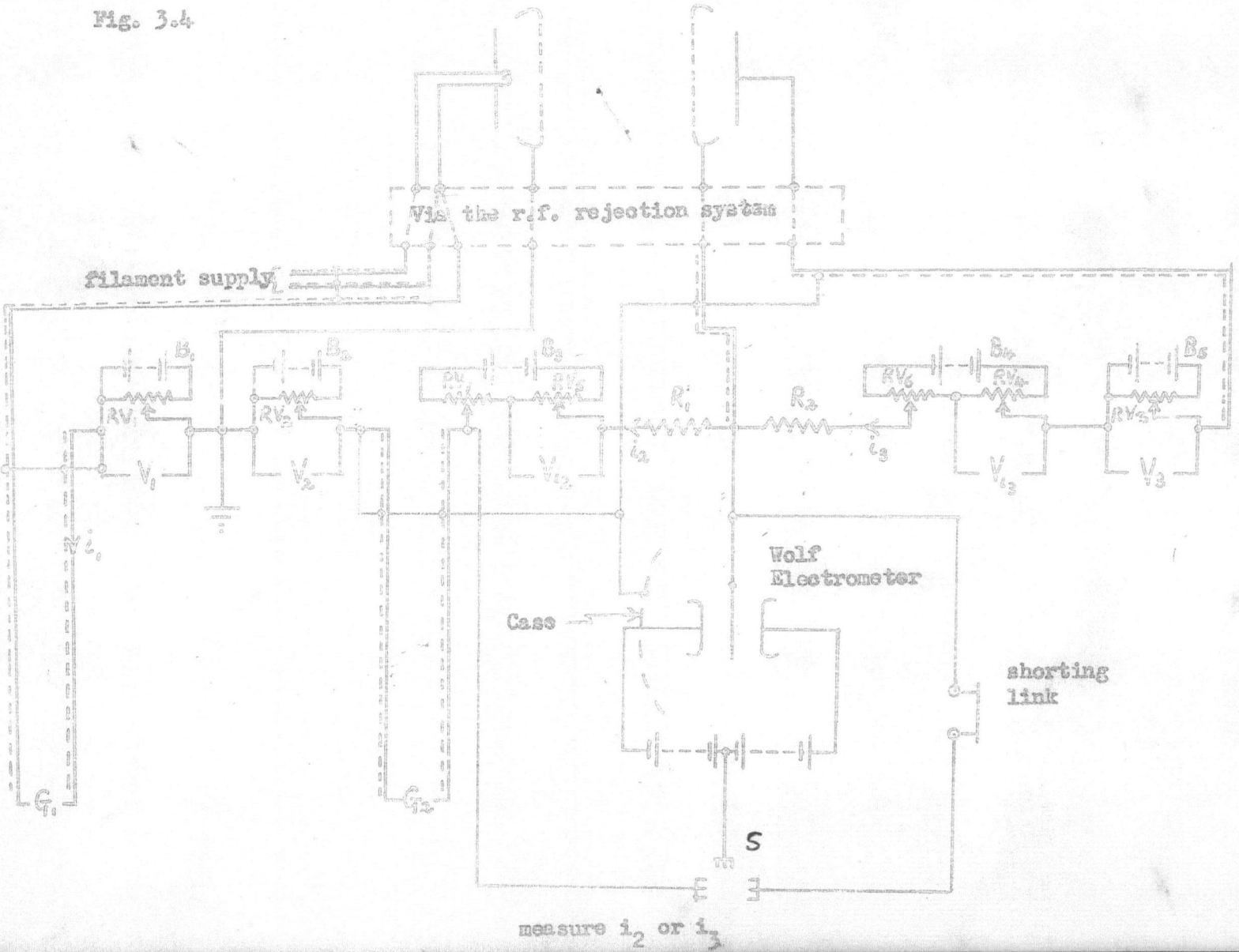
Via the r.f. rejection system
filament supply
Wolf
Electrometer
Case
shorting
link
S
measure i_2 or i_3

flowing. To overcome this difficulty the system was made into a null-device by including a reverse voltage source in series with the resistor. The electrometer then measured the voltage across the sourse and resistor in series and thus the difference between the source voltage and that dropped across the resistor by the current being measured. The voltage source was then adjusted to give zero voltage difference as observed on the electrometer. Thus provided this null position is achieved, there is zero voltage across the resistor-source combination and thus no variation in the voltage applied to the electrodes. The voltage dropped across the resistor and thus the current may then be measured as the voltage of the source by the use of an ordinary voltmeter.

The complete circuit is shown in figure 3.4. There R_1 and R_2 are the resistors and B_3 and B_4 provide the voltage sources which may be varied by using potentiometers RV_5 and RV_4 respectively. A switching device, S, is provided for connecting the electrometer across either combination.

When no current is flowing between the electrodes, there are certain currents flowing in the measuring circuits due to leakage through the insulation. The voltage dropped when these flow through R_1 and R_2 may be backed off using potentiometers RV_7 and RV_6. The voltages read across RV_5 and RV_4 are then those due to gap current only.

The values of R_1 ($10^{11}\Omega$) and R_2 ($10^{12}\Omega$) determine the sensitivity obtainable. A gap current of 10^{-13} amp flowing through R_2 can readily be detected.

To reduce the flow of leakage currents, leads in the system are coaxial cables whose screens are at the potential of the inner core. The earthing point (figure 3.4) eliminates leakage flow via the filament control system through the measuring circuits of i_2 and i_3. Thus the filament control system is isolated from the current measuring circuits of i_2 and i_3 as far as leakage to earth is concerned. The large body of apparatus attached to the filament with its consequent large leakage currents to earth, can therefore not affect the measurement of the small currents i_2 and i_3.

3.4 Protection of the Galvanometer, G_2

In an experiment to measure the amplification, it is considered desirable to make frequent checks of the initial gap current, i_{20}. However, if during these experiments breakdown should occur, the resultant large current caused the zero of the galvanometer measuring the gap current to drift. The extent of this drift could only be estimated by reducing i_{20} to zero and thus changing the experimental conditions. Thus to retain continuity of conditions in these experiments and to enable fluctuations in i_{20} to be recorded, it was considered desirable to provide a protection device against large currents occuring at breakdown.

The basic requirement was to operate a relay from the spot of a

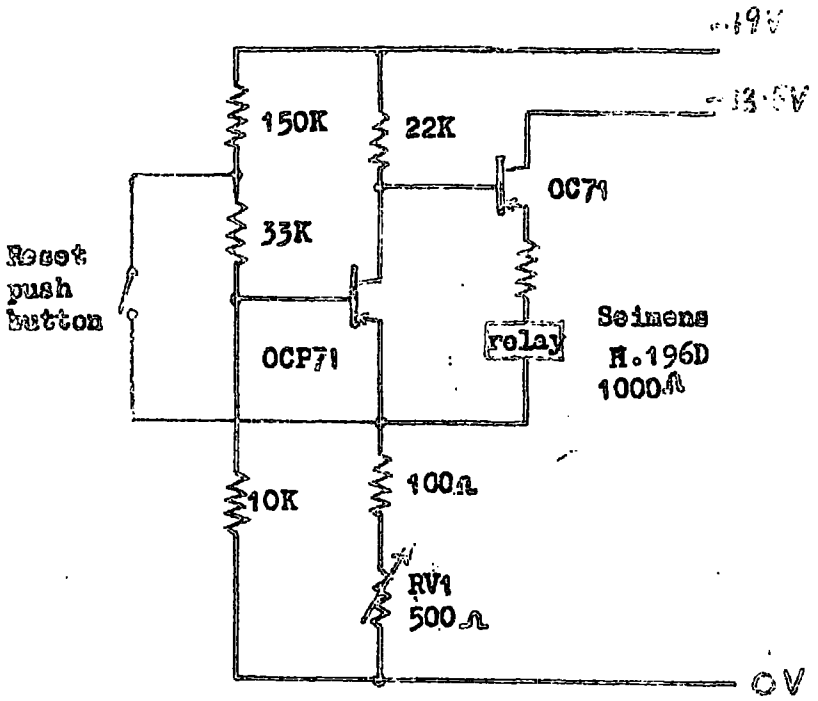
-19V
-13·5V
150K
22K
OC71
33K
Reset
push
button
OCP71
relay
Seimens
H.196D
1000Ω
10K
100Ω
RV1
500Ω
0V

Fig. 3.5

sensitive galvanometer, so that in the event of an abnormally high current occuring the galvanometer was automatically shorted. The rate of rise of this current was found to be such that the speed with which the spot passed a phototransistor was too great to develop a pulse of sufficient length to bring in a high speed relay. It was thus not possible to employ self holding relay techniques. A relatively fast photosensitive bistable circuit was therefore developed to operate the shorting relay. The further requirement that the unit be isolated from earth so as to reduce leakage from the galvanometer leads to earth, necessitated the use of transistors. The complete circuit is shown in figure 3.5.

A bistable circuit of this type has been treated by Wolfendale, 1957, for non-phototransistors. He has shown that both stable states are controled by T1, one with T1 bottomed and the other with T1 cut off. It remained to modify the design equations when T1 is a phototransistor. This has been attempted (Appendix 1), and it has been concluded that the circuit may be reliably triggered from the state with T1 cut off, by the incidence of a galvanometer spot on T1, the level of illumination required depending on the emitter resistance (RV1). Further in the triggered state (T1 bottomed) the circuit may be made insensitive to illumination or temperature fluctuations.

The relay, RLA, is energised during the light sensitive state, when it is arranged to leave the galvanometer unshorted. The relay is then

released and the galvanometer short circuited either by a light pulse incident on TR1 or by failure of the supply batteries. The circuit thus has a right side failure characteristic.

The battery supplies for the circuit are switched with the galvanometer range. In the 'shorted' position of this switch, the supply batteries are switched off, so that the galvanometer is short circuited both by the galvanometer range switch and by the relay. As a consequence of the right side failure characteristic, on switching on, the relay contacts remains closed and the galvanometer cannot be released until the circuit is reset by the push button (figure 3.5). Failure of the relay to short the galvanometer, initially, indicates a circuit fault, whereas failure to reset indicates either a circuit fault or an incorrect setting of the background compensation control, RV1. The switching on process thus provides a check on the working of the protective device.

The background illumination may be compensated by adjusting the triggering level of the bistable. This adjustment may be achieved by adjusting RV1 so that the circuit just triggers with background illumination only and then turning RV1 to increase the trigger level slightly to provide a safety margin.

This procedure corrects for long term variations in background illumination and temperature. The sensitivity of the circuit is then limited by the short term fluctuation in background illumination and temperature. In the present case the former is thought to be the most important. To ensure this causes no failures a lens was used to

concentrate the spot onto the sensitive area of the phototransistor and thus provide a greater signal to noise ratio in the incident light. This greatly reduced the sensitivity of the circuit to background fluctuations and made the setting of RV1 much less critical. However, it has been found quite reliable to use this circuit in sunlight provided that variations in illumination are not too great.

The phototransistor is mounted at the for end of the galvanometer scale so that the deflection is limited to the range of the scale.

3.5 Stabilisation of Current emitted into the gap

3.5.1 Introduction

Ideally the current emitted into the gap during amplification measurements, should be constant, independent of gap conditions. Prior to some theory of emission of electrons into the gap, through the hole in the emitting electrode, it is assumed that the criterion for constant emitted current is a constant current flow to the inside of the emitting electrode shell, i_1. Thus the stability of the current, i_1, flowing from the filament to the emitting electrode shell is regarded as the criterion for constant emitted current.

This current (i_1) was, however, found to be susceptible to short and long term drifts; the latter result from decreasing emissive power of the filament. In the measuring system large capacitors are charged by small current giving long time constants so that the effect

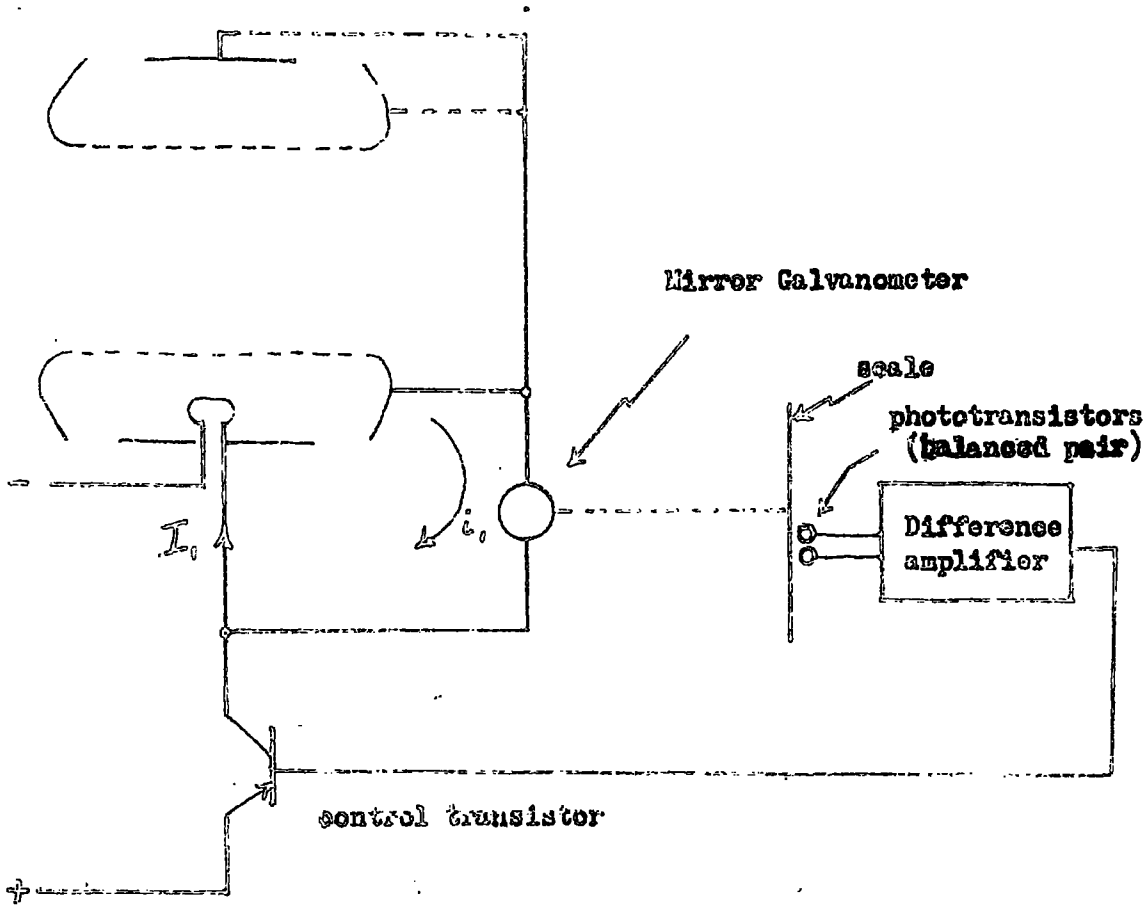

Fig. 3.6 Outline of system for the stabilisation of the current emitted by the filament

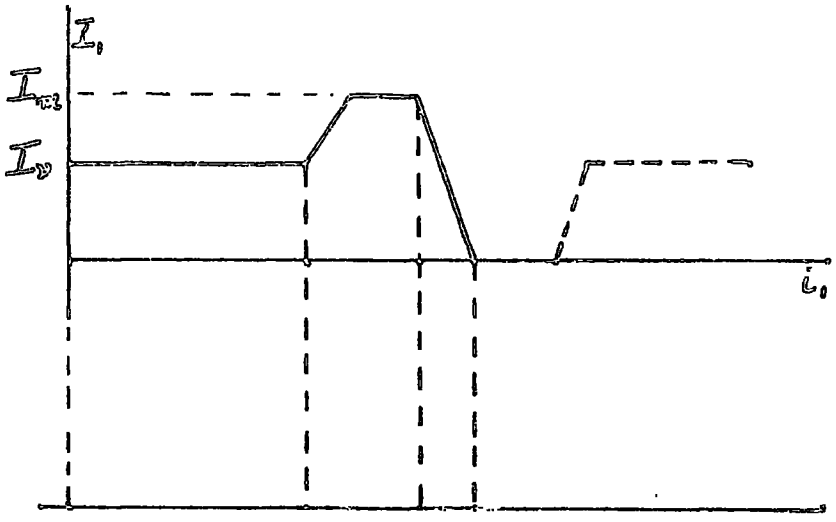

Fig. 3.7 Variation of the output current (I) of the control amplifier with spot position (i_0)

of variations of i_1 tends to be masked. Hence some stabilisation of i_1 was considered desirable.

A system shown diagrammatically in figure 3.6 was therefore developed. Two phototransistors placed close together on the scale of the galvanometer measuring i_1, feed currents into a difference amplifier which depend on the position of the spot and thus on the value of i_1. The amplified difference signal is applied to a transistor in series with the filament. As a consequence of the characteristics of this system, the filament current, I, is a function of i_1 as shown diagrammatically in figure 3.7. The filament warms up under a variable initial current, I_v, until the spot is caught by the phototransistors and held on portion, A, of the curve. Since with high current amplification the slope of A is high, and the filament emission is critically dependent on I, a high degree of stabilisation of i_1 is obtained.

3.5.2 The circuit (Figure 3.8)

The circuit may be divided into three sections, the pick-off unit which is mounted on the galvanometer scale, the difference amplifier, and the power amplifier which feeds the filament. The pick-off unit consists of two phototransistors, OCP71, in a long tailed pair circuit with provision (RV1 and RV2) for balancing the circuit for a given background illumination.

The advantages of long tail pair circuits in both this and the difference amplifier are two fold. Firstly a balanced system enables

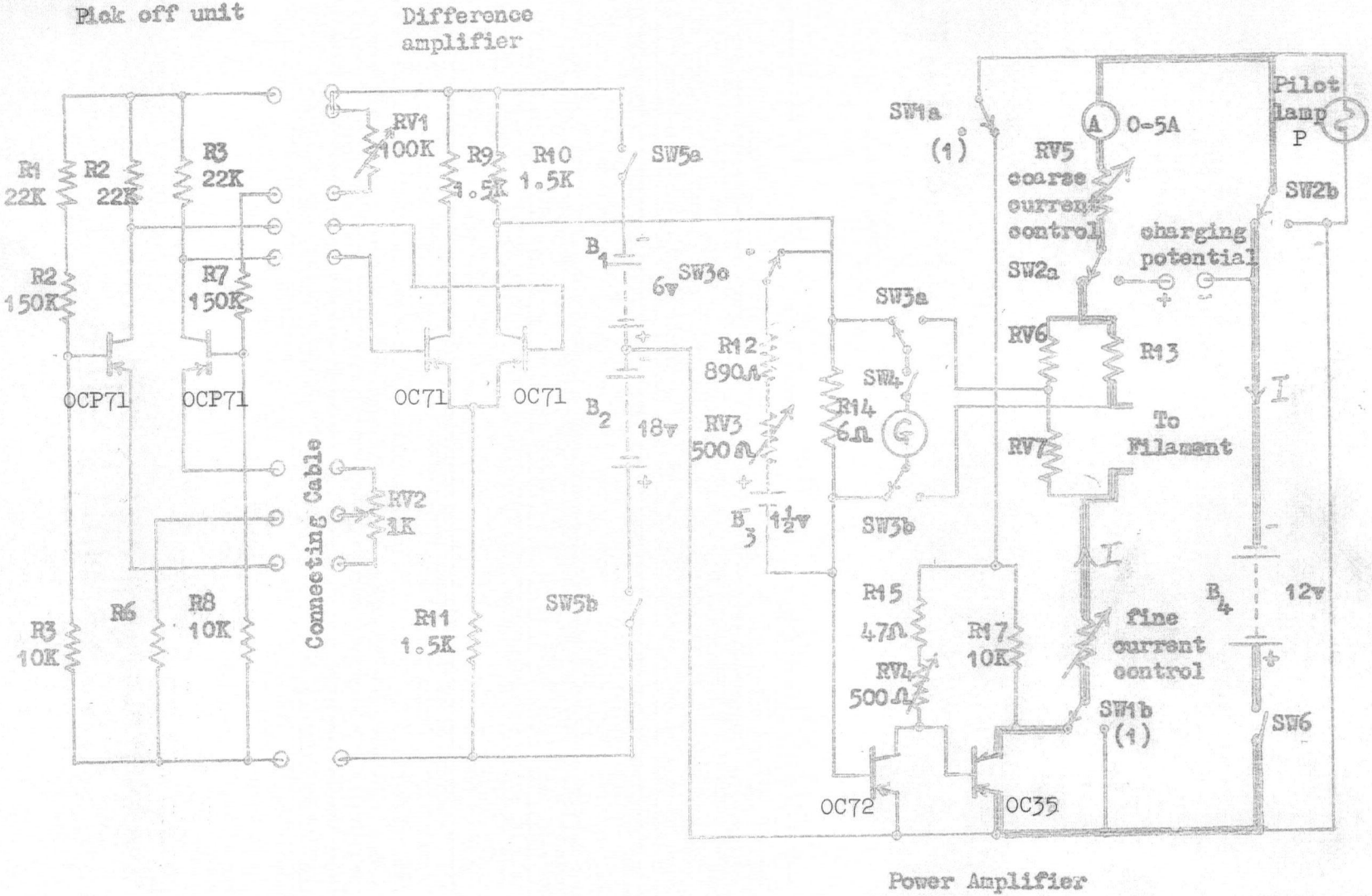
Pick off unit
Difference amplifier
R1 22K
R2 22K
R3 22K
R2 150K
R7 150K
OCP71
OCP71
R3 10K
R6
R8 10K
RV1 100K
R9 1.5K
R10 1.5K
SW5a
B1
6v
SW3c
OC71
OC71
B2
18v
Connecting Cable
RV2 1K
R11 1.5K
SW5b
R12 890Ω
RV3 500Ω
B3 1½v
SW3a
SW4
R14 6Ω
SW3b
SW1a (1)
A 0-5A
RV5 coarse current control
SW2a
RV6
R13
RV7
To Filament
Pilot lamp P
SW2b
charging potential
I
I
B4 12v
R15 47Ω
RV4 500Ω
R17 10K
fine current control
SW1b (1)
SW6
OC72
OC35
Power Amplifier

Fig. 3.8

background illumination to be balanced out. Secondly, drift, one of the chief problems in direct coupled, temperature variant systems, is reduced in these early stages where signal amplitude is small.

The balance of background illumination:

The pick off unit may be balanced to compensate for a wide range of background illumination. The criterion for balance is judged by monitoring the output current of the difference amplifier. This current is passed through a 6Ω resistor (R14) and measured as the voltage across it by means of the centre zero galvanometer, G (when SW3 is suitably switched).

In the absence of a difference signal from the phototransistor pair, there is a steady current through R14, which will be referred to as the zero current. A bias current is provided by B_3 across R12 and RV3 to back off this zero current, to allow the full range of the galvanometer to be used and to facilitate the adjustment of balance as a gradual approach to a zero value.

The variable resistor, RV3, allows the bias current to be set so that the zero current corresponds to the zero of the meter, G. At balance the phototransistor, when exposed to the same illumination, provide equal inputs in opposite phase into the difference amplifier so that the resultant difference signal is zero. Since the range of outputs of the two phototransistors are equal, it is convenient if the zero level of the output current of the difference amplifier be in the centre of its range. This is arranged by finding the limits, by exposing each transistor in turn to a bright light, and then

estimating the centre of these limits and adjusting RV3 so that this centre corresponds to the zero of the meter, G.

The actual balancing process may now be carried out using the balance controls RV1 and RV2 and two light sources of differing intensities. The criterion for balance is that the output current of the difference amplifier remains at its zero value, when the ambient light intensity changes, provided the intensity at both transistors changes equally. Thus the phototransistors are exposed to a light source and one of the balance controls used to adjust the reading of G to zero. This is repeated with the other light source and the other balance control. Repetition of these adjustments results in a gradual reduction in the change in output current upon changing the light intensity, eventually reaching the zero level.

The Power Amplifier:

With SW1a and SW1b (Figure 3.8) in position (i), the current through the filament is manually controlled by adjustment of RV5 and RV8. When SW1 is switched from this condition so that the control system is operative, the output transistor operates with a maximum possible current, I_m, of the value observed with SW1 in the manual position. Thus RV5 is used to arrange a safe limit to the current which can be passed through the filament.

Since emission from the filament is only appreciable over a small current range, it is not necessary that the difference amplifier should drive the output transistor over its full range of output

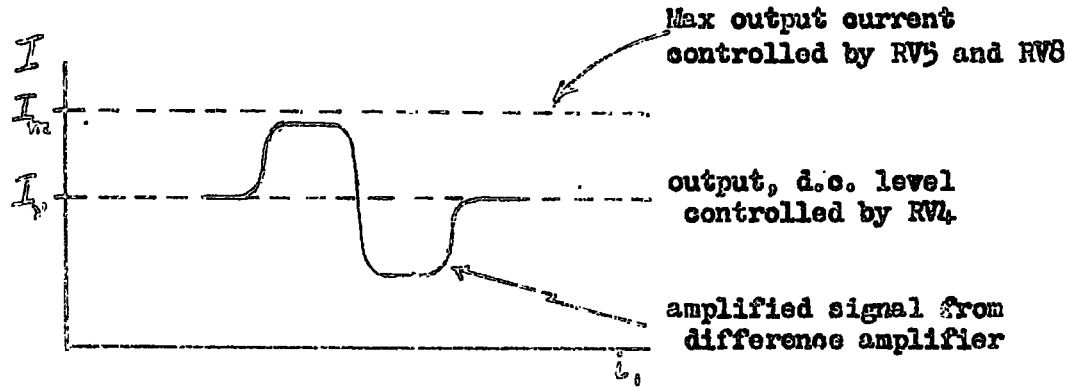

a.

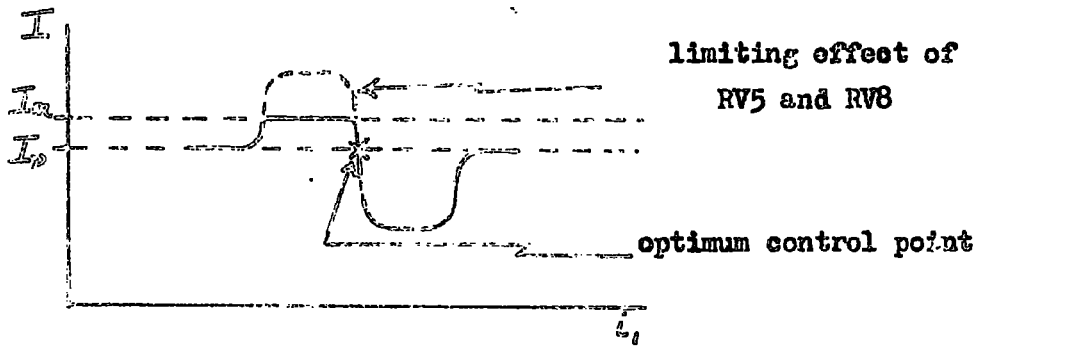

b. Normal control conditions

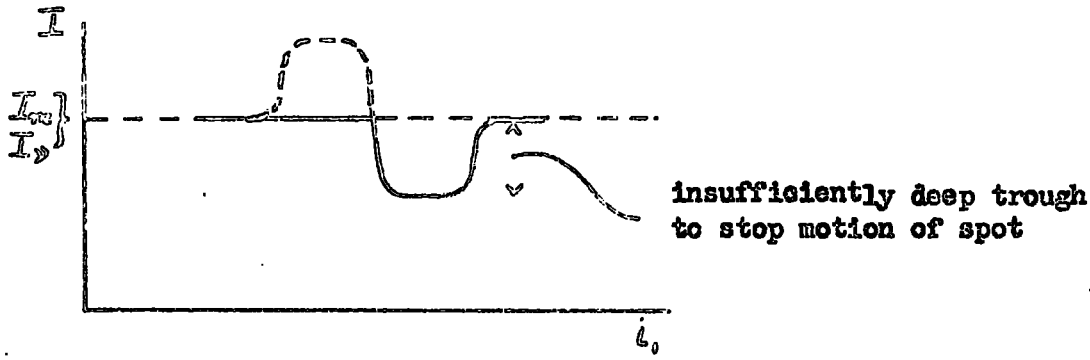

c. Too high a d.c. level.

Fig. 3.9

currents. Thus, for economy, the difference amplifier controls the output current over a small current range (Figure 3.9a). The position of this range over the full range (0 to I_m) is controlled by RV4, which effectively controls the zero level of the output current, I_v.

The filament is warmed up by raising this zero level, I_v, using RV4. Initially the emission current, i_1, is too small for the spot to impinge on the phototransistors and the filament warms up under the current, I_v. When, however, the spot impinges on the phototransistors there is an initial increase of I causing slight acceleration in the rise of i_1. When the control region is reached there is a rapid decrease of I (figure 3.9b) and the movement of the spot is rapidly damped and held at some point on this region which will be referred to as the control point.

The position of the control point over the range of the control region may be observed using G to measure the input current to the power amplifier and may be adjusted using RV4 to adjust I_v. Ideally the control point should be at a value of filament current equal to I_v (i.e. the control point should be adjusted so that the galvanometer, G, reads zero). Under such conditions failure of the system by which the spot no longer impinges on the phototransistors (e.g. galvanometer lamp failure) will leave the zero current flowing and the spot remains close to its stabilised position.

If I_v be excessively increased during the warming up period, the trough following the control region (figure 3.9c) may be insufficient to damp the motion of the spot, so that the spot flies past. However, this does not result in an excessive current flowing through the filament if correct adjustment of I_m(RV5) has been made.

Instabilities in the system:

For a given position of the phototransistors, the actual stabilised current will depend on the shunt across the galvanometer measuring i_1. For higher sensitivities oscillations of i_1 are observed. Overdamping of the galvanometer has reduced these to small amplitude and they become completely absent for lower sensitivities. Loss of sensitivity due to the large damping required is no disadvantage since the apparatus is used with lower sensitivities only.

The mechanism responsible for the generation of these oscillations is as follows. The large momentum obtained as the spot passes through the maxima or transition region (figure 3.7) carries the spot into the minimum. Here the filament cools rapidly to below emission level while the motion of the spot is damped out. The spot, therefore, drifts back well into the region of the maximum before the filament warms up again and the process is repeated.

The amplitude of these oscillations depends on the maximum current available, I_m. Observations of this amplitude is thus a useful indication of the difference between the stabilised and maximum currents.

The filament is run at a temperature somewhat below that of fusion. Nevertheless on the grounds of safety it is thought advisable to adjust the maximum so that the difference between stabilised and maximum currents is as small as is practicable. In practice this condition was met when the amplitude of the oscillation had been reduced, by reduction of I_m, to be just undetectable.

Measurement of filament temperature is made possible by including a bridge circuit in the load of the output transistor. The variable arms are provided by RV6 and RV7 while R13 is a standard resistance and the filament completes the bridge. The filament is of platinum wire and thus an absolute measurement of the temperature on the platinum resistance scale is possible. However, this has not been found necessary and in general the bridge is used simply as an indicator of filament temperature. In particular as the emission decreases, the temperature will be increased by the stabiliser in an attempt to restore the emission. Thus variation in temperature becomes a measure of the variation in emission.

Provision is made for charging the accumulator block B_4. A switch is provided (SW2) to switch B_4 into a suitable position for charging from an external source applied between the points indicated in figure 3.8. A Rheostat RV5 limits the current, which is indicated by the ammeter, A. This also indicates filament current, thus indication of a current by A is not necessarily an indication that there is a filament current flowing. Hence a pilot lamp, P, is incorporated, which lights only when power is available across the filament.

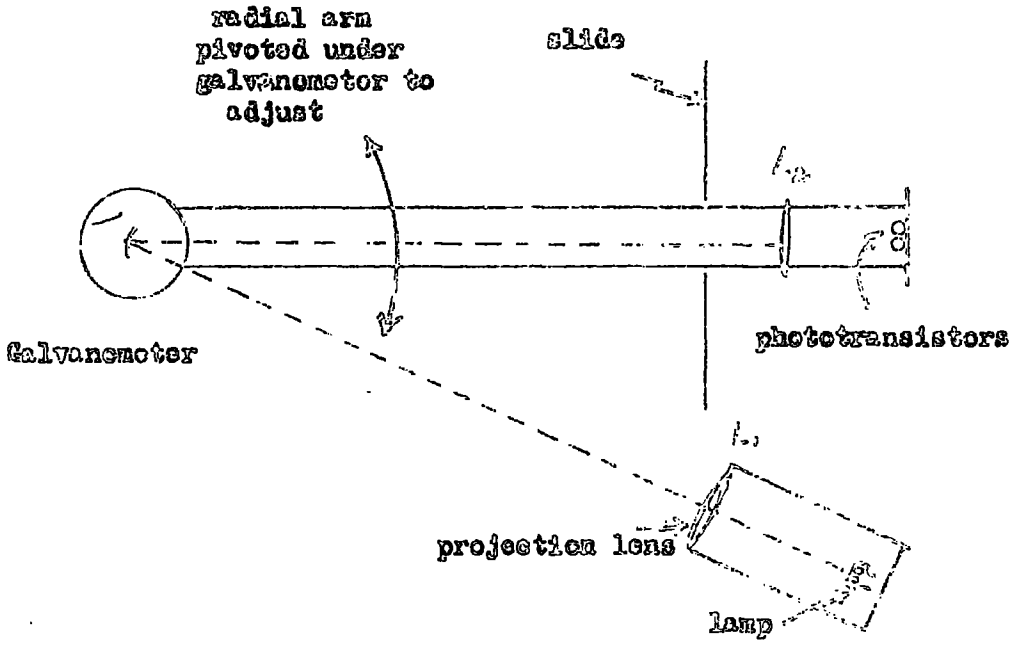

Fig. 3.10a Plan of optical system

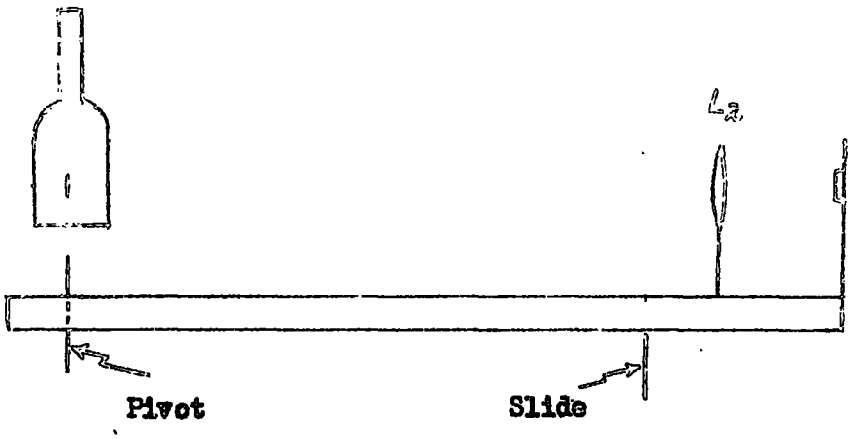

Fig. 3.10b Elevation of optical system

3.5.3. The Optical System

Although the background illumination can be largely balanced out, any change in the distribution of this over the two phototransistors gives rise to a zero drift. Thus fluctuations in position of objects in the room can affect the stability of i_1. Fundamentally the problem is to arrange a large signal to noise ratio at the phototransistors, which implies that the background intensity be much less than that of the spot.

This is achieved by the use of an efficient projection system (figure 3.10) which is conventional except for the lens L_2. Since the sensitive area of a phototransistor is small considerable increase in signal to noise ratio can be obtained by converging the spot onto the sensitive area, by L_2. In addition a box covers the galvanometer system, open only at the end near the scales, limiting the general intensity of ambient light.

The Sensitivity of the Pick-off system.

The output current from a phototransistor depends on the total flux of light incident on the sensitive area. The principle used to detect spot movement is to arrange the edge of the spot to sweep across the light-sensitive areas, to expose more of one and less of the other.

The output current of an OCP71 as a straight edge is moved across it is shown in figure 3.11. It will be seen that the most sensitive

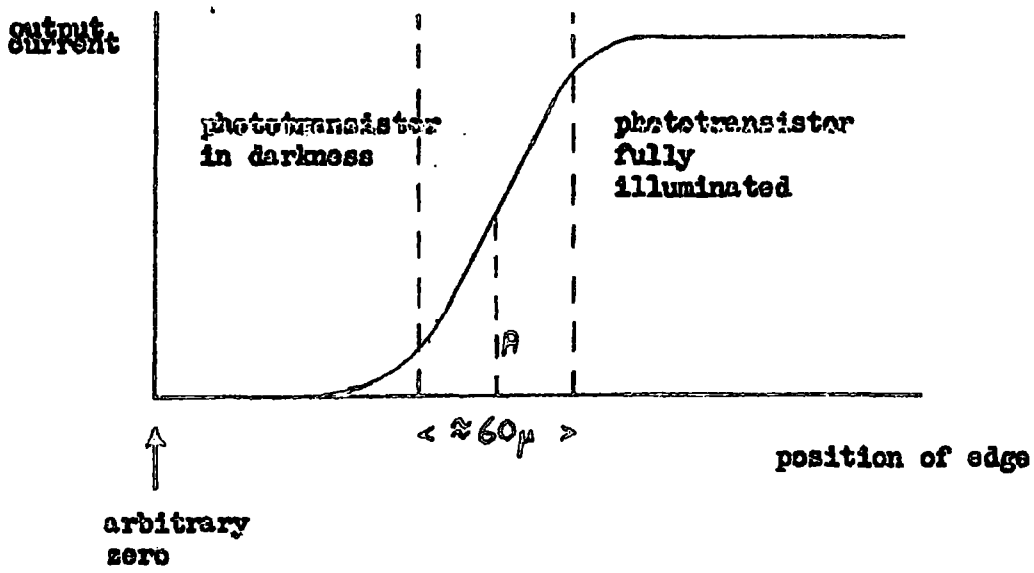

Fig. 3.11 The movement of a straight edge over a phototransistor

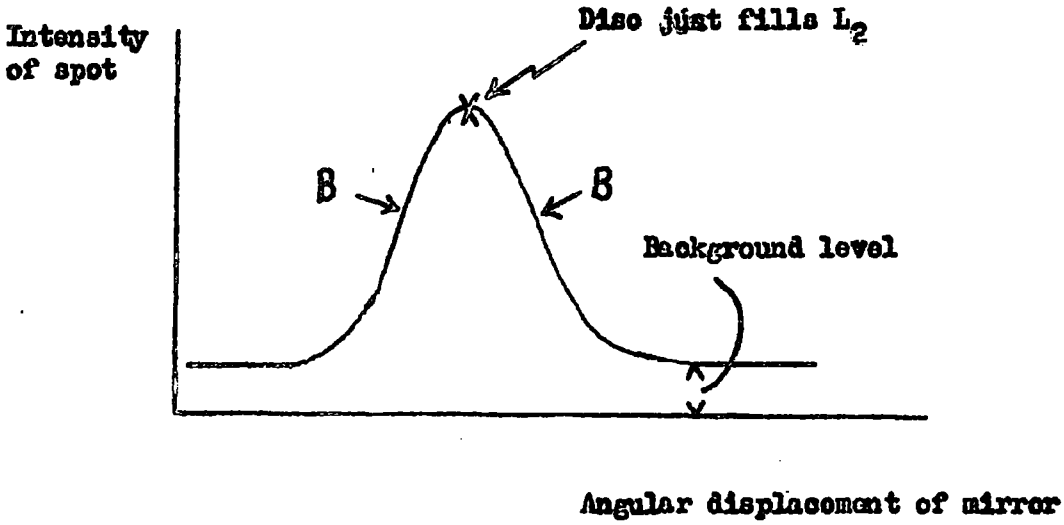

Fig. 3.12 The intensity of the spot impinging of the phototransistors as the disc of light moves across L_2

region for the spot edge to lie is at A. Thus maximum sensitivity is obtained by arranging the spot diameter to be the distance between the positions, A, of the two phototransistors. This is achieved by suitable adjustment of the position of L_2 : an adjustment which is found to critically control the sensitivity of the system.

It will be realised that the focussing of the spot onto the phototransistors by L_2, is accompanied by a reduction in the movement of the spot, for a given mirror rotation, by a factor of m, where m is the linear magnification introduced by L_2. However, it leads to an increase in the intensity of the spot by a factor of $\frac{1}{m^2}$ so that the change of light flux incident on the phototransistor for a given rotation of the mirror increases as spot size is reduced, improving the sensitivity of the system. Hence the phototransistors were placed as close together as possible.

As the galvanometer mirror rotates, a disc of light, the image of L_1, moves across L_2. The intensity of the spot impinging on the phototransistors is then dependent on the fraction of this disc striking L_2. Thus the rotation of the mirror has been translated into modulation of the intensity of the spot as shown diagrammatically in figure 3.12. It will be seen that the greatest sensitivity of this translation process occurs in regions, B. However, the disc of light only half fills L_2 in this region, giving a decrease in intensity of the spot by a factor of about $\frac{1}{2}$. Since the sensitivity for actual movement of the spot over the phototransistors is dependent on this intensity, it

is necessary to find a compromise. Thus the position and misalignment of L_2 is adjusted from optimum sensitivity.

Variation of i_1 may be achieved by moving the phototransistors along the galvanometer scale. The adjustment of L_2 in relation to the galvanometer mirror and the phototransistors is then retained by mounting L_2 and the transistors on an arm (figure 3.10) pivoted directly below the axis of the galvanometer suspension. Rotation of this arm provides a simple means of adjusting i_1 to the required value.

3.5.4 The Accuracy of Stabilisation

No variations of i_1 are observable on the galvanometer scale. Assuming this may be read to within $\pm$ .2 mm. the accuracy for a typical deflection of 20 cms. is therefore better than $\pm$ .1%.

The output current of the difference amplifier is a measure of position of the spot over about .2 mm. of the scale. With the meter, G, used, a variation in i_1 of $\pm$ .001% could be detected. However, there was a drift of i_1 attributed to the decreasing emissive power of the filament. If use is made of RV4 to retain the control point at the zero of the meter G, this drift may be easily held to within $\pm$ .02% of i_1. This may thus be regarded as the overall accuracy of the system.

The current emitted into the gap is measured as the initial gap current, i_{20}. This degree of stabilisation of i_1 should, by consideration of the variation of i_{20} as a function of i_1, correspond to a stabilisation of i_{20} to within $\pm$ .05%. However, certain fluctuations and drifts of i_{20} have been observed despite this stabilisation of i_1.

These will be discussed in later chapters, where they are interpreted as the result of a variation in conditions in the interelectrode gap rather than a variation in the current flow through the holes. Thus it is likely that stabilisation of i_1, has resulted in a stabilisation of the current emitted from the holes, but variation of the drift field in the gap alters the fraction of this current which reaches the collecting electrode, forming i_{20}.

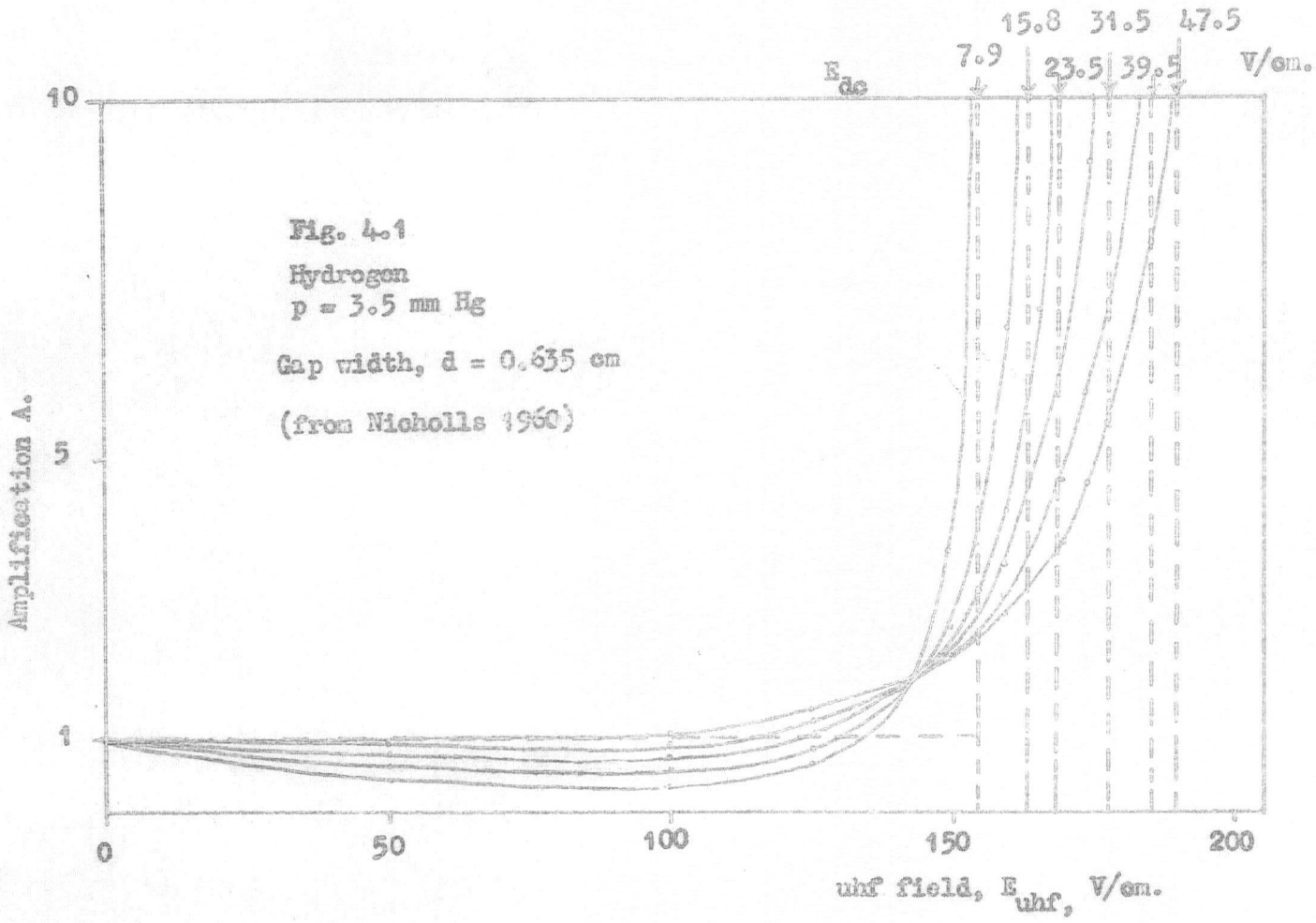

Fig. 4.1

Hydrogen
p = 3.5 mm Hg

Gap width, d = 0.635 cm

(from Nicholls 1960)

CHAPTER 4

EXPERIMENTAL MEASUREMENTS OF AMPLIFICATION

4.1 The method of measurement

When the filament current has stabilised, a current (i_{20}) flows between the electrodes under drift field only and is measured by the galvanometer G_2 (figure 3.4). This current is defined as the initial gap current. The u.h.f. field is then applied gradually (since abrupt switching of the field often causes breakdown) when there is in general, a corresponding change in the current reaching the collecting electrode, i_2.

The amplification, A, is given by

$$A = \frac{i_2}{i_{20}}$$

and is unity for zero u.h.f. field.

Hydrogen was used in all the experiments to be described.

4.2 The preliminary work of Nicholls (1960)

This work was carried out without stabilisation of i_1 to the extent of later measurements, and in general the calibration of the various instruments was only approximate.

However, several curves of Amplification against u.h.f. field, E_{uhf}, at various drift fields and gas pressures were obtained for hydrogen. Figure 4.1 is a typical curve. It will be observed that, for a given drift field E_{dc}, the curve initially falls and then rises as breakdown is approached. The vertical lines on the right of the figure represent experimentally determined breakdown field values.

The amplification curves were found to be asymptotic to these lines.

This work firmly establishes the presence of an initial drop in the amplification curve and a reduction in this drop with increased drift field. Further the rapid rise of amplification to breakdown is established and has been considered to be the result of collision ionization.

4.3 Further Amplification Measurements

Following this work of Nicholls an attempt has been made to make more accurate measurements of amplification, with stabilisation of emitted current.

4.3.1 Precautions taken

It was found that the initial gap current, i_{20}, showed variation, despite the stabilisation of the total current emitted by the filament and incident on the back of the emitted electrode, i_1. These variations were of two types:-

a) A slow decrease over periods of days.

b) An apparent rise, followed by a decay (of time constant 1.5 to 2.0 minutes) after breakdown or large gas amplification.

An analysis of these effects and their possible cause will be attempted in later chapters.

To reduce as far as possible the effects of these variations on measurement of electron amplification, experiments were carried out

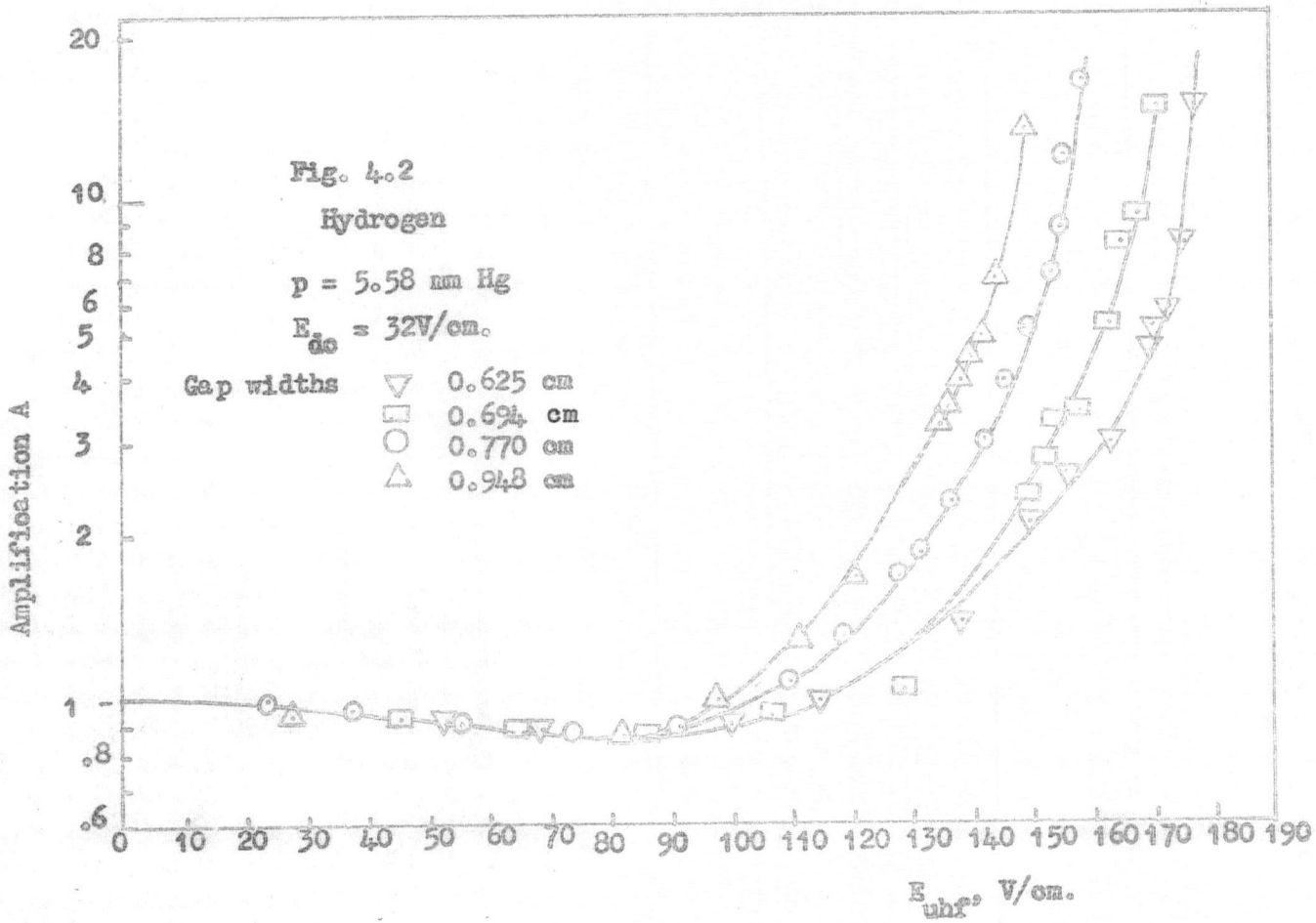
Fig. 4.2
Hydrogen
p = 5.58 mm Hg
E_{dc} = 32V/cm.
Gap widths
0.625 cm
0.694 cm
0.770 cm
0.948 cm
Amplification A
20
10
8
6
5
4
3
2
1
.8
.6
0 10 20 30 40 50 60 70 80 90 100 110 120 130 140 150 160 170 180 190
E_{uhf}, V/cm.

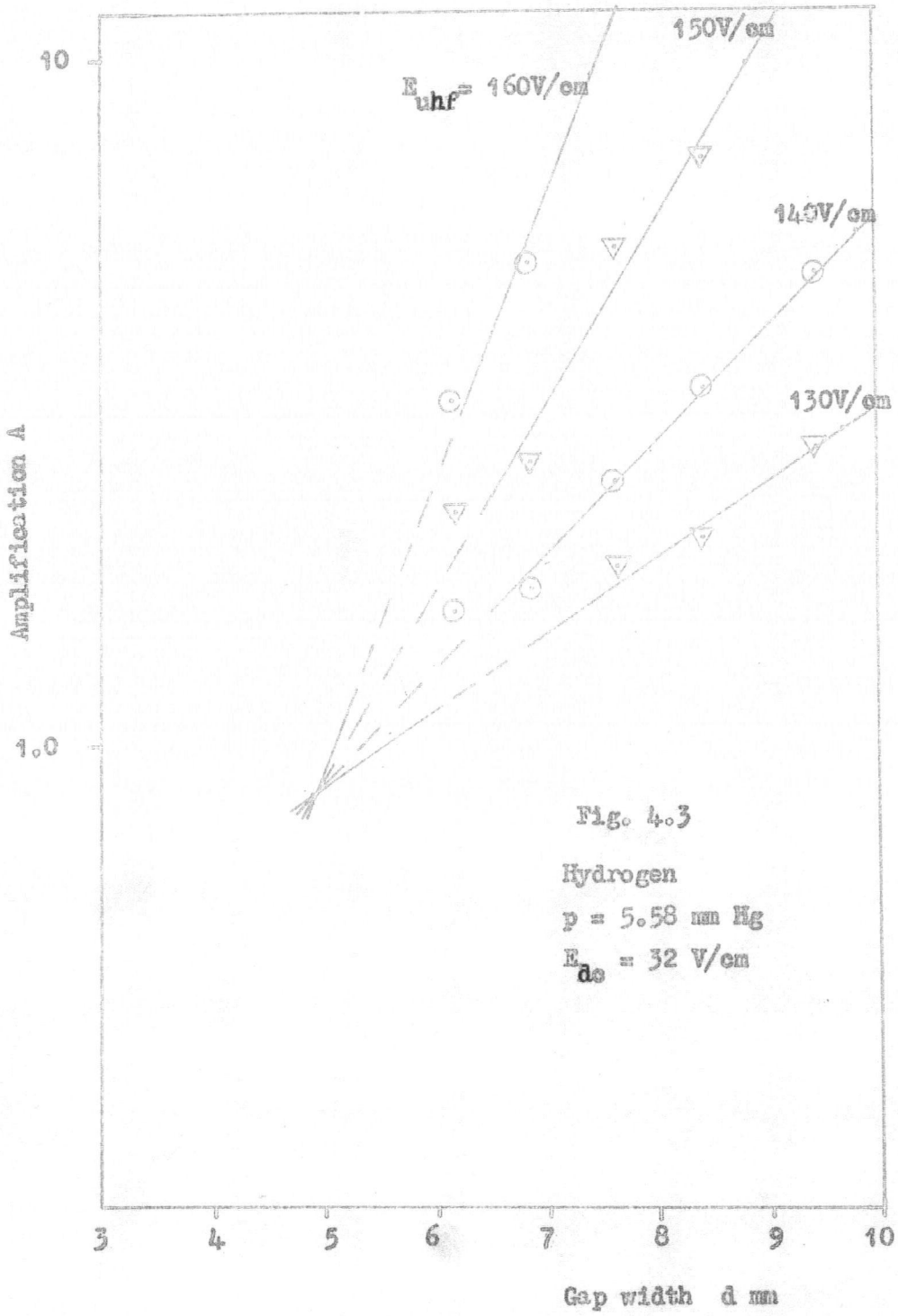

Fig. 4.3

Hydrogen

p = 5.58 mm Hg

E_{dc} = 32 V/cm

in which i_{20} was measured before and after an amplification measurement. Its value at the time of the experiment was then determined by interpolation.

To bring to light any time dependency the points for any given amplification curve were measured at random intervals of time and in random order. The distribution of points on the plot is then an indication of any time dependency. The more randomly distributed they are about the curve the more likelihood of there being some time dependent factor present. In fact their distribution gave some indication of such a factor but this was by no means conclusive.

4.3.2 Results

By this technique a series of plots of amplification, A, as a function of u.h.f. field, E_{uhf}, were obtained for a pressure of 5.58 mm Hg. of hydrogen with a drift field of 32 V/cm, and a range of gap widths from .625 cms to .948 cms. These are shown in figure 4.2.

It will be recalled that measurements of amplification as a function of gap-width at constant ionizing field, corresponds closely to the method used in the measurement of Townsends first ionization coefficient, α. Plots of amplification against gap-width with E_{uhf} as parameter are shown in figure 4.3. These curves suggest that for a given u.h.f. field, the amplification is an exponential function of gap-width of the form:

$$A = A_o \epsilon^{(\zeta d + b)} = A_o' \epsilon^{\zeta d}$$

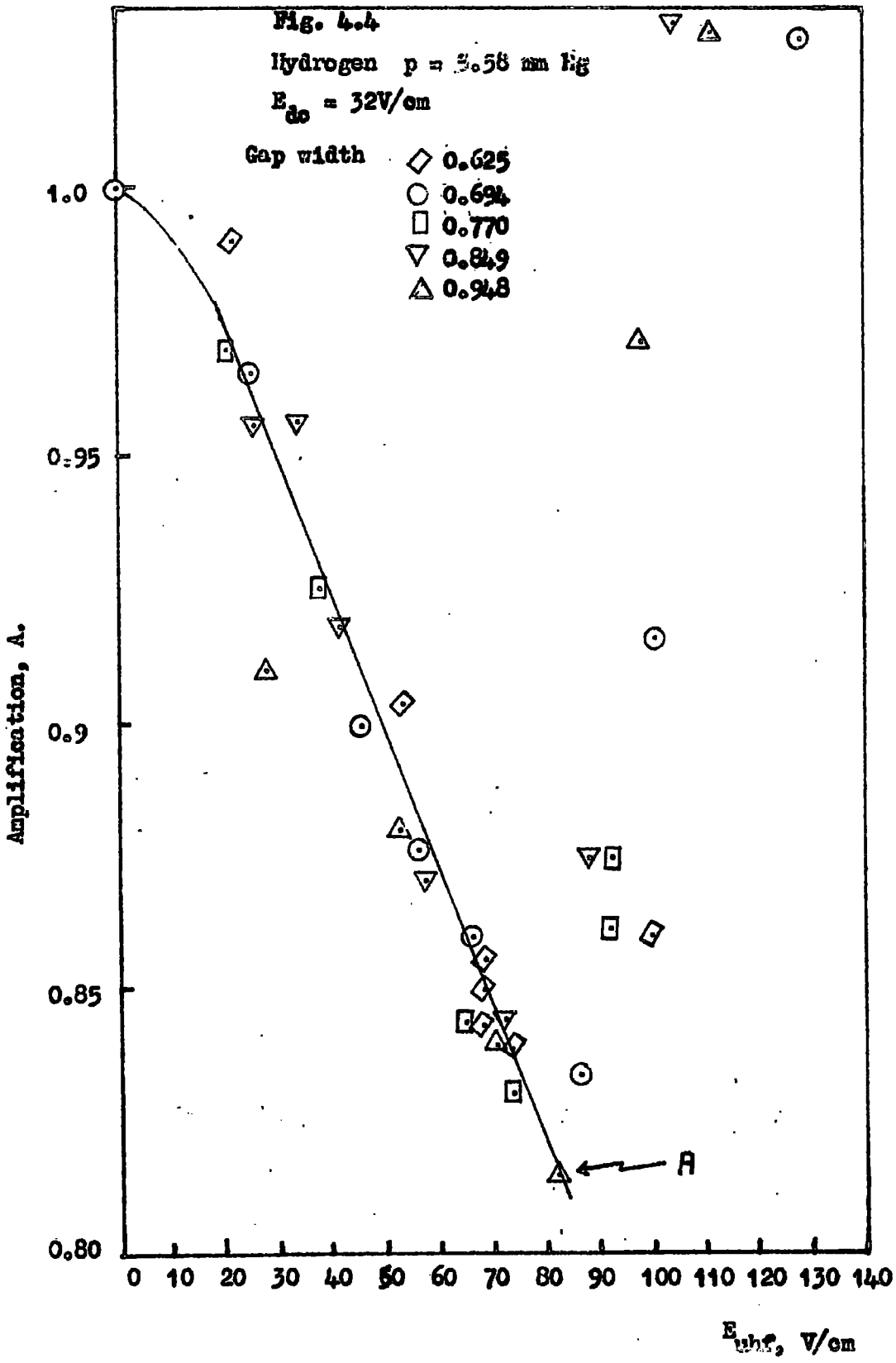
Fig. 4.4
Hydrogen p = 3.58 mm Hg
E_{dc} = 32V/cm
Gap width
0.625
0.694
0.770
0.849
0.948
1.0
0.95
0.9
0.85
0.80
Amplification, A.
A
0 10 20 30 40 50 60 70 80 90 100 110 120 130 140
E_{rhf}, V/cm

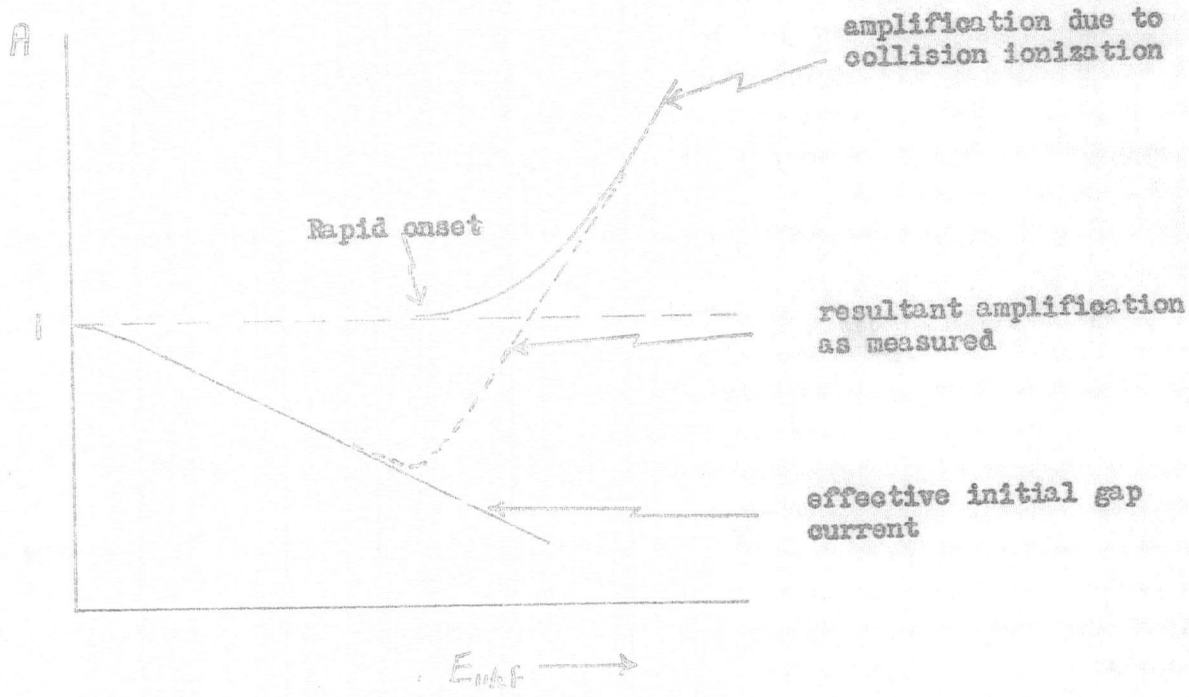
A
amplification due to
collision ionization
Rapid onset
resultant amplification
as measured
effective initial gap
current
E with t

Fig. 4.5

where A_o, A_o' and b are constants independent of E_{uhf}

($A_o = .84$, $b = .50$ cms and $A_o' = A_o \epsilon^b$).

This is similar to the equation, $A = A_o \epsilon^{\alpha d}$, derived by Townsend for an electron avalanche in a unidirectional field only.

However, extrapolation of these curves does not go through unity. Regarding the initial drop of the amplification curve as a progressive decrease in the fraction of emitted electrons crossing the gap, it follows that effectively the stream of initial electrons crossing the gap and thus the effective initial current is less the higher E_{uhf}. Under such conditions these curves would be expected to cross the axis at a value of A somewhat below unity. Some attempt to correct for this decrease in the effective initial current, will be discussed in detail in a later chapter.

Figure 4.4 shows an enlarged plot of the initial drop of the A-E_{uhf} curves of figure 4.1. From this it may be concluded that the initial drop is independent of gap-width. Further the sudden break in the curve at point A suggests that the onset of collision ionization is well defined (figure 4.5).

The results of these measurements indicate that for low electron energies ($A \approx 1$) the amplification is independent of the injected current and thus of the initial gap current, i_{2o}, but for higher energies the amplification is found to increase with increasing i_{2o}. The range of initial currents was from 10^{-10}A to 2×10^{-9}A. There is uncertainty as to the precise cause of this. It would be expected that the charge densities were too small for space charge to control

the electron flow appreciably. However, there may be some effect associated with the flow of electrons from the holes into the larger concentrations of ions and electrons which are in the inter-electrode gap at higher amplifications. Further there may be an effect due to polarization of the electrode surfaces. This will be investigated in a later chapter.

The measurements described here were found to be subject to several long time constant phenomena and certain instabilities. On investigation, these appeared to be associated with the charging and discharging of an insulating film on the electrodes. Hence this series of experiments was terminated pending a full investigation of this phenomenon, which will be dealt with, in detail, in the later part of this thesis. It will suffice, at this stage, to point out that this work has thrown considerable doubt on the effective value of the unidirectional field in the experiments described in this chapter. For example, in the curve of figure 4.2 which corresponds to a gap-width of .770 cms, the field is probably the geometrical field of 32 volts per cm over the initial region, but the breakdown stress reveals that this reduces to about 20 volts per cm at high amplifications. Thus, this variation must be removed before reliable amplification measurements may be made. Attempts to remove this film have not been completely successful.

CHAPTER 5

A THEORETICAL STUDY OF ELECTRON FLOW IN THE INTERELECTRODE GAP, IN THE ABSENCE OF IONIZATION

5.1 Introduction

In the results described in the previous chapter, it was observed that there was an initial drop in the amplification - E_{uhf} curves (figure 4.2). From the expanded plot of figure 4.4 it appears that this drop is independent of gap width. Previous work (Nicholls, 1960) has shown that this drop is less for larger drift fields. Present work has confirmed this. Further it is expected that no ionization occurs in this region.

In the present chapter some explanation will be given for this drop, in terms of variations in the electron flow pattern in the gap.

Electrons moving in the gap are acted upon by both u.h.f. and drift fields. Since the u.h.f. field is predominant in supplying the electron energy, their random velocity is important as well as their drift velocity. Hence the flow is one in which diffusion and drift play comparable parts.

Of a given electron stream entering the gap, the fraction reaching the far electrode will be reduced by an increase in random velocity, which may account for the fall in gap current when the u.h.f. field is increased. Nicholls, 1960, has considered a hypothetical case of a parallel plate gap of infinite extent in which there is a uniform flow of injected electrons across the emitting electrode. He deduced the relation between the electron concentration, n, at some point, x, y, z,

in the gap and that over the plane of the emitting electrode ($z = 0$), n_o, as

$$n = n_o \frac{(\epsilon^{\mu/D.E_{dc}.z} - \epsilon^{\mu/D.E_{dc}.d})}{1 - \epsilon^{\mu/D.E_{dc}.d}} \qquad \ldots\ldots\ldots 5.1$$

where μ/D is the ratio of mobility to diffusion coefficient for electrons at the energy of those in the gap. From this he concluded that, in the absence of ionization,

$$A = \frac{i_2}{i_{20}} = \frac{\mu}{\mu_o} \qquad \ldots\ldots\ldots 5.2$$

where μ is the mobility when the u.h.f. field is applied (and the gap current is i_2) and μ_o is that under drift field only (when the initial gap current i_{20} flows).

Values calculated from this equation differ from the experimental ones by a factor of 2, but do describe the general trend.

In the following sections the existence of descrete sources over the emitting electrode and the dimensions of the electrodes will be taken into account.

5.2 The Physical Picture of Electron Flow

The emitting electrode may be regarded as a large electron sink with small electron sources distributed, largely at random over the electrode surface. The proximity of source and sink suggests that a considerable flow of electrons from source to sink must take place, without the electrons having a very large excursion in the gap.

The electron cloud enters from a hole by a mechanism involving both diffusion and drift. In the absence of any large concentration

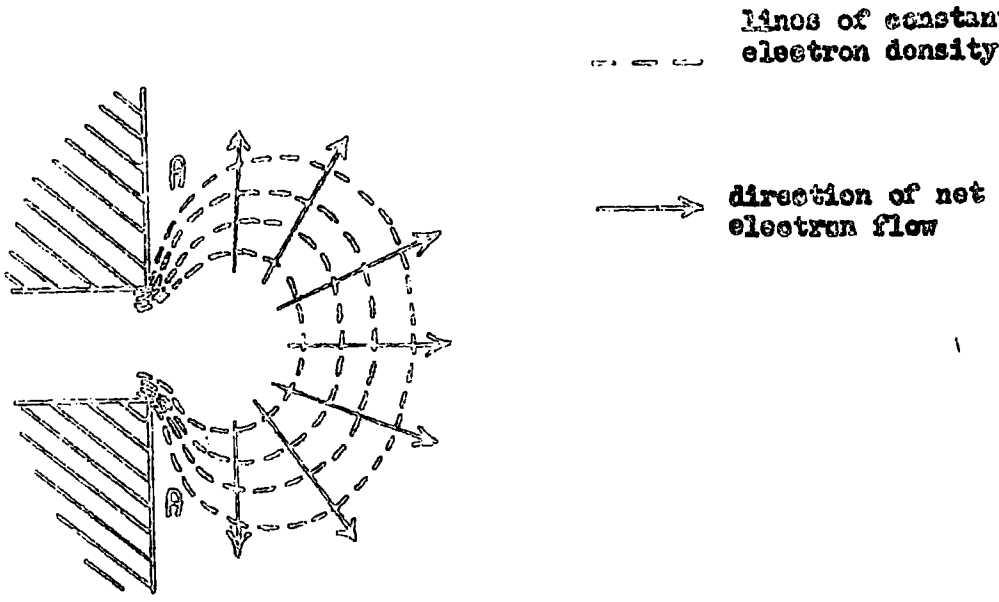

Fig. 5.1 Diffusive flow of electrons from a hole.

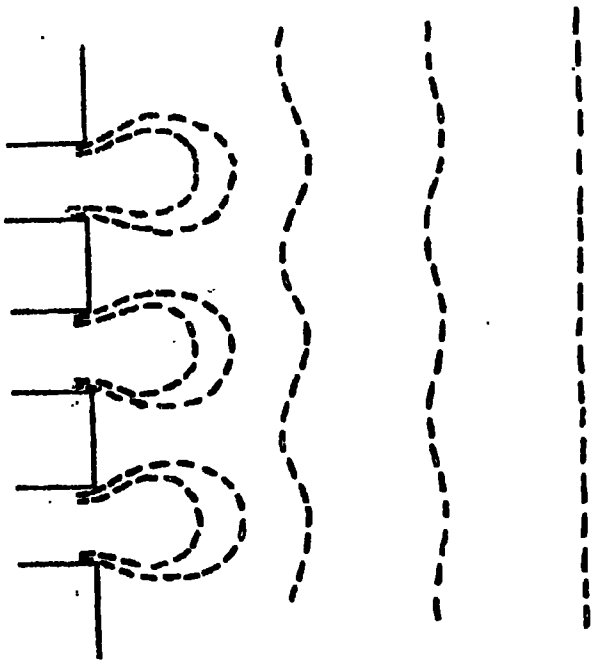

Fig. 5.2 The electron concentration pattern.

of electrons in the gap (i.e. in the absence of ionization), the net diffusive flow will be directed outwards from the hole in all directions (figure 5.1). The presence of the sink is expected to give a larger concentration gradient in region A (figure 5.1) so that larger electron flow may be expected in this region. This implies a large radial current flow, most of which is lost to the boundaries.

The drift field tends to draw the electron cloud away from the surface and thus increases the current flowing into the gap itself. This, therefore modifies the concentration pattern round the hole by displacing it in the field direction, as shown in figure 5.2.

From figure 5.2, it will be observed that there are concentrations of electrons opposite the holes, but between the holes the electron density falls. Thus the electron distribution is expected to be far from uniform over the region close to the electrode surface. However, at further distances from the electrode, the electron concentration may be expected to become, as a consequence of lateral diffusion, more and more uniform over a plane parallel to the electrode surface.

In the work that follows it will be assumed that the holes behave as an assembly of point sources distributed over the conducting electrode.

5.3 Solution of the equation of continuity for Point Sources over the Emitting Electrode.

In the steady state the equation of continuity for a continuous stream of electrons moving under a drift field, E_{dc}, directed along the z-axis is (in the absence of ionization) (Townsend, 1925, Pidduck, 1925)

$$\nabla^2 n = 2\lambda \frac{\partial n}{\partial z} \qquad \ldots\ldots 5.3$$

where n represents the electron density at the point, x, y, z, and $2\lambda = \frac{\mu E_{dc}}{D}$ for the case when the electron energy at the point x, y, z is such that the mobility is μ and the diffusion coefficient D. In the present experiment λ is about 20 cm^{-1}.

On entering the gap, emitted electrons will, in general, take a finite time to gain their equilibrium energy (Compton, 1923, Compton and Langmuir, 1930). In the present case it is likely that there is field penetration into the holes so that the fraction of this time, during which electrons are in the gap itself, may be expected to be small. It will therefore be assumed that the time taken for an electron to gain its equilibrium energy on entering the gap is small compared to its lifetime in the gap. The electron energy and hence μ, D and λ, are then independent of gap position, and can be regarded as constants dependent only on the energy supplied by the combined drift and u.h.f. fields.

Huxley, 1940, has applied this to derive an expression for the electron density distribution due to a point source on a conducting plane, emitting into a region of infinite extent. Using an infinite

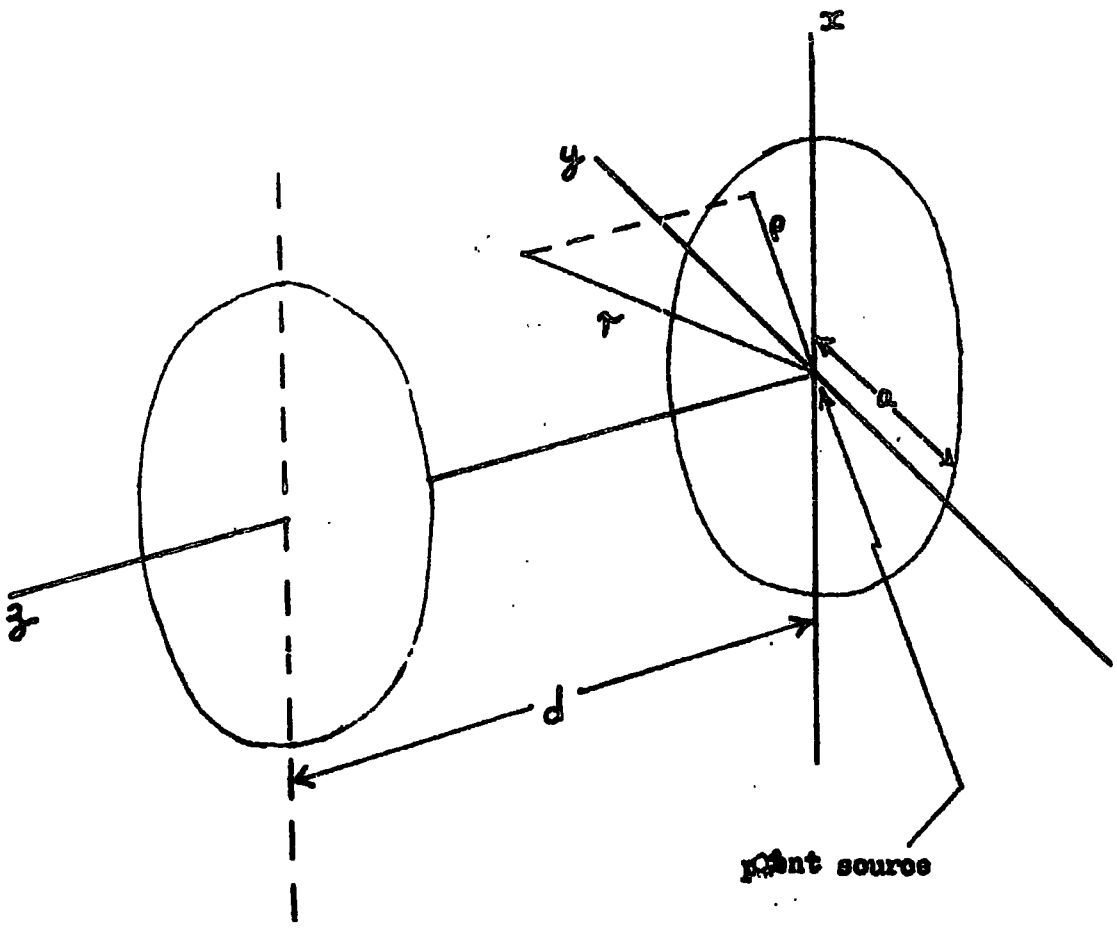

Fig. 5.3

number of these point sources distributed along the z-axis, he derived the electron density distribution for a point source at the origin (figure 5.3) and in the surface of one electrode of a parallel plate gap, with the condition that n = 0 over the electrode surfaces, as the infinite series,

$$n = B\,\epsilon^{\lambda z}\left[\frac{z}{r}\frac{d}{dr}\left(\frac{\epsilon^{-\lambda r}}{r}\right) + \frac{(z-2d)}{r_1}\frac{d}{dr_1}\left(\frac{\epsilon^{-\lambda r_1}}{r_1}\right) + \frac{(z+2d)}{r_2}\frac{d}{dr_2}\left(\frac{\epsilon^{-\lambda r_2}}{r_2}\right) + \frac{(z-4d)}{r_3}\frac{d}{dr_3}\left(\frac{\epsilon^{-\lambda r_3}}{r_3}\right) + \ldots\ldots\right] \quad \ldots\ldots 5.4$$

where,

$$r^2 = \rho^2 + z^2;\ r_1^{\,2} = \rho^2 + (z-2d)^2;\ r_2^{\,2} = \rho^2 + (z+2d)^2$$
$$r_3^{\,2} = \rho^2 + (z-4d)^2 \text{ etc.} \quad \ldots\ldots 5.4a$$
$$\rho^2 = x^2 + y^2$$

and B is an integration constant, representing the strength of the source.

If the electron source is displaced relative to the axis in the x,y plane over the electrode surface, equation 5.4 still holds with a modified r. However, all such equations are solutions of equation 5.3 and thus the solutions are additive. The electron density at any point is then the sum of the separate contribution made by each source. Thus, if we regard the holes in the emitting electrode as aggregate point sources or single point sources and if N is the total number of such point sources, the total electron density at a point x, y, z is:-

$$n = \sum_{k=1}^{N} n_k \qquad \ldots\ldots 5.5$$

The unidirectional current density vector, Γ, at some point, for the case when drift is superimposed upon diffusion is (Varnerin and Brown, 1950):

$$\Gamma = n \cdot \mu E_{dc} - D \cdot \nabla n \qquad \ldots\ldots 5.6$$

Separating the component in the z-direction and expressing n in terms of the individual point sources using equation 5.5, equation 5.6 becomes:

$$\Gamma_z = \sum_{N}' n_k \mu E_{dc} - D \cdot \sum_{N}' \left(\frac{dn_k}{dz} \right)_{x,y,z} \qquad \ldots\ldots 5.7$$

At the surface of the collecting electrode, z = d, n = 0 is the boundary condition so that,

$$\Gamma_z = -D \sum_{N}' \left(\frac{dn_k}{dz} \right)_{x,y,d} \qquad \ldots\ldots 5.8$$

The vector Γ_z incident on an area dx.dy of the electrode surface, makes a contribution to the collected current, i_2, of

$$di_2 = \Gamma_z \cdot dx \cdot dy$$

Thus integrating and introducing Γ_z from equation 5.8 the current flow to the far electrode assembly is

$$i_2 = -D \sum_{N}' \iint_{\substack{\text{over} \\ \text{electrode} \\ \text{surface}}} \left(\frac{\partial n_k}{\partial z} \right)_{x,y,d} dx \cdot dy \qquad \ldots\ldots 5.9$$

Hence, i_2 is the sum of the current densities due to each of the holes considered separately.

Consider a single point source at the origin. The contribution of this source to i_2 is (equation 5.9)

$$\Delta i_2 = -D \iint_{\text{over electrode}} \left(\frac{\partial n}{\partial z}\right)_{x,y,d} dx.dz \qquad \ldots\ldots 5.10$$

Writing this in terms of ρ ($\rho^2 = x^2 + y^2$, see figure 5.3) gives:

$$\Delta i_2 = -D \int_{\rho=0}^{a} \left(\frac{\partial n}{\partial z}\right)_{\rho,d} 2\pi\rho.d\rho \qquad \ldots\ldots 5.11$$

where a is the effective radius of the electrode. Since $r^2 = \rho^2 + d^2$ and d, the gap width, is a constant, $\rho d\rho = rdr$ and equation 5.11may be integrated, using equation 5.4, to give:

$$\Delta i_2 = -4\pi\ B.D.\ \epsilon^{\lambda d}\left[\frac{\epsilon^{-\lambda r_a}}{r_a} + \frac{\epsilon^{-\lambda r_{2a}}}{r_{2a}} + \ldots - \frac{\epsilon^{-\lambda d}}{d} - \frac{\epsilon^{-\lambda 3d}}{3d} - \ldots\ldots\right] \qquad \ldots\ldots 5.12$$

where, suffix 'a' refers toquantities defined in equations 5.4a with $\rho = a$ and $z = d$.

In practice, $\lambda \approx 20\ cm^{-1}$, $d \approx .8$ cms and $a \approx 1.5$ cms, thus

$$\frac{\epsilon^{-\lambda r_a}}{\epsilon^{-\lambda r_{2a}}} \approx \epsilon^{27} ,$$

$$\frac{\epsilon^{-\lambda d}}{\epsilon^{-\lambda 3d}} \approx \epsilon^{28} \quad \text{and} \quad \frac{\epsilon^{-\lambda r_a}}{\epsilon^{-\lambda d}} \approx \epsilon^{-14}$$

Hence, all but the $\frac{\epsilon^{-\lambda d}}{d}$ term of the bracket of equation 5.12 are negligible and

$$\Delta i_2 = \frac{4\pi B.D.}{d} \qquad \ldots\ldots 5.13$$

Since terms envolving a are negligible, it follows that the equation

is not critically dependent on the boundary condition, $\rho = a$, from which these terms originate. Physically this implies that the current density vector decreases rapidly as ρ increases. Thus most of the current flow, is to the central region of the electrode. It is therefore proper to make the approximation that all the holes lie at the centre of the emitting electrode. Thus the sum of equation 5.9 may be evaluated from equation 5.13 to give,

$$i_2 = N.\Delta\, i_2$$

$$= N.4\pi.\ B.D./d$$

$$= B'.\ D/d \qquad \ldots\ldots\ 5.14$$

where, $B' = 4\pi.N.B.$

The diffusion coefficient, D, of equation 5.14 depends on the electron energy, hence i_2 is a function of the u.h.f. field. The amplification, in the absence of ionization, is therefore,

$$A = \frac{i_2}{i_{20}} = \frac{B'D}{B'_o D_o} \qquad \ldots\ldots\ 5.15$$

where the suffix, o, refers to the case when the drift field only is applied.

Equation 5.4 suggests that the integration constant, B, represents the strength of the sources, since it controls the electron density at all points. Thus B' may be expected to depend on the nature of electron flow from the holes.

The arbitrary assumption that the strength of these sources is independent of gap conditions gives $B' = B'_o$ and $A = D/D_o$, leading to

an increase of A with u.h.f. field, whereas experimentally A is found to decrease. This suggests that the effective point source has a strength which decreases as the energy of electrons in the gap increases.

The study of electron flow within the holes has been found intractable. Thus instead of pursuing the consequences of the theory by the evaluation of B' it has been found more satisfactory to consider the subdivision of the electron currents in the gap. If i_e is the total current emitted from the holes, it is lost from the gap by:

a) diffusion back to the emitting electrode; the resultant flow across this boundary being defined as the back diffusion current, i_B.

b) the current collected by the far electrode assembly, i_2, and

c) latteral flow from the gap, which from equations 5.4 and 5.6 may be shown to be negligible.

Hence: $$i_e = i_2 + i_B \qquad \ldots\ldots 5.16$$

A convenient quantity in which to consider the fraction of i_e reaching the far electrode is the gap transmission coefficient, T_g, which is defined by, $i_2 = T_g\, i_e$. This coefficient depends only on gap conditions and will be evaluated independently of the nature of the flow from the holes, provided that emission from them may be regarded as the result of an assembly of point sources.

Using equation 5.16, T_g will be evaluated from $T_g = \dfrac{i_2}{i_2 + i_B}$, which requires calculation of i_B. This may be obtained by an argument

similar to that above by which i_2 is derived.

Following through this argument, putting z = 0 in equation 5.7 gives the z-component of the current density vector over the emitting electrode surface. Further, this surface is an electron sink so that n = 0 over the electrode. Thus

$$\Gamma_z(x,y,0) = -D \sum_{k=1}^{N} \left(\frac{\partial n_k}{\partial z}\right)_{x,y,0} \qquad \ldots\ldots 5.17$$

The current, i_B, may be obtained by integrating this vector over the electrode surface. Assuming again that all the holes may be considered at the centre of the electrode and to have a radius, b, equation 5.17 may be integrated to give,

$$i_B = -D. \sum_{N} \int_{\rho=b}^{\rho=a} \left(\frac{\partial n_k}{\partial z}\right)_{\rho,0} 2\pi\rho d\rho \qquad \ldots\ldots 5.18$$

Evaluating $\frac{\partial n}{\partial z}$ from equation 5.4 and integrating the L.H.S. of equation 5.18 gives:

$$i_B = -2\pi.B.D.N \left[\frac{\epsilon^{-\lambda r}}{r} + \frac{2\epsilon^{-\lambda r_1}}{r_1} + \ldots\right]_{\rho=b}^{\rho=a}$$

$$= -\frac{B'}{2}.D \left[\frac{\epsilon^{-\lambda r_a}}{a} + \frac{2\epsilon^{-\lambda r_{1a}}}{r_{1a}} + \ldots \right.$$

$$\left. - \frac{\epsilon^{-\lambda b}}{b} - \frac{2\epsilon^{-\lambda r_{1b}}}{r_{1b}} - \ldots\ldots\ldots\right] \qquad \ldots\ldots 5.19$$

Where the suffixes a and b refer to quantities defined in equation 5.4a with $\rho = a$, $\rho = b$ respectively and $z = 0$.

As before, $\frac{\epsilon^{-\lambda a}}{a} >> \frac{\epsilon^{-\lambda 1 a}}{r_{1a}}$, $\frac{\epsilon^{-\lambda b}}{b} >> \frac{\epsilon^{-\lambda r_{1b}}}{r_{1b}}$ and $\frac{\epsilon^{-\lambda a}}{a} << \frac{\epsilon^{-\lambda b}}{b}$ etc.

Hence all but the $\frac{\epsilon^{-\lambda b}}{b}$ term of the bracket may be neglected so that,

$$i_B = \frac{B'D}{2}\frac{\epsilon^{-\lambda b}}{b} \qquad \ldots\ldots 5.20$$

From equation 5.16:

$$i_e = i_B + i_2$$

$$= B'D\left[\frac{\epsilon^{-\lambda b}}{2b} + \frac{1}{d}\right] \qquad \ldots\ldots 5.21$$

Hence, the gap transmission factor may be evaluated as:

$$T_g = \frac{i_2}{i_e} = \frac{1/d}{\left(\frac{\epsilon^{-\lambda b}}{2b} + \frac{1}{d}\right)} \qquad \ldots\ldots 5.22$$

Since $\lambda \approx 20\ cm^{-1}$, $b \approx .02$ cms and $d \approx .8$ cms, it follows that $T_g \approx .02$. Thus of the electrons emitted less than 2% cross to the collecting electrode.

Normalising T_g to unity for $\lambda = \lambda_1$, gives

$$T_{gn} = \frac{\frac{d}{2b}\epsilon^{-\lambda_1 b} + 1}{\frac{d}{2b}\epsilon^{-\lambda b} + 1} \qquad \ldots\ldots 5.23$$

the suffix, n, indicating a normalised value. Since $\frac{d}{2b}\epsilon^{-\lambda b} \gg 1$, this may be approximated to

$$T_{gn} \approx \epsilon^{-b(\lambda_1 - \lambda)} \qquad \ldots\ldots 5.23a$$

By definition $T_g = \frac{i_2}{i_e}$, and thus $T_{gn} = \frac{i_2}{i_e} \Big/ \frac{i_{20}}{i_{eo}}$ where i_2 and i_e correspond to $\lambda = \lambda$ and i_{20}, i_{eo} to $\lambda = \lambda_1$. Thus, T_{gn} may be expressed in terms of the amplification, A, defined as $A = \frac{i_2}{i_{20}}$, by

$$T_{gn} = A\frac{i_{eo}}{i_e} \qquad \ldots\ldots 5.24$$

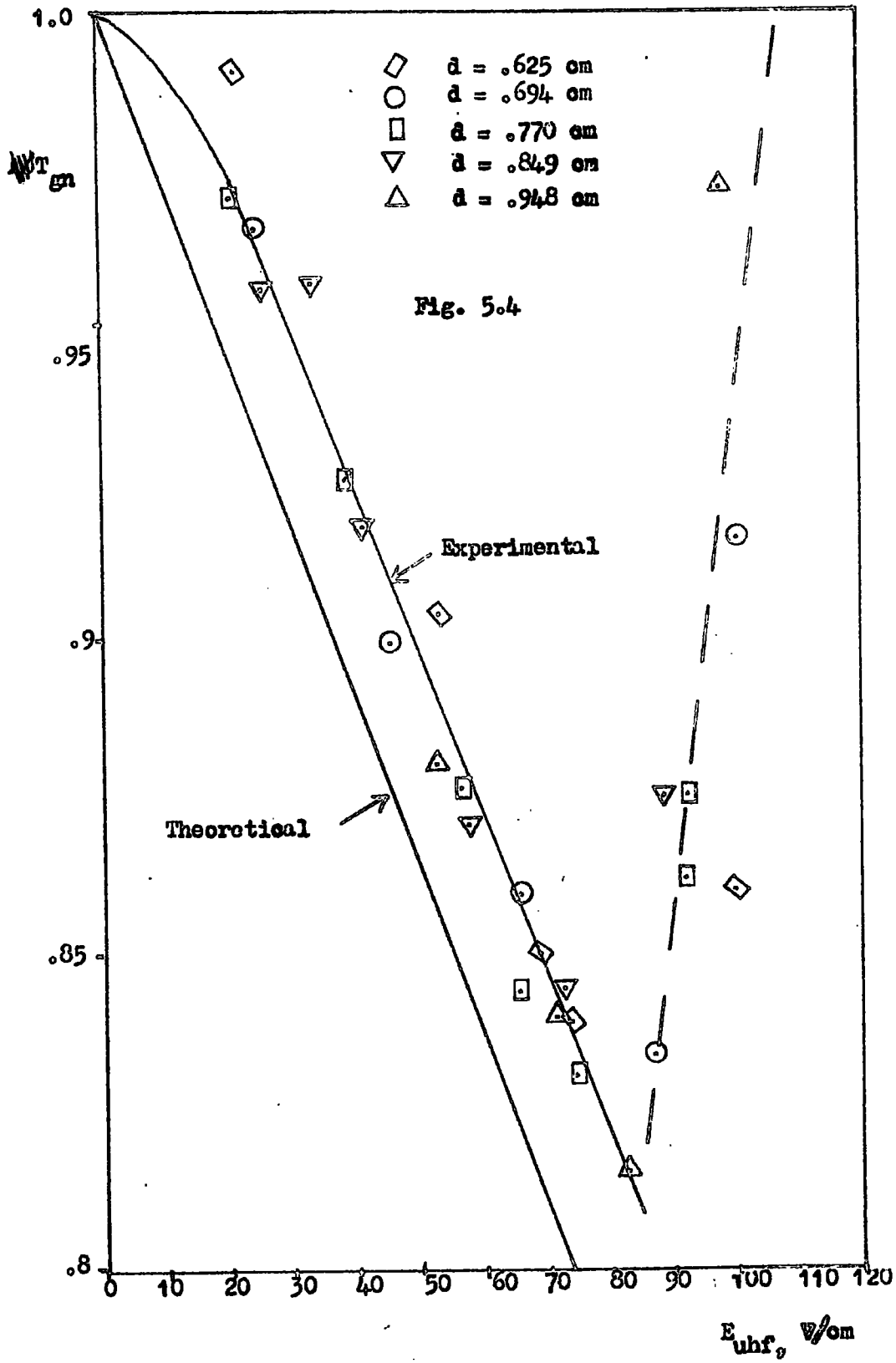
1.0
.95
.9
.85
.8
T_{gn}
d = .625 cm
d = .694 cm
d = .770 cm
d = .849 cm
d = .948 cm
Experimental
Theoretical
0
10
20
30
40
50
60
70
80
90
100
110
120
E_{uhf_g} v/cm

Fig. 5.4

provided λ_1 corresponds to the electron energy under drift field only. Hence, T_{gn} is only equivalent to A if $i_{eo} = i_e$ i.e. the emitted current is a constant. In fact, however, some variation of i_e may be expected due to variations in the electron flow and density patterns in the gap.

It, therefore, becomes necessary to define a hole transmission coefficient, T_H, defined by $i_e = T_H\, i_1$, where i_1 is the measured total current emitted by the filament. Since i_1 is stabilized the normalized hole transmission coefficient is

$$T_{Hn} = \frac{i_e}{i_1} \Big/ \frac{i_{eo}}{i_{1o}} = \frac{i_e}{i_{eo}} \qquad \ldots\ldots 5.25$$

Thus strictly the amplification, as measured is

$$A = T_{Hn} \cdot T_{gn} \qquad \ldots\ldots 5.26$$

It has been pointed out that evaluation of T_H from diffusion and drift theory has not yet been found possible. Thus it is assumed that T_{Hn} is unity i.e. there is no variation of i_e with the energy of electrons in the gap. (This does not imply that B is constant, since B controls the electron density pattern in the gap, not the flow of electrons through the holes). Under these conditions, T_{gn}, as given by equation 5.23, is directly comparable with amplification over the initial part of the A - E_{uhf} curves. Figure 5.4 shows a plot of T_{gn} for the case of Figure 4.4 with the experimental curve superimposed. The calculation of T_{gn} was based on values of $\frac{\mu}{D}$ derived from Hall (1955) and Varnerin and Brown (1950). It will be seen that these curves are in close agreement. The results therefore afford considerable support for the theory.

CHAPTER 6

A THEORETICAL STUDY OF ELECTRON FLOW IN THE INTERELECTRODE GAP, WHEN IONIZATION OCCURS.

In this chapter the theory by which the initial drop of the A-E_{uhf} curves may be explained is extended to a study of the electron flow pattern in the case when ionization occurs. From this study a method of calculating the ionization rate from the amplification curves is suggested.

6.1 The physical picture of electron flow when ionization occurs.

It has been shown in the previous chapter that, as a consequence of the superimposition of diffusion upon drift, the fraction of the emitted current crossing the gap in the absence of ionization is dependent on the u.h.f. field. This suggests that the variation of the current collected by the far electrode, i_2, on applying the u.h.f. field may, in general, be expected to have two components. The first is due to a decrease in the number of injected electrons crossing the gap, as suggested by the preceeding chapter. The second component is due to the onset of collision ionization by this electron stream to give an increase in current to the far electrode. The problem is to separate these components so that the amount of ionization occurring, and thus the ionization rate may be derived.

Following Townsend the simple view, based on the assumption that drift is the predominant transport mechanism (Chapter 2) is that a continuous stream of electrons crosses the gap, ionizing the gas as it flows, to give an exponential increase of current across the

gap. This assumes that the initial electron stream is there independently of the presence of ionization. It may now be seen that as a consequence of diffusion, this is an oversimplified picture. Firstly, the stream of injected electrons crossing the gap is energy dependent, as suggested in the previous chapter. Secondly the onset of ionization changes the electron flow pattern so that the partition of electrons to each electrode is likely to be altered. Thus the presence of ionization itself may be expected to alter the stream of initial electrons, so that the assumption that the stream is present unchanged when ionization occurs is unjustified. Further this implies that the two components of i_2 mentioned above are both dependent on the electron density and flow patterns, and thus are interdependent and not separable.

Thus to estimate the ionization coefficient it is necessary to derive an expression for electron flow when ionization occurs. In the present case positive ions, as well as electrons, contribute to the gap current. Assuming there are no space charge effects, electrons and position ions will move independently of each other. Thus the total charge flow in the gap may be represented as an electron flow pattern with a positive ion flow pattern superimposed upon it. These flow patterns may therefore be derived separately, and the current vectors due to the two types of carriers added to give the net charge flow at any required point in the gap.

6.2 The Electron Density Distribution

When ionization is small itspresence may be regarded as a small perturbation superimposed upon the injected electron density pattern.

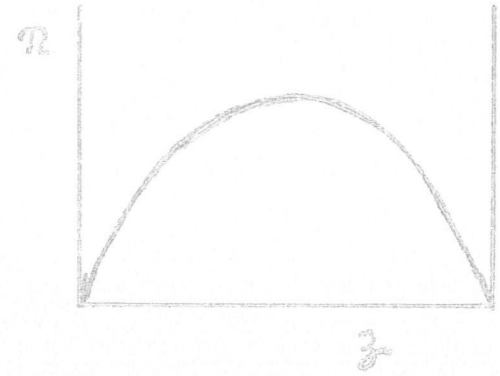

Fig. 6.1

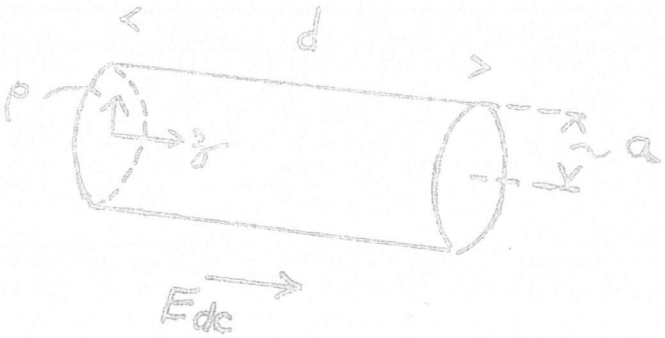

Fig. 6.2

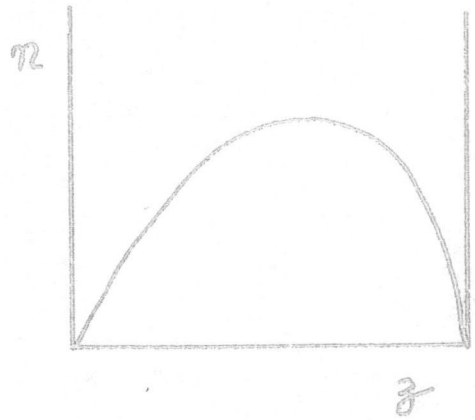

Fig. 6.3

From such a simple picture, an exponential rise of electron density across the gap resulting from collision ionization (c.f. Townsend's treatment of the electron avalanche) is to be expected.

On the other hand, at very high amplifications the predominant electron source is no longer at the emitting electrode but is distributed throughout the gap. As a consequence, the electron density distribution is expected to be similar to that for pure u.h.f. discharges (which is a sine function as shown in figure 6.1) but deformed as a result of drift.

Varnerin and Brown (1950) have analysed the electron density pattern for the present field system under conditions of breakdown and without injected current. They obtained for the cylindrical gap of figure 6.2:

$$n = B.e^{\lambda z}. \sin\left(\frac{\pi}{d} z\right). \quad J_o\,(k_1 \rho) \qquad \ldots\ldots\ 6.1$$

where $k_1 = \frac{2.404}{a}$ and J_o is the zero order bessel function. Here the exponential factor represents a deformation of the simple sine function applicable to pure u.h.f. discharges, to give a density distribution across the gap as shown in figure 6.3.

The presence of injected current might be regarded as a small perturbation of this density pattern so that the density function should approach equation 6.1 at higher amplifications. Hence as ionization increases a change from an exponential density distribution to one of sinusoidal form is to be expected. This concept is further analysed mathematically in the next section.

6.2.1 The Electron Flow Pattern as a Consequence of the Equation of Continuity

The equation of continuity (equation 1.4) for the present case, expresses the scalar electron density in terms of drift, diffusion and ionization (Townsend, 1947) as

$$\nabla^2 . n - 2\lambda \frac{\partial n}{\partial z} + \frac{\psi}{D} . n = 0 \qquad \ldots\ldots 6.2$$

where $2\lambda = \frac{\mu}{D} . E_{dc}$.

Drift is controlled by E_{dc}, which is a vector directed along the z-axis. The drift term is thus asymmetrical in space co-ordinates and is a function of z only. However, this term may be transformed into a symmetrical space function using the transform $n = U . \epsilon^{\lambda z}$, when

$$\nabla^2 . U - \frac{\nu^2}{D} U = 0 \qquad \ldots\ldots 6.3$$

where,

$$\frac{\nu^2}{D} = \lambda^2 - \frac{\psi}{D}$$

The particular solution of this equation, which is applicable to a given set of boundary conditions, is dependent on whether ν is real or unreal and thus on the value of ψ.

By solving the equation of continuity, Varnerin and Brown have derived the condition for breakdown when a small drift field is superimposed upon the u.h.f. field, as

$$\psi . \frac{\Lambda_m^2}{D} = 1 \qquad \ldots\ldots 6.4$$

where the modified diffusion length, Λ_m, is given by

$$\frac{1}{\Lambda_m^2} = \frac{1}{\Lambda^2} + \lambda^2 \qquad \ldots\ldots 6.5$$

The value of ψ given by equation 6.4 corresponds to breakdown and therefore represents the upper limit obtainable in the present experiment, so that the range of ψ is

The gap in real space

The gap in U-space

Fig. 6.4 The exponential deformation of space.

$$0 < \psi < D\left\{\frac{1}{\Lambda^2} + \lambda^2\right\} \qquad \ldots\ldots 6.6$$

Remembering that $\frac{\nu^2}{D} = \lambda^2 - \frac{\psi}{D}$, the range of ν^2 is then:

$$\lambda_1^2 > \frac{\nu^2}{D} > -\frac{1}{\Lambda^2} \qquad \ldots\ldots 6.7$$

where λ_1 corresponds to $E_{uhf} = 0$, when the initial gap current is flowing.

Over part of this range $\nu^2 < 0$ so that ν is unreal. Then putting $\frac{\nu}{D}_1 = \frac{\nu'}{jD} = \sqrt{\left\{\frac{\psi}{D} - \lambda\right\}}$ equation 6.3 becomes:

$$\nabla^2 U + \frac{\nu_1^2}{D} U = 0 \qquad \ldots\ldots 6.8$$

Solutionsof equation 6.8 ($\nu^2 < 0$) are of sinusoidal form, whereas solutions of equation 6.3, $\nu^2 > 0$, are exponential functions. Thus $\nu = 0$ represents point at which the form of the density distribution function changes.

The significance of this change in terms of the flow pattern may be seen if equation 6.3 is written:

$$D.\nabla^2 U - D\lambda^2 U + \psi U = 0 \qquad \ldots\ldots 6.9$$

Here, U is related to the electron density, n, by the relation $n = U\epsilon^{\lambda z}$. Thus U represents the electron density in an exponentially deformed space which will be referred to as U-space, figure 6.4. The three terms of equation 6.9 may then be seen to represent, in U-space, the rate at which electrons diffuse into a region, the rate of loss by drift and the rate of generation by ionization respectively.

Here drift is represented as a loss of electrons in the volume of the gas, and may be considered in a similar manner to recombination i.e. as the presence of a partial electron sink distributed over the gap. Thus the scalar coefficient, $D\lambda^2$, represents the loss rate due to drift

per individual electron.

In place of ψ, which is the net volume generation rate for electrons in real space (i.e. the ionization rate less the attachment and recombination rates), we introduce ν_1^2 to have similar properties in U-space. In U-space there is the drift rate, as well as the attachment and recombination rates, to be subtracted from the ionization rate to give the net volume generation rate. Thus,

$$\nu_1^2 = \psi - D\lambda^2$$

and may be positive or negative according to the relative values of ionization and drift rates. In the steady state these electrons must be removed by diffusion. Thus the electron density pattern in U-space is essentially diffusion controlled, so that the theory of diffusion controlled discharges may be applied to discharges in U-space.

A similar conclusion may be obtained by comparing the equation of continuity for electrons in U-space (equation 6.8), with that for real space in the absence of a drift field (Herlin and Brown, 1948),

$$\nabla^2 n + \frac{\psi}{D} \cdot n = 0$$

For $\nu_1 = 0$, $\psi = D\lambda^2$ and the rate of loss of electrons by drift is equal to the rate of gain by ionization so that the diffusion rate from any given point is zero ($D \cdot \nabla^2 U = 0$). For lower values of ψ ($\nu_1^2 \leq 0$) the amount of ionization is not sufficient to balance the flow rate, and diffusion thus maintains the balance by providing a net rate of flow into the region. If, however, ψ increases so that $\nu_1^2 > 0$, diffusion is relied upon to remove the excess electrons so that diffusion must be outwards from the region. For a net inward flow to any point,

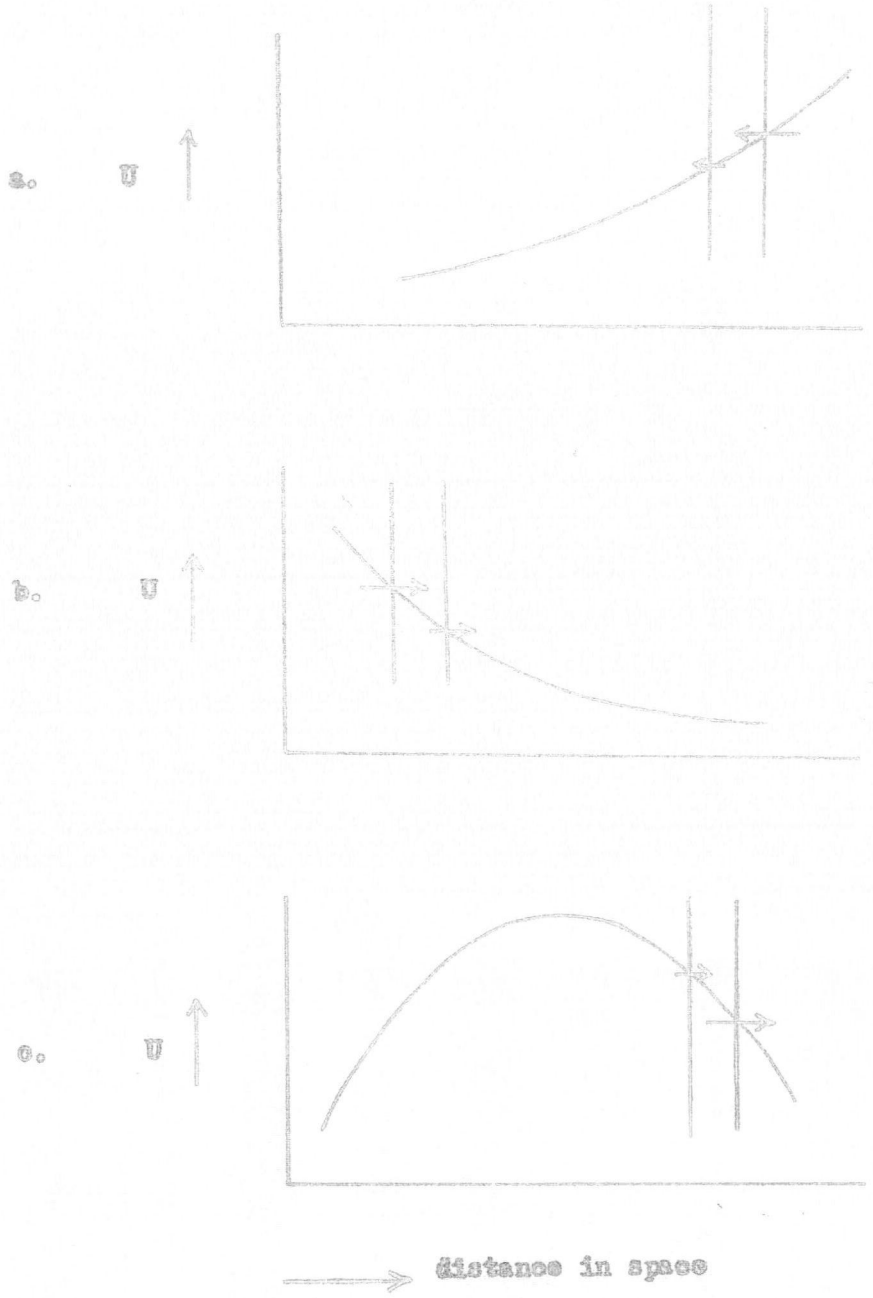

Fig. 6.5 Arrows represent diffusion rates across boundaries indicated. Their lengths are an indication of their magnitude.

the gradient of U must increase with U i.e. U must form a concave surface in space. Thus the equation of continuity may be solved for $\nu_1^2 < 0$ ($\nu^2 > 0$), if U is an exponential function of space co-ordinates (figure 6.5 a and b).

On the other hand for $\nu_1^2 > 0$, there must be a net outward flow of electrons and U must be a convex surface to satisfy the condition of continuity (figure 6.5c). Positive parts of sinusoidal functions satisfy this condition, exponential functions do not. Thus $\nu_1 = 0$ represents a basic change in the density pattern in the gap.

So far attempts to obtain satisfactory values of the electron distribution pattern for $\nu_1^2 > 0$ ($\nu^2 < 0$) have not been successful. The following sections are therefore confined to a discussion of the case $\nu_1^2 < 0$ ($\nu^2 > 0$) for which quantitative estimates of the electron distribution pattern are made.

6.3 Calculation of the Electron Flow Pattern for $\nu^2 > 0$

This will be derived along similar lines to the case in the absence of ionization and follows Huxley's method of solution of the equation of continuity.

As already seen this equation (equation 6.2) may be transformed using $n = e^{\lambda z}.U$, into the equation

$$\nabla^2 U = \frac{\nu^2}{D} U. \qquad \ldots\ldots 6.3$$

Huxley operated in the same way on the equation of continuity, applicable when there is no ionization (equation 5.3), to obtain

$$\nabla^2 U = \lambda^2 U \qquad \ldots\ldots 6.10$$

Comparing equations 6.3 and 6.10 shows that any solution of 6.10 will be a solution of 6.3 provided λ^2 be replaced by ℓ^2, where $\ell^2 = \frac{\nu^2}{D}$.

Hence a solution may be obtained from equation 5.4, to give the electron density distribution due to a point source on one electrode of a parallel plate gap as,

$$n = B\,\epsilon^{\lambda z}\left[\frac{z}{r}\,\frac{d}{dr}\left(\frac{\epsilon^{-\ell r}}{r}\right) + \frac{z-2d}{r_1}\,\frac{d}{dr_1}\left(\frac{\epsilon^{-\ell r_1}}{r_1}\right) + \frac{z+2d}{r_2}\cdot\frac{d}{dr_2}\left(\frac{\epsilon^{-\ell r_2}}{r_2}\right) + \frac{z-4d}{r_3}\cdot\frac{d}{dr_3}\left(\frac{\epsilon^{-\ell r_3}}{r_3}\right) + \ldots\ldots + \ldots\ldots\right] \qquad \ldots\ldots 6.11$$

The electron current flowing to the collecting electrode, i_{2-}, and the electron back diffusioncurrent, i_{B-}, may then be derived as for the non-ionization case, as

$$i_{2-} = -B'\epsilon^{\lambda d}\left[\frac{\epsilon^{-\ell r_a}}{r_a} + \frac{\epsilon^{-\ell r_{2a}}}{r_{2a}} + \ldots\ldots - \frac{\epsilon^{-\ell d}}{d} - \frac{\epsilon^{-\ell\cdot 3d}}{3d} - \ldots\ldots\right]_{z\,=\,d} \qquad \ldots\ldots 6.12$$

and

$$i_{B-} = -\frac{B''}{2}\left[\frac{\epsilon^{-\ell r_a}}{r_a} + 2.\,\frac{\epsilon^{-\ell r_{1a}}}{r_{1a}} + \ldots\ldots - \frac{\epsilon^{-\ell r_b}}{r_b} - 2.\,\frac{\epsilon^{-\ell r_{1b}}}{r_{1b}} - \ldots\ldots\right]_{z\,=\,0} \qquad \ldots\ldots 6.13$$

where suffixes a and b refer to the quantities defined in equation 5.4a with $\rho = a$ and $\rho = b$ respectively, and $B'' = 4\pi N.B.D.$

With values of a and b for the present experiment ($b \approx .02$ cm. and $a \approx 1.5$ cm.) these equations may be approximated to within 1%, provided

X an ionizing collision

Fig. 6.6

$d > \cdot 6$ cm and $\ell > 5$ cm^{-1}, to give

$$i_{2-} = B'' \cdot \frac{\epsilon^{(\lambda-\ell)d}}{d} \qquad \ldots\ldots 6.14$$

$$i_{B-} = \frac{B''}{2} \cdot \frac{\epsilon^{-\ell b}}{b} \qquad \ldots\ldots 6.15$$

6.4 The Positive Ion Flow Pattern

As with electrons, positive ions can have the random motion of diffusion superimposed upon their drift motion. Thus there is a flow of positive ions to each electrode in the same way as with electrons. The cases of figure 6.6 show that as a consequence, collision ionization close to an electrode need not provide any contribution to the flow of gap current. In the case of the far electrode this may be allowed for by saying that the net current collected, i_2, is composed of an electron current, i_{2-}, and a positive ion current, i_{2+}, so that

$$i_2 = i_{2-} - i_{2+} \qquad \ldots\ldots 6.16$$

Positive ions will be generated in the volume of the gap and move by drift and diffusion towards the boundaries. It will be seen that positive ion flow will obey similar laws to electron flow and thus be controlled by the ratio, $\frac{\mu}{D}$, for positive ions. It may be shown that this ratio is a factor of 100 greater than that for electrons, which suggests that diffusion is less prominent in the flow of positive ions than in the flow of electrons.

Consider the hypothetical case of a sheet source of positive ions of density, n_s, in the centre of a parallel plate gap. The ratio of the current flow to the anode to that to the cathode may be shown to be

$$\frac{1 - \epsilon^{-\mu E_{dc}/D \cdot d}}{1 - \epsilon^{+\mu E_{dc}/D \cdot d}}$$

which is of the order of 10^{-100}. For an electron source under similar conditions, the ratio of the current to the cathode to that to the anode is of the order of 10^{-1}. Thus it is concluded that the diffusion of positive ions against the drift field (back diffusion) is much less than with electrons. It is therefore considered justified to assume $i_{2+} \ll i_{2-}$, when equation 6.16 reduces to $i_2 = i_{2-}$.

6.5 Evaluation of the Gap Transmission Coefficient

Since only the resultant gap current is measured in the external circuit, it is convenient to define the gap transmission coefficient, T_g, in terms of the net current, i_2, collected by the far electrode. Thus as in the non-ionization case we define:

$$T_g = \frac{i_2}{i_e} = \frac{i_{2-} - i_{2+}}{i_e} \qquad \ldots\ldots 6.17$$

Here, T_g is again a function purely of gap parameters and independent of the nature of the electron flow through the holes. It represents the net flow of charge carriers across the gap for a given injected current and is an expression of the various processes (diffusion, drift and ionization) occurring in the gap.

The value of i_e may, on the principle of continuity, be calculated as the difference between the total electron current lost from the gap and the total rate of generation within the gap. If Γ_n represents the electron current density vector normal to the boundary of the discharge, the electron current leaving the gap is $\iint \Gamma_n \cdot dS$ integrated over all the

boundaries of the discharge but omitting the holes. Since the net rate of generation must be $\psi\iiint n\, dV$ over the gap the principle of continuity may be expressed as:

$$i_e + \psi\iiint n\, dV = \iint \Gamma_n dS \qquad \ldots\ldots 6.17$$

If i_s is the current lost from the sides of the discharge,

$$\iint \Gamma_n dS = i_{B-} + i_{2-} + i_{s-} \qquad \ldots\ldots 6.18$$

and

$$i_e = \left[-\psi\iiint n.dV + i_{B-} + i_{2-} + i_{s-} \right] \qquad \ldots\ldots 6.19$$

This relation is quite general and leads to a general expression for T_g of

$$T_g = \frac{i_{2-} - i_{2+}}{\left(-\psi\iiint n.dV + i_{B-} + i_{2-} + i_{s-}\right)} \qquad \ldots\ldots 6.20$$

It may be shown from equation 6.11 that in the present case the current, i_{s-}, is negligible compared with i_{2-} and i_{B-}. Further it is shown in section 6.4 that the assumption, $i_{2-} \gg i_{2+}$ is justified. Hence equation 6.20 reduces to

$$T_g = \frac{i_{2-}}{i_{B-} + i_{2-} - \psi\iiint n.dV} \qquad \ldots\ldots 6.21$$

and it remains to evaluate $\psi\iiint n.dV$.

Since there is cylindrical symmetry about the z-axis, dV may be expressed in terms of ρ and z so that

$$\psi \iiint_{\text{over gap}} n \cdot dV = \psi \int_{z=0}^{z=d} \int_{\rho=0}^{\rho=a} n \cdot 2\pi\rho \cdot d\rho \cdot dz \qquad \ldots\ldots 6.22$$

Evaluating n from equation 6.11 and remembering there are N sources which may be assumed to be at the centre of the emitting electrode, the second integral may be evaluated to give, after the elimination of negligible terms:

$$\frac{\psi}{D} \cdot B'' \int_{z=0}^{z=d} \epsilon^{\lambda z} \left(-\epsilon^{-\ell z} + \epsilon^{-\ell(z-2d)} - \epsilon^{-\ell(z+2d)} \right) \cdot dz \qquad \ldots\ldots 6.23$$

This may be integrated to give

$$B'' \left[(\lambda+\ell) - 2\ell\epsilon^{(\lambda-\ell)d} \right] \qquad \ldots\ldots 6.24$$

after elimination of negligible terms.

The gap transmission coefficient, T_g, may now be evaluated. Using the approximate expression for i_{2-} and i_{B-} derived above (equations 6.14 and 6.15), a value of T_g applicable to the range $\ell > 5$ cm^{-1} and $d > .6$ cm;, may be obtained from equation 6.21 as:

$$T_g = \epsilon^{(\lambda-\ell)d} \Big/ \epsilon^{(\lambda-\ell)d} (1 + 2\ell d) - d(\lambda+\ell) + \frac{d}{2b} \epsilon^{-\ell b} \qquad \ldots\ldots 6.25$$

Normalising to the case when $\lambda = \lambda_1$ and there is no ionization:

$$T_{gn} = \left\{ 1 + \frac{d}{2b} \cdot \epsilon^{-\lambda_1 b} \right\} T_g \qquad \ldots\ldots 6.26$$

where T_g is given by equation 6.25.

As in the case when no ionization occurs, for constant emission current from the filament, i_1, the amplification as measured is

$$A = T_{gn} \cdot T_{hn} \qquad \ldots\ldots 6.27$$

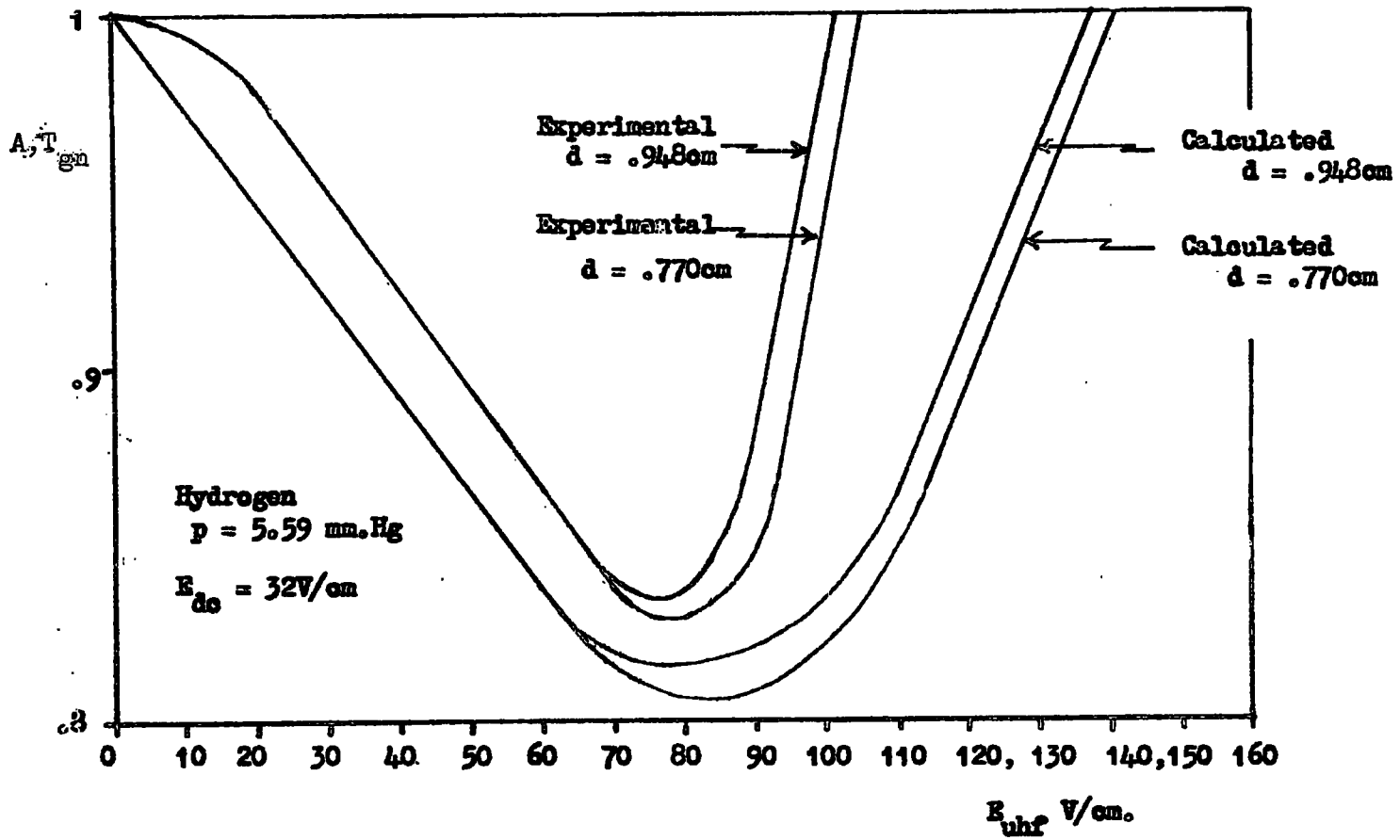
1
.9
.8
$A_2 T_{gn}$
Experimental
d = .948cm
Experimental
d = .770cm
Calculated
d = .948cm
Calculated
d = .770cm
Hydrogen
p = 5.59 mm.Hg
E_{dc} = 32V/cm
0 10 20 30 40 50 60 70 80 90 100 110 120, 130 140,150 160
E_{uhf} V/cm.

Fig. 6.7

Again in the absence of a detailed theory of the flow of electrons through the holes, T_{hn} will be assumed to be independent of gap conditions and equal to unity. The amplification is then directly comparable with T_{gn}. This assumption is equivalent to saying that the current emitted from the holes is a constant independent of gap conditions.

Putting $\ell = 5$ in equation 6.26 gives $T_{gn} \approx 1$. This implies that the equation is applicable up to cases where A, defined as $\frac{i}{i_{20}}$, is less than unity. // Since the electron energy distribution in the present case is similar to that in discharges in pure unidirectional fields (Varnerin and Brown, 1950) the values of ψ may be expected to be similar in the two cases. It should thus be possible to use values of ψ measured in unidirectional fields to calculate (from equation 6.26) the amplification curve obtained in the present experiment.

Using the values of ionization efficiency, η, measured by Leiby (1954, reproduced in Brown 'Basic Data of Plasma Physics' p. 136) and values of $\frac{\mu}{D}$ taken from Varnerin and Brown, 1950, T_{gn} is evaluated for two gap widths and plotted in figure 6.7. It will be seen that the calculated and experimental curves are of the same form, beginning to curve upwards at the same value of E_{uhf}. However, there is a far more rapid rise in the experimental curve than in that calculated. This might imply that the ionization rate in the present experiment is somewhat above that with unidirectional fields and electrons of the same energy. There is, however, some doubt as to the value of E_{dc} in the

experimental curves due to the presence of insulating films on the electrode surfaces. In this region their effect is expected to increase the drift field as a consequence of the flow of charge through the films. Such an increase might account for the difference observed between the experimental and theoretical curves. An exact verification of the theory must therefore await measurements of amplification in which there is less uncertainty in the value of the drift field.

CHAPTER 7

TRANSIT TIMES - THEIR MEASUREMENT AND SIGNIFICANCE

7.1 Method of Measurement

The method employed is to modulate the injected current by superimposing a sine wave of radio frequency (100 kc/s to 7 Mc/s) on the drift voltage, V_1, applied between the filament and the emitting electrode shell. The resultant bursts of electrons after transmission across the gap, are gated by a similar field in reverse phase applied between the collecting electrode shell and the internal collector plate (Figure 2.1, on the back cover).

The fraction of the current, i_2, incident on the collecting electrode, which reaches the inner collecting plate depends on the phase of the internal field. The current, i_3, collected by this plate will be a maximum when arrival of a puff of electrons coincides with the maximum value of the internal field when this is directed so that electrons drift onto the collecting plate. If f is the modulation frequency, the transit time, t_t, is given by this condition as:

$$t_t = \frac{q}{2f} \qquad \ldots\ldots 7.1$$

where q is the number of puffs present in the gap at any given time. Thus $\frac{i_3}{i_2}$ is measured for a range of gating frequencies and the frequency at which $\frac{i_3}{i_2}$ is a maximum determined. From this the transit time may be calculated using equation 7.1.

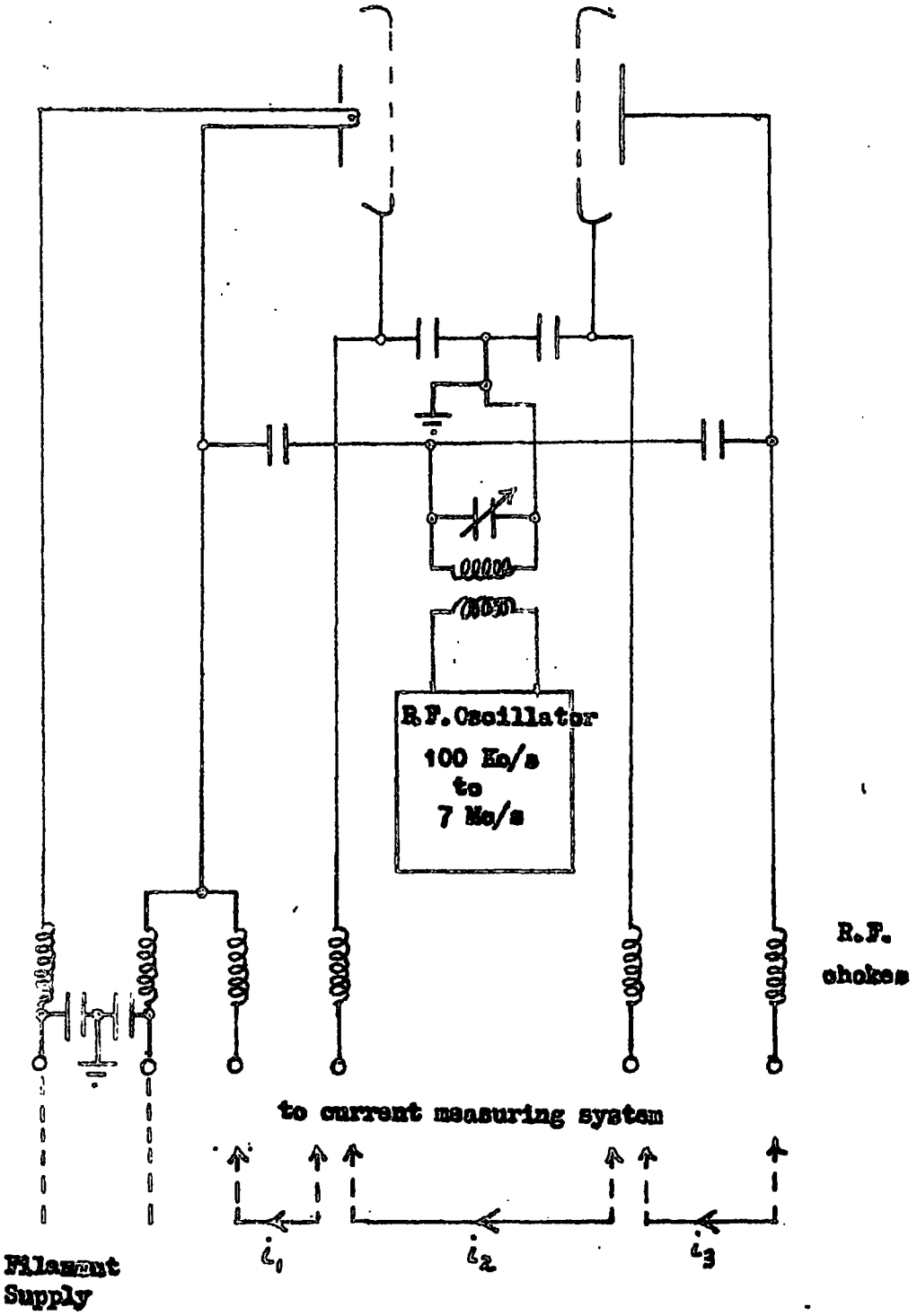
R.F. Oscillator
100 Ko/s
to
7 Mo/s
R.F.
chokes
to current measuring system
Filament
Supply
i_1
i_2
i_3

Fig. 7.1

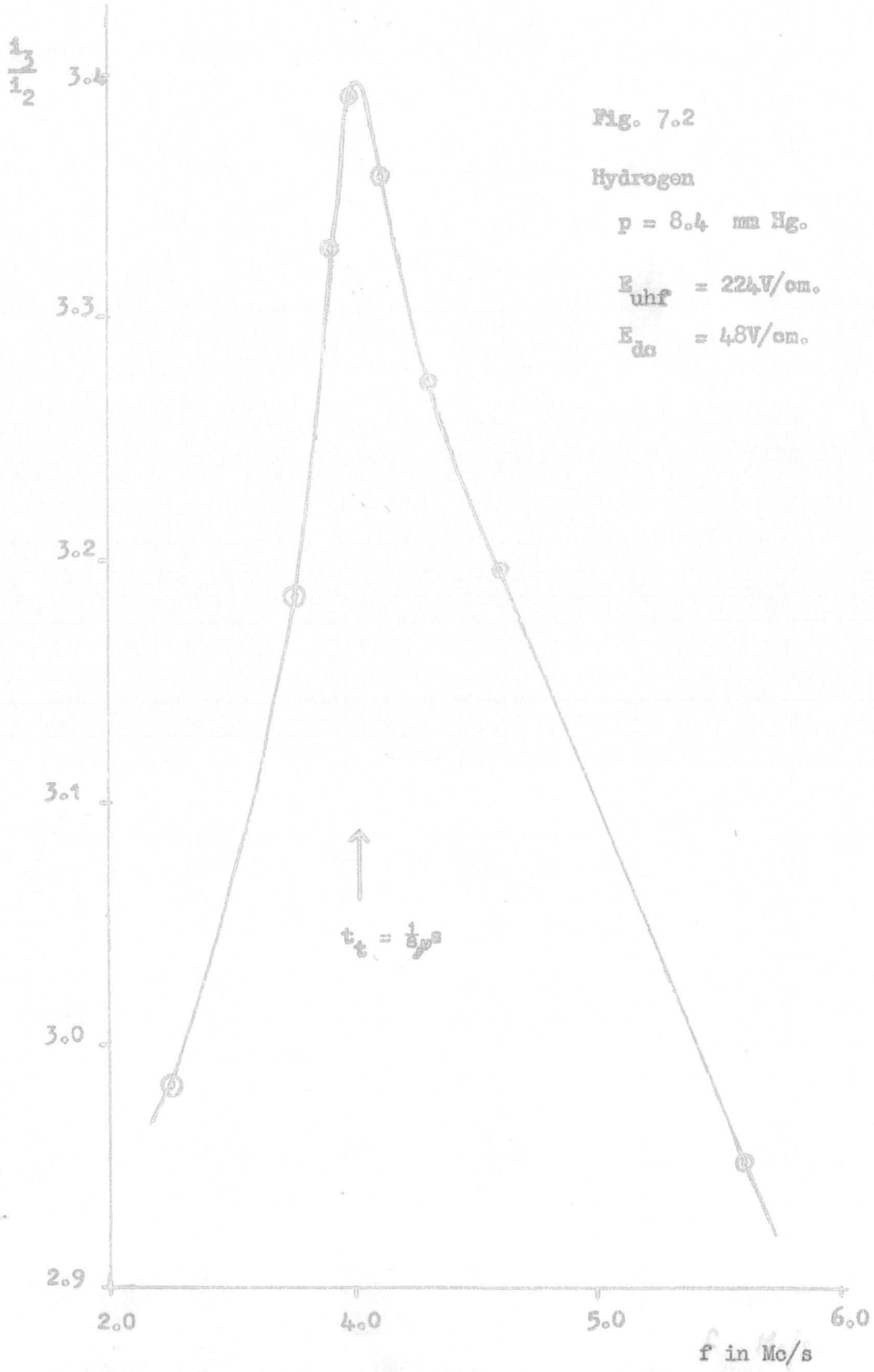

Fig. 7.2

Hydrogen

p = 8.4 mm Hg.

E_{uhf} = 224V/cm.

E_{dc} = 4.8V/cm.

The circuit used to supply the radio-frequency gating voltages is shown in figure 7.1. Radio-frequency chokes are used between the electrodes and the current measuring system to prevent r.f. currents flowing through these circuits. High insulation blocking capacitors are used so that the small unidirectional currents flowing between the electrodes do not leak through the r.f. supply system.

7.2 Preliminary Measurements of Transit Time

Preliminary measurements of $\frac{i_3}{i_2}$ have been made for a range of modulating frequencies and for conditions close to breakdown. A typical plot of $\frac{i_3}{i_2}$ against f is shown in figure 7.2

For this case, assuming q = 1, equation 7.2 gives $t_t \approx \frac{1}{8}\mu S$. This value is in good agreement with that calculated from breakdown data using the method given by Nicholls, 1960.

The feasibility of this method of measurement has thus been demonstrated. However, in view of the uncertainty in the drift field resulting from surface phenomena investigated later in this thesis, no attempt has been made to make systematic measurements of t_t over a range of conditions. Like the amplification measurements these await removal of the uncertainty in the drift field caused by the presence of surface films.

7.3 The expected accuracy of measurement of t_t

Drift velocities of electrons in various gases have been measured by Bradbury and Nielson (1936 and 37) using the electrical shutter method. Crompton, Hall and Macklin (1957) have found that markedly different drift velocities could apparently be obtained using the same apparatus but with

different distances between the shutters. Duncan (1957) has shown that such an effect is theoretically predictable when diffusion is appreciable. However, differences calculated from his work are considerably smaller than those observed. It is suggested by Crompton and his collaborators that this may be due to certain assumptions made in the boundary conditions of the diffusion equation used by Duncan.

In the present experiment it has been shown that diffusion is appreciable so that electron transit times cannot be considered to be controlled exclusively by drift. The electron density and flow patterns may be expected to be considerably altered by the modulation of the electron source. Thus a pulse of electrons would be expected to diffuse both backwards and forwards in its passage across the gap, distorting the shape of the pulse. It is this distortion which might account for the observations of Crompton and his collaborators. The effects of this distortion on measurements of transit times in the present experiment is therefore of interest.

7.4 The Electron Flow and Density Pattern with Modulation of Emitted Current

In the measurement of transit time the electron stream emitted into the gap is modulated by a sinusoidal field applied between filament and emitting electrode shell. The electrons are thus emitted according to some time function and the electron density and flow patterns in the gap vary with time.

The emitted electron stream may be considered to be a partial modulation of the static stream of electrons already considered (Chapter 6). For the general case the modulated waveform may be represented by a

fourier series of sinusoidal waveforms. Thus the electron density at any point in the gap is a time function of the form:

$$n = \sum_{s=0}^{s=\infty} N_s \, \epsilon^{js\omega t} \qquad \ldots\ldots 7.2$$

where s is an integer, ω is the angular frequency of the fundamental component and N_s defines the amplitude and phase of the sth sinusoidal component.

The amplitude and phase of each component may be expected to vary over the gap as the waveform is distorted by diffusion and drift. It will be assumed that the component frequencies of the emitted waveform are sufficient to express the waveform at any other point.

The equation of continuity (Equation 1.2) applicable to these conditions is:-

$$D.\nabla^2 n - \mu E_{dc}. \frac{\partial n}{\partial z} + \psi n = \frac{\partial n}{\partial t} \qquad \ldots\ldots 7.3$$

The time dependent function may be removed by employing equation 7.2 to give:-

$$\left\{\nabla^2 - 2\lambda \frac{\partial}{\partial z} + \frac{\psi}{D}\right\}. \sum_{s=0}^{s=\infty} N_s = \sum_{s=0}^{s=\infty} \frac{js\omega}{D} . N_s \qquad \ldots\ldots 7.4$$

which may be split into an infinite series of equations of which the sth is

$$\left\{\nabla^2 - 2\lambda \frac{\partial}{\partial z} + \frac{\psi}{D} - \frac{js\omega}{D}\right\}. N_s = 0 \qquad \ldots\ldots 7.5$$

Each of these equations is similar to the equation of continuity for the steady state condition (equation 6.2) provided $\frac{\psi}{D}$ is replaced by $\left(\frac{\psi}{D} - \frac{js\omega}{D}\right)$. Thus as before, Huxley's method of solution may be followed. It is thus possible to derive, for a point source at the origin, on a conducting plane

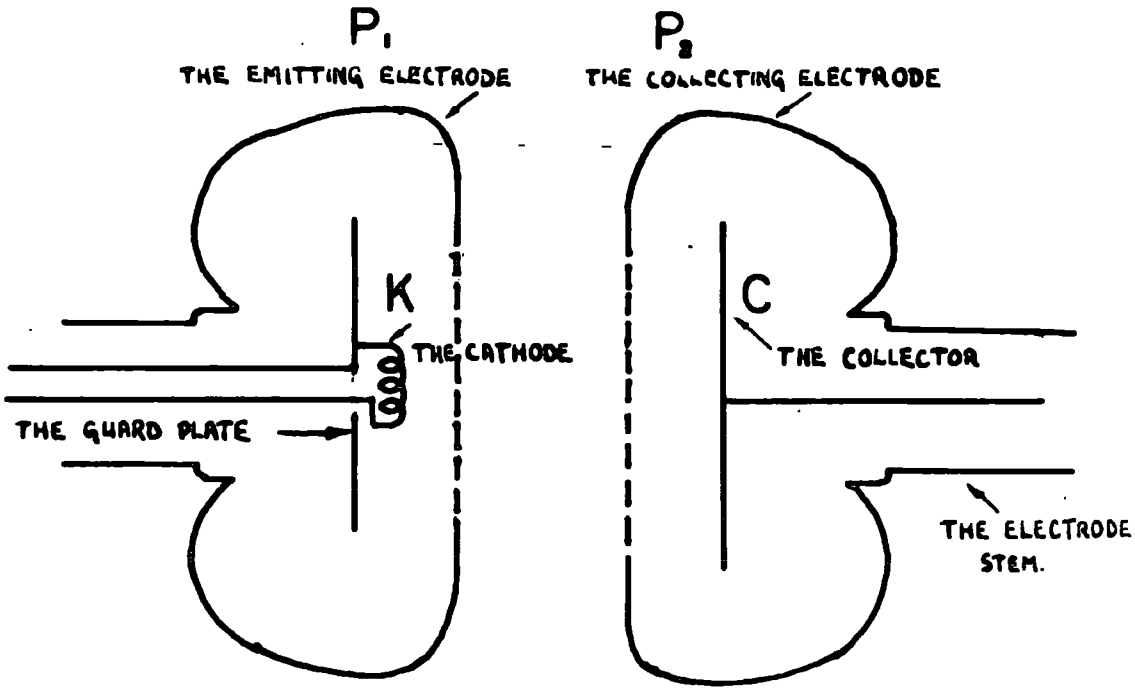

FIG. 2.1 A SCHEMATIC DIAGRAM OF THE ELECTRODE SYSTEM.

emitting into an infinite medium, an electron density distribution in space given by

$$n = \sum_{s=0}^{s=\infty} N_s = \sum_{s=0}^{s=\infty} B_s \, \epsilon^{\lambda z} \cdot \frac{z}{r} \cdot \frac{d}{dr}\left(\frac{\epsilon^{-\ell_s r}}{r}\right) \cdot \epsilon^{js\omega t} \quad \ldots\ldots 7.6$$

where, $\ell_s^2 = \ell^2 + \frac{js\omega}{D}$. This is subject to the condition that ℓ_s is real or $\lambda^2 > \left(\frac{\psi}{D} - \frac{js\omega}{D}\right)$. Here ℓ_s is complex and may be written in the form $g_s + jh_s$ where,

$$g_s^2 = \tfrac{1}{2}\left\{\ell^2 + \sqrt{\left(\ell^4 + \left(\frac{s\omega}{D}\right)^2\right)}\right\} \quad \ldots\ldots 7.7$$

and $$h_s^2 = \tfrac{1}{2}\left\{\sqrt{\left(\ell^4 + \left(\frac{s\omega}{D}\right)^2\right)} - \ell^2\right\} \quad \ldots\ldots 7.8$$

Equation 7.6 shows that the component of the electron density pattern corresponding to the sth frequency component of the emitted waveform, is proportional to $\epsilon^{(js\omega t - \ell_s r)}$, which may be expanded to $\epsilon^{-g_s r} \cdot \sin(s\omega t - h_s t)$. Thus the electron density pattern consists of a sinusoidal waveform travelling out radially from the point source. Further it is seen that the wavelength of the sth component in the plasma is $\frac{2\pi}{h_s}$, so that the velocity of propagation, V_s, of a sinusoidal electron density pattern of frequency $\frac{s\omega}{2\pi}$ is $\frac{s\omega}{h_s}$. Substituting for h_s from equation 7.8 gives

$$V_s = \frac{\sqrt{2} \cdot s\omega}{\sqrt{\left\{\sqrt{\left[\ell^4 + \left(\frac{s\omega}{D}\right)^2\right]} - \ell^2\right\}}} \quad \ldots\ldots 7.9$$

which is an increasing function of frequency.

The propagation of a pulse across the gap may therefore be expected to be analogous to propagation down a transmission line, the effect being to delay the component frequencies by different times. It is thus expected

that the shape of the emitted pulse of electrons is distorted in its passage across the gap. This effect may be further considered in terms of the phase of the electron current, i_{2-}, incident on the collecting electrode.

Again following Huxley, the collecting electrode may be introduced into the system considered above, and the electron density put to zero over its surface, by the introduction of a distribution of point sources emitting in phase. Thus for a single point source on the emitting electrode N_s is given by equation 6.11, with n and ℓ replaced by N_s and ℓ_s respectively. The current flowing to the collecting electrode, i_{2-}, may then be derived as in the previous chapter to give (corresponding to equation 6.14)

$$i_{2-} = \frac{\epsilon^{\lambda d}}{d} \cdot \sum_{s=0}^{s=\infty} \left\{ B_s'' \cdot \epsilon^{-g_s d} \cdot \epsilon^{j(s\omega t - h_s d)} \right\} \qquad \ldots\ldots 7.10$$

which is true to within 1% if $\ell_s > 5\text{cm}^{-1}$ and $d > .6\text{cm}$.

The current which the collecting electrode would receive if placed very close to the emitting electrode may be obtained by letting d tend to zero in equation 7.10, to give

$$i_{2-} \rightarrow \sum_{s=0}^{s=\infty} \frac{B_s''}{d} \cdot \epsilon^{js\omega t} \qquad \ldots\ldots 7.11$$

Regarding this current as the input current to the gap, it will be seen that the phase difference across the gap for a given component of the emitted waveform is the phase difference between that component of the currents of equations 7.10 and 7.11 i.e. $h_s d$ for the sth component.

This phase difference is frequency dependent and is an alternative way of expressing the varying velocities of the various frequency components.

Further, comparison of equations 7.10 and 7.11, shows that the sth component of the waveform is attenuated by a factor $\frac{\epsilon^{(\lambda-g_s)d}}{d}$. Equation 7.7 shows g_s to be an increasing function of frequency. Thus there is expected to be a tendency for the higher frequency components to be filtered out. It is therefore reasonable to assume that the collected pulse is composed largely of the fundamental component so that the delay time of the maximum of the pulse is that of the component, s = 1. The behaviour of the system is then the behaviour of this component and the phase difference across the gap is $h_1 d$.

The condition for maximum current to the internal collecting plate of the collecting electrode is that the current received by the collecting electrode should be in antiphase with that emitted, i.e. that the phase difference across the gap is a multiple of π. Thus

$$h_1 d = q\pi \qquad \ldots\ldots 7.12$$

where q is an integer. The transit time, t_t, as measured, is given by

$$t_t = \frac{d}{V_1} = \frac{dh_1}{\omega} = \frac{q\pi}{\omega} \qquad \ldots\ldots 7.13$$

Here V_1 is given by equation 7.9 with s = 1 and is an increasing function of ω. Thus it will be seen that the transit time measured is that for a pulse of fundamental frequency, $\frac{\omega}{2\pi}$, rather than that of the electrons flowing in the steady state ($\omega = 0$). It would therefore appear that for any experiment measuring drift velocities by noting the transit time

of a burst of electrons, measures, not the drift velocity of the electrons but the velocity of propagation of the pulse.

As the frequency tends to zero equation 7.9 shows that the propagation velocity, V_s, approaches the drift velocity, μE_{dc}. In general however the propagation velocity is greater than the electron drift velocity in the steady state ($\omega = 0$).

The variation of drift velocities with gap width observed by Crompton Hall and Macklin (1957) may be explained qualitatively in this way. Since the gating frequency (ω) for maximum current transmission through the collecting gate decreases with gap width, the measured velocity, given by equation 7.9, likewise decreases with gap width, as was observed. Quantitative predictions, however, require values of the diffusion coefficient, D, which are independent of drift velocity measurements. These do not appear to be available in the range of $\frac{E}{p}$ applicable to these results. However, approximate calculations, using 'accepted' values of D, are in substantial agreement with experiment.

When diffusion is small, the electrons may be expected to move across the gap with the drift velocity, μE_{dc}. The value of h_s, when diffusion is small may be obtained from equation 7.8, by letting D tend to zero when,

$$h_s \rightarrow \frac{s\omega}{\mu E_{dc}}$$

The velocity of propagation of an electron density pattern of any frequency is then $\frac{\omega}{h_s} = \mu E_{dc}$, as would be expected.

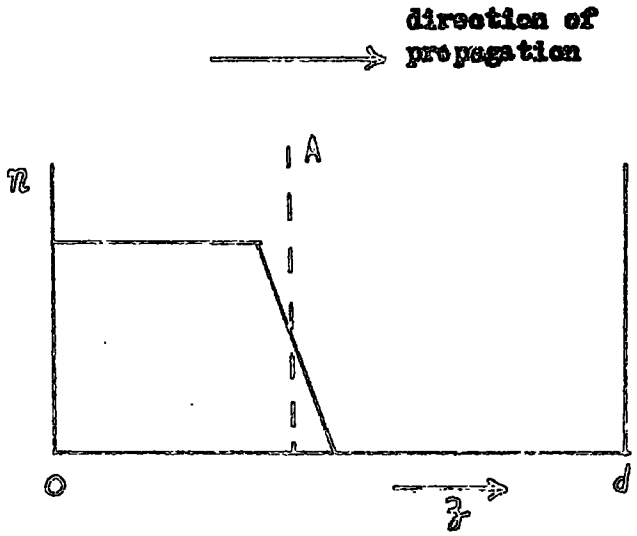

Fig. 7.3

It is therefore seen that the differing velocities observed for the various frequency components are the result of diffusion. Physically the mechanism may be seen by considering the propagation of a sharp increase in electron density (a step function) of the form of figure 7.3. The current crossing the plane A is composed of a drift plus a diffusion current both acting to propagate the step. Thus, if k is the slope of the step, the z-component of the electron density vector is

$$\Gamma_z = \mu E_{dc} \cdot n + Dk$$

The effective drift velocity of electrons crossing A is therefore

$$\frac{\Gamma_z}{n} = \mu E_{dc} + \frac{Dk}{n}$$

which is the propagation velocity of the step. Considering this as part of a sinusoidal density distribution, the higher the frequency, the larger k and thus the larger the velocity of propagation.

It has been seen that the transit time measured is that for a particular frequency, $\frac{\omega}{2\pi}$. The value of h for any frequency may be obtained from a plot of $\frac{i}{i_2}$ against d, retaining ω constant. Maxima of $\frac{i}{i_2}$ should then be observed when (equation 7.13), $d = \frac{q\pi}{h} = \frac{q\pi}{\omega} \cdot V_s$ so that h or V_s could be calculated. Knowing h, $\frac{\omega}{D}, \frac{\mu}{D}$ it is possible to calculate ℓ and hence $\frac{\Psi}{D}$, from equation 7.8. This could therefore provide a means of measuring $\frac{\Psi}{D}$ independently of the amplification method, but based on similar theoretical concepts. It may therefore play a useful part in confirming the validity of the theory. At present, however, insufficient results are available to allow a quantitative evaluation.

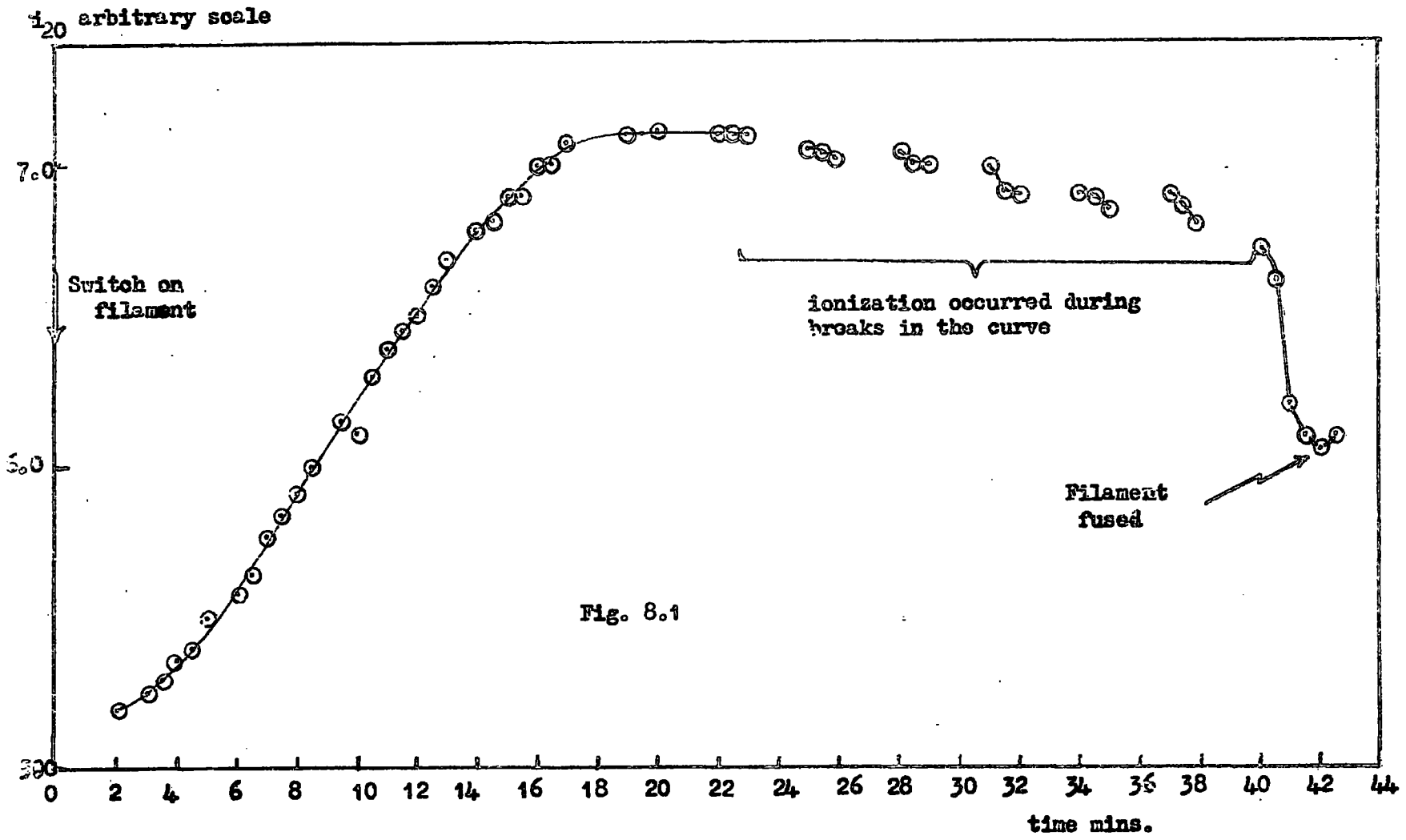
i_{20} arbitrary scale
7.0
5.0
3.0
Switch on filament
ionization occurred during breaks in the curve
Filament fused
0 2 4 6 8 10 12 14 16 18 20 22 24 26 28 30 32 34 36 38 40 42 44
time mins.

Fig. 8.1

CHAPTER 8

LONG TIME CONSTANT EFFECTS

8.1 The Experimental evidence

During the measurements of amplification, several variations of i_{20} and i_2 were observed which possessed long time constants. As pointed out in Chapter 4, these were eliminated as far as possible from the amplification measurements by employing a timed sequence of experiments. In the present Chapter these effects will be described and analysed in more detail.

Fluctuations and drift in the initial gap current, i_{20}

These may be separated into two groups, those which occur in the absence of gap ionization and those which occur after, and presumably during, the period when collision ionization occurs in the gap. The former is a gradual drift of i_{20} with time which is independent of the application of u.h.f. fields and the presence of ionization. Superimposed upon this there is a fluctuation of i_{20} following experiments in which ionization in the gap was high. These variations are shown in figure 8.1, which relates to an experiment in which the total emission from the filament was kept to within 0.1% by the stabilizer, while the current reaching the far electrode (i_{20}) was measured.

This curve shows that after switching on the filament and the total emission current from the filament, i_1, had stabilized, there was a gradual rise of i_{20} over the first 18 mins. This was followed by a gradual decrease until the stabilizer, at 40 mins., could no longer retain the current, i_1, and the filament fused. The initial

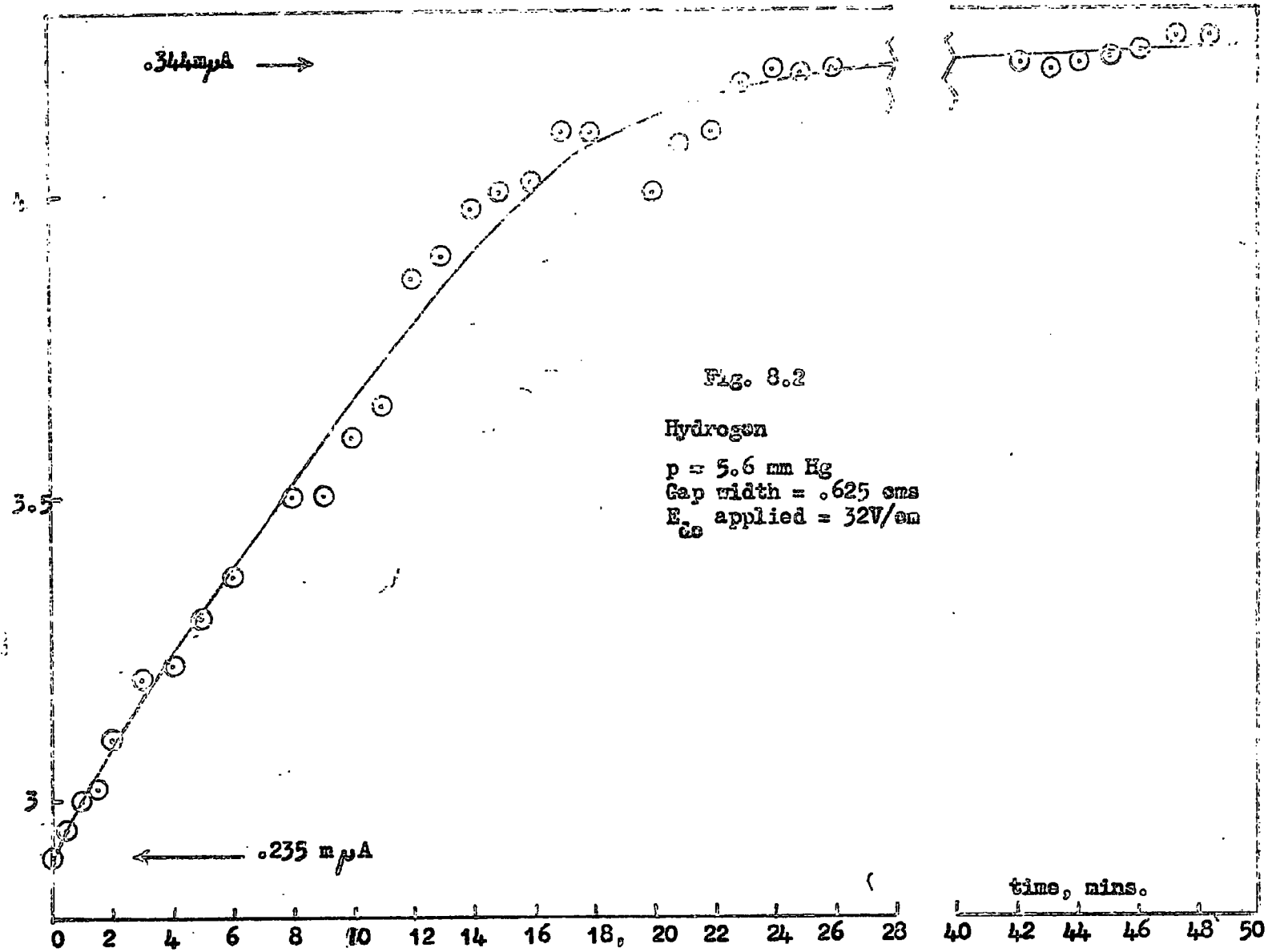

Fig. 8.2

Hydrogen

p = 5.6 mm Hg
Gap width = .625 cms
E_{co} applied = 32V/cm

rise of this curve is quite typical of the observed behaviour, the drop between 20-40 mins. is, however, not a typical case. In general this decrease would occur over a period of several hours. Figure 8.1, however, serves to show this drift on a reduced scale. Figure 8.2 is a typical curve over the same time range.

During the slow decrease in i_{20} shown in figure 8.1, a u.h.f. field was applied periodically and ionization occurred. On removal of this field i_{20} may be seen to have fluctuated from the value expected for a smooth drift.

In many cases the initial rise of these curves was not observed. The value of i_{20} remained at its low initial value although i_1 was equal to that of figures 8.1 and 8.2. Further, the maximum value of i_{20} varied widely from experiment to experiment, for any given value of i_1.

This suggests that the fraction of the electron current incident on the inside of the electrode, which gets through the holes, varies from experiment to experiment. Although the total current flowing to the back of the electrode, i_1, is the same, its distribution over the inside surface of the electrode might cause a change in current flowing through the holes. Thus a decrease in current density in the region behind the holes, with corresponding increases in other regions might be expected to cause a decrease of the current flowing through the holes. Thus a limitted variation from experiment to experiment could result from changes in the current distribution pattern inside the electrode, which could be caused by changes in filament and

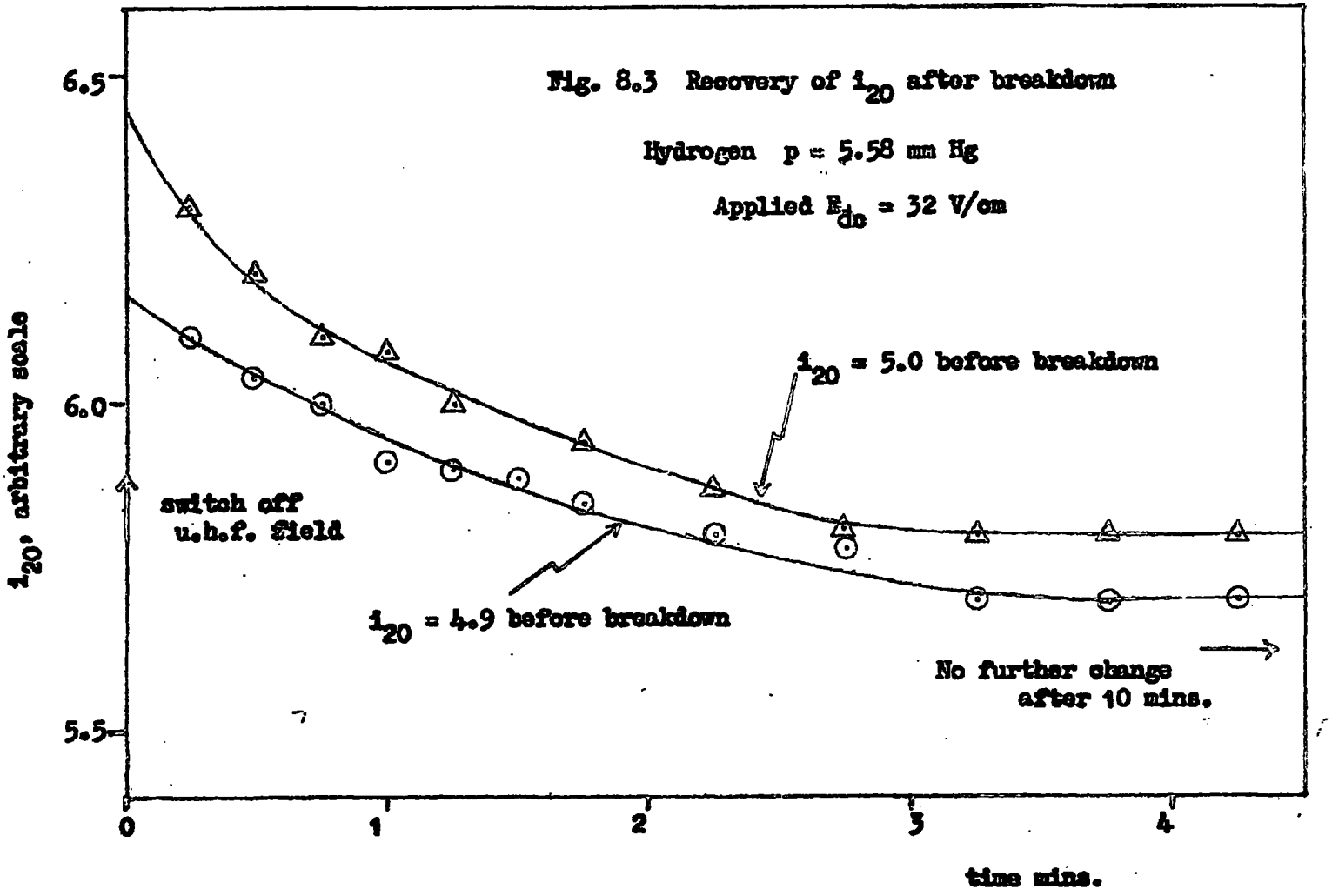

Fig. 8.3 Recovery of i_{20} after breakdown

Hydrogen p = 5.58 mm Hg

Applied E_{dc} = 32 V/cm

shield positions after installing a new filament. The time rise might then be explained by thermal expansion of the electrode structure. However, deliberate variation of filament position did not give the required variation of i_{20}.

Alternatively, since the measurements are made on currents crossing the gap, it is possible that the properties of the gap itself may have to be considered. This is discussed in detail in the following chapter.

If, after i_{20} has stabilized to its nearly constant value, the gap is broken down, then on extinguishing the discharge, i_{20} is found to have increased. This rise of i_{20}, which presumably took place during the discharge, then decays with a time constant of about $1\frac{1}{2}$ mins. Figure 8.3 shows this for two initial values of i_{20}.

Similar effects occur after amplification in the gap has risen to large values. The extent of the rise of i_{20} occurring increases with increasing amplification. It is accompanied by a rise of i_2 during the period when the u.h.f. field is applied. This will be dealt with in the next section.

There is the possibility that this effect is caused by the flow of ions and electrons from the gap through the holes. This could interfere with the electron flow pattern in the emitting electrode by providing a further current source contributing to the current flowing between filament and the electrode shell, i_1. The action of the stabilizer would then be to decrease the emitted current from the filament to retain i_1 a constant. On extinguishing the discharge, the stabilizer would increase the current again with

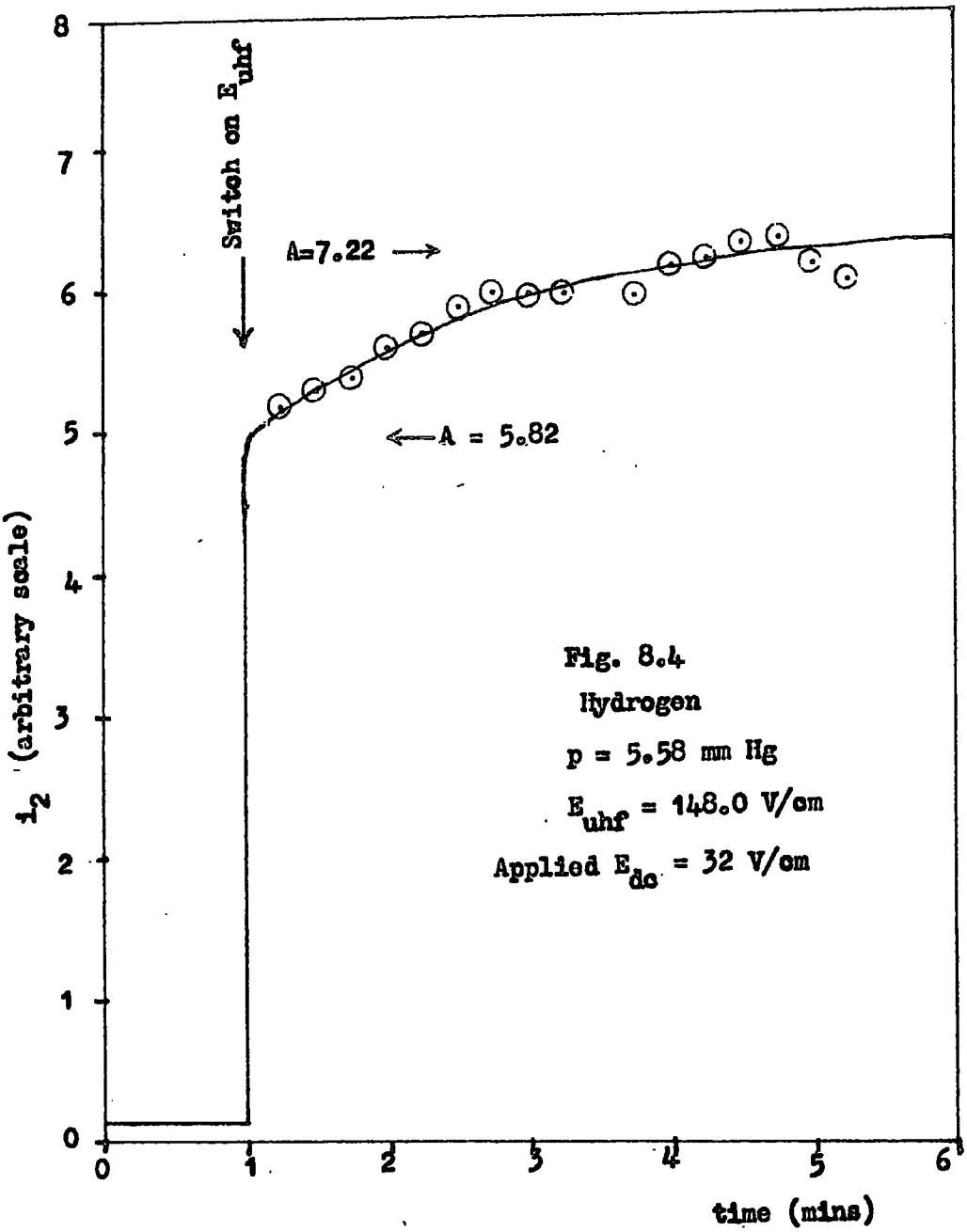

Fig. 8.4

Hydrogen

p = 5.58 mm Hg

E_{uhf} = 148.0 V/cm

Applied E_{dc} = 32 V/cm

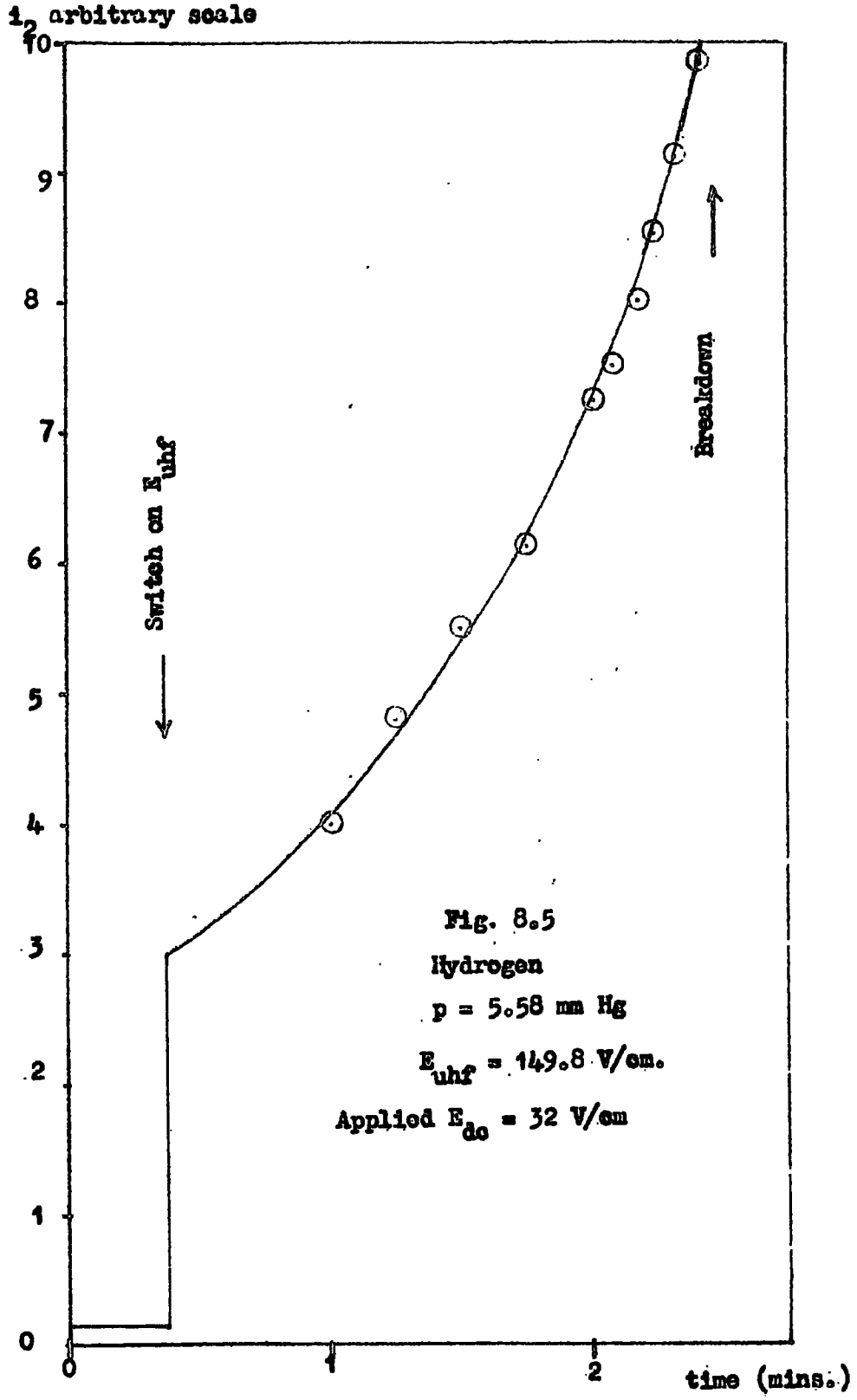

Fig. 8.5

Hydrogen

p = 5.58 mm Hg

E_{uhf} = 149.8 V/cm.

Applied E_{dc} = 32 V/cm

the thermal time constant of the filament which is about $\frac{1}{3}$ min. Such a mechanism, however, gives an apparent decrease of i_{20} rather than an increase. Further the expected recovery time constant is too short to explain those observed (1.5 mins.).

8.2 The Drift of i_2 with time

If the initial gap current, i_{20}, varies, then the current, i_2, crossing the gap when a u.h.f. field is applied, can be expected to show a corresponding variation. This could account for the observed drift of i_2 in certain cases. However, when large values of i_{20} are used, instability of i_2 is observed which cannot be explained in this way.

For lower u.h.f. fields this instability took the form of a slow rise of i_2 with time eventually resulting in some stable value (figure 8.4 is a typical curve). At higher u.h.f. fields a progressive rise of i_2, eventually resulting in breakdown, was observed, of which figure 8.5 is a typical curve. These instabilities were observed despite stabilization of i_1, which showed no variation greater than 0.1% over any of these experiments.

These instabilities only occurred at higher i_{20} values. In practice this meant that this only occurs in experiments in which the initial rise of i_{20} was observed. Attempts to obtain higher values of i_{20} without the initial rise, necessitated over-running the filament. In the few cases where this was achieved, there appeared no sign of any instability. Thus it is suggested that the phenomena causing the initial rise also control these instabilities, and that the onset of

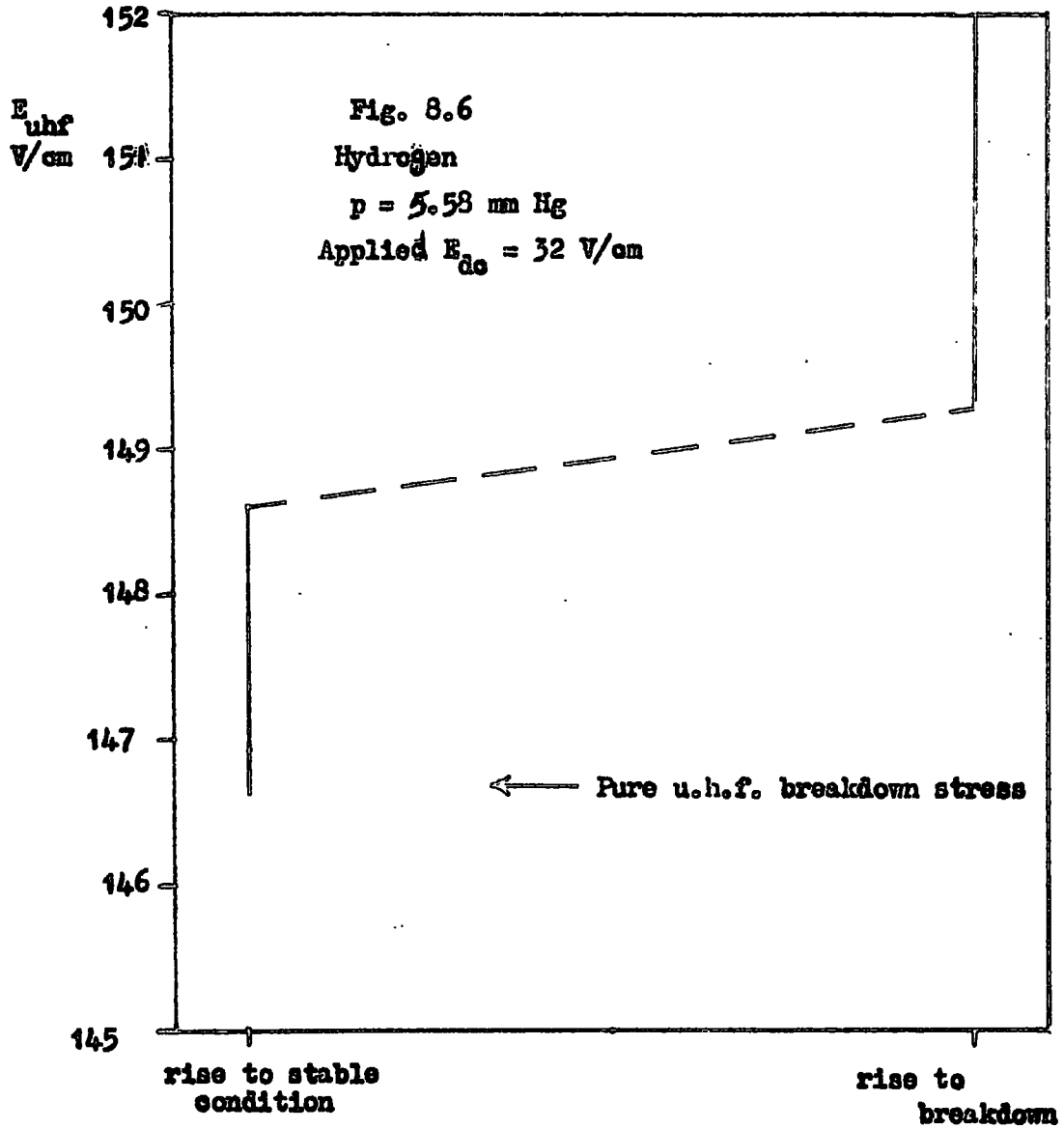
152
151
150
149
148
147
146
145
E_{uhf} V/cm
Fig. 8.6
Hydrogen
p = 5.58 mm Hg
Applied E_{dc} = 32 V/cm
Pure u.h.f. breakdown stress
rise to stable condition
rise to breakdown

these instabilities is independent of i_{20} itself. The fact that these observations do not always occur, suggests that their common cause is not always present.

There appears to be a definite u.h.f. field above which there was a progressive rise to breakdown and below which a stable value was obtained. Figure 8.6 is a plot of the applied field in terms of the type of instability observed. This shows a transition at about 149 V/cm.

The rate of rise of the instability curves was found to decrease with the u.h.f. field applied. Further at low fields the extent of the drift of i_2 with time became very small and disappeared in cases where the amplification was less than about 2.

Since i_1 remains constant and the variation of i_{20} was too small to explain this increase (andcould not explain the rise to breakdown), these curves imply a slow rise of gas amplification with time. The time constant of these phenomena is of the order of 1.5 mins.

This appears to be due to some phenomenon occurring in the gap and hence deserves further investigation.

8.3 Analysis of the instability curves in terms of the concept of positive feedback

The two forms of the instability curves for i_2 (figures 8.4 and 8.5) may be understood to be different forms of the same phenomenon if considered in terms of a system with positive feedback.

The gas amplification process is essentially equivalent to a current amplifier with an input of the emitted current, i_e, and an output of i_2. If it is postulated that this current amplifier is composed of a amplifier of gain, G, and a positive feedback loop with a feedback

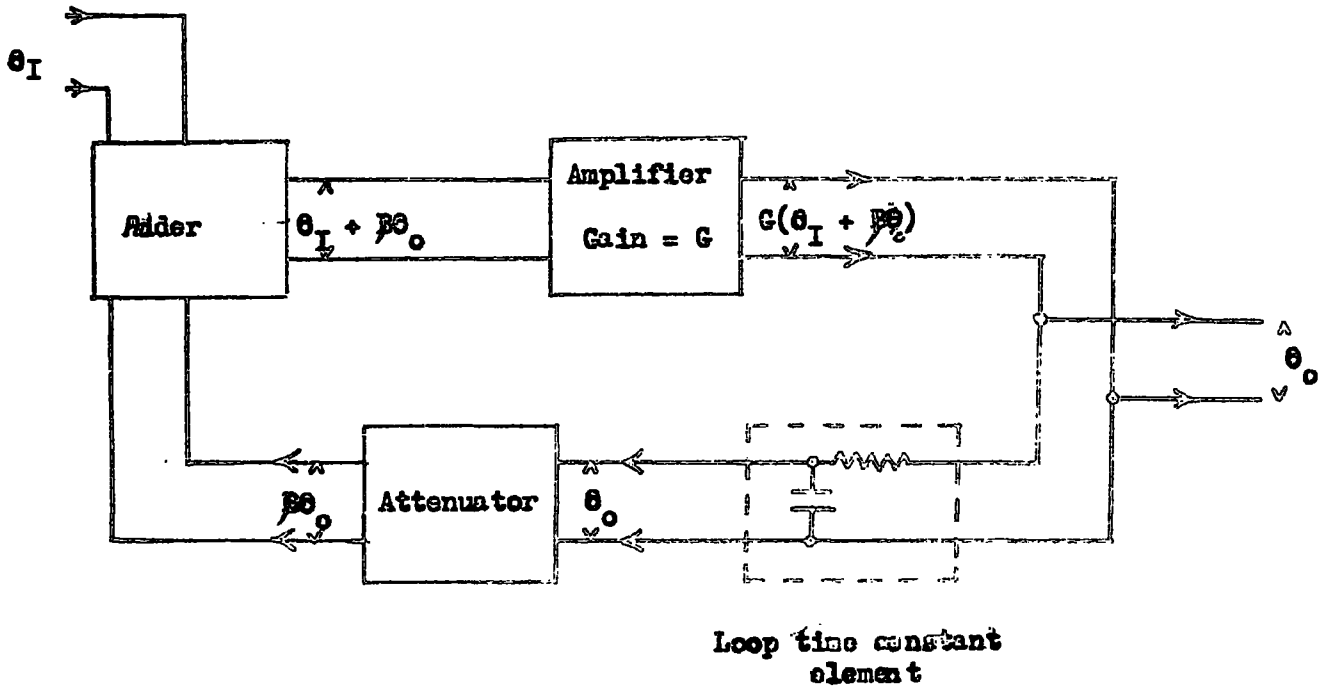
θ_I
Adder
$\theta_I + \beta\theta_o$
Amplifier
Gain = G
$G(\theta_I + \beta\theta_o)$
θ_o
$\beta\theta_o$
Attenuator
θ_o
Loop time constant element

Fig. 8.7

factor, β, and a time constant of τ (figure 8.7), its response may be shown (Appendix 2) to be similar to that of figures 8.4 and 8.5.

It is well known that such systems are stable if $G\beta < 1$, but unstable if $G\beta > 1$. For example, in a discharge with unidirectional field only, secondary emission provides a positive feedback loop and β is then a function of secondary processes, the gain, G, being provided by collision ionization. In this case, $G\beta = 1$ represents the onset of the breakdown condition (the Townsend criterion for breakdown) when the output current tends to infinity and then becomes independent of the input current. It would appear that a similar feedback system is present in the experiments described, but it is unlikely that secondary emission is responsible. On the grounds of the time scale involved, the charging and discharging of insulating films on the electrode surfaces is shown in the next chapter to be the most likely mechanism.

Referring to the circuit of figure 8.7, the time for the steady condition to be established depends on the effective time constant of the feedback loop, τ. Thus if a step increase of gain from 1 to G_1, occurs, the output waveform does not rise to its maximum value immediately but approaches it with a time constant controlled by τ. This has been analysed in detail in Appendix 2, where it is shown that if θ_I is the input to such a system, the output, θ_O, when an increasing step from 1 to G_1 (figure 8.8a) is applied to G, is a time function as shown in figures 8.8 b and c for the cases $G_1\beta > 1$ and $G_1\beta < 1$ respectively. In the former case there is a gradual rise to

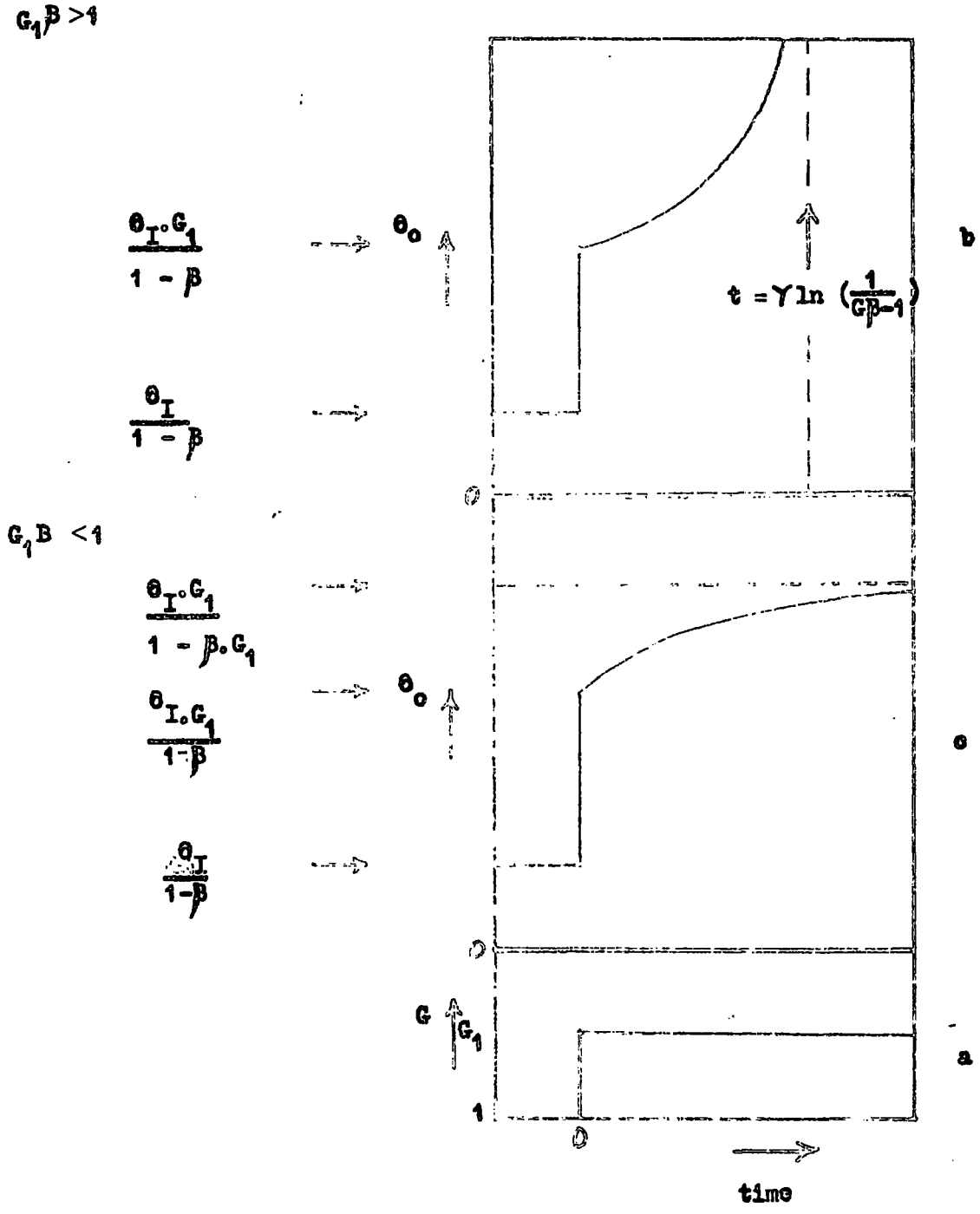
$G_1\beta > 1$
$\frac{\theta_I \cdot G_1}{1-\beta}$
θ_o
$\frac{\theta_I}{1-\beta}$
$t = \gamma \ln\left(\frac{1}{G\beta - 1}\right)$
b
$G_1 B < 1$
$\frac{\theta_I \cdot G_1}{1-\beta \cdot G_1}$
θ_o
$\frac{\theta_I \cdot G_1}{1-\beta}$
$\frac{\theta_I}{1-\beta}$
c
G
G_1
1
a
time

Fig. 8.8

instability (breakdown) and in the latter case a gradual rise to a stable value.

The curves of figures 8.8 c and b will be seen to be very similar to those of figures 8.4 and 8.5 respectively. Thus the output of a circuit employing positive feedback is seen to exhibit instabilities similar to those if i_2, so that θ_o may be identified as the gap current i_2. In the case of i_2, the controlling condition for transition between the two types of curve is shown in figure 8.6 to be a certain value of the u.h.f. field. This implies a certain value of gas amplification. Thus, as in the system analysed by Townsend, G may be regarded as the result of collision ionization. The application of a step function to G is then seen to correspond to an increase of u.h.f. field from zero to give a gas amplification of G_1, resulting from collision ionization.

A comparison of figures 8.8c and 8.8b with 8.4 and 8.5 respectively, suggests that the initial steady value of θ_o before G is increased, corresponds to the steady value of i_{20}. Thus

$$i_{20} \equiv \frac{\theta_I}{1 - \beta} \qquad \ldots\ldots 8.1$$

The instantaneous rise of θ_o to $\frac{\theta_I G_1}{1-\beta}$ on increasing the gain may now be seen to be i_{20} amplified by the gap amplification (G), in the absence of feedback. The subsequent onset of feedback then causes the progressive drifts observed. The time constant with which this feedback loop comes into operation must, to explain the observed phenomenon, be of the order of minutes. This is shown in the next chapter to be too long

to be explained in terms of gas phenomena and it is concluded that surface phenomena in the interelectrode gap are responsible.

The dependence of the rate of rise of the curves of figure 8.5 on the u.h.f. field, may be explained on this hypothesis since the rate of rise is controlled by loop gain, βG, as well as the loop time constant, τ. It is shown in Appendix 2 that the time to reach breakdown after applying a step to G (when $G\beta > 1$) is

$$\tau . \ell n \frac{1}{G\beta - 1} \qquad \ldots\ldots 8.2$$

Increase in the u.h.f. field is expected to increase the ionization rate and thus the gas amplification, G, so that from equation 8.2, the rate of rise may be expected to decrease.

It may be concluded, from the above, that the observed instabilities of i_2 may be completely explained in terms of a positive feedback mechanism with a time constant of the order of minutes. It remains to see whether such an hypothesis can also explain the observed variations of the initial gap current, i_{20}.

8.4 Analysis of the variation of i_{20} in terms of positive feedback

The initial gap current, i_{20}, is the current flowing across the gap when the drift field only is applied. Since there is no u.h.f. field there is no gas amplification and the current reaching the far electrode may then be regarded as the output of the feedback amplifier of figure 8.7 with G = 1.

The action of switching on the filament and subsequently monitoring i_{20}, is equivalent to applying an increasing step function to θ_I and monitoring θ_o which would then be given by (Appendix A2, equation A2.1)

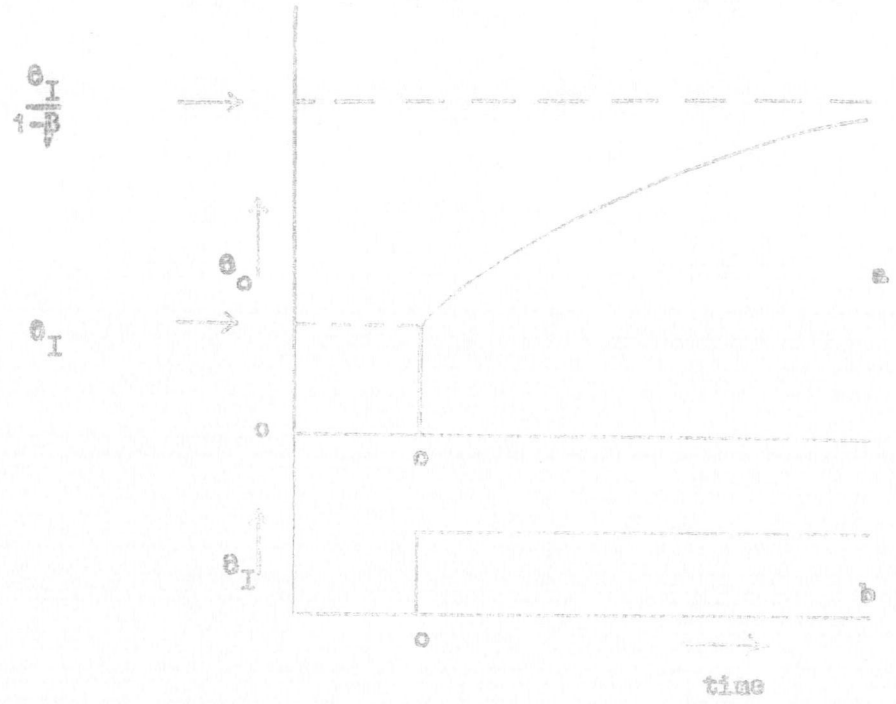

Fig. 8.9

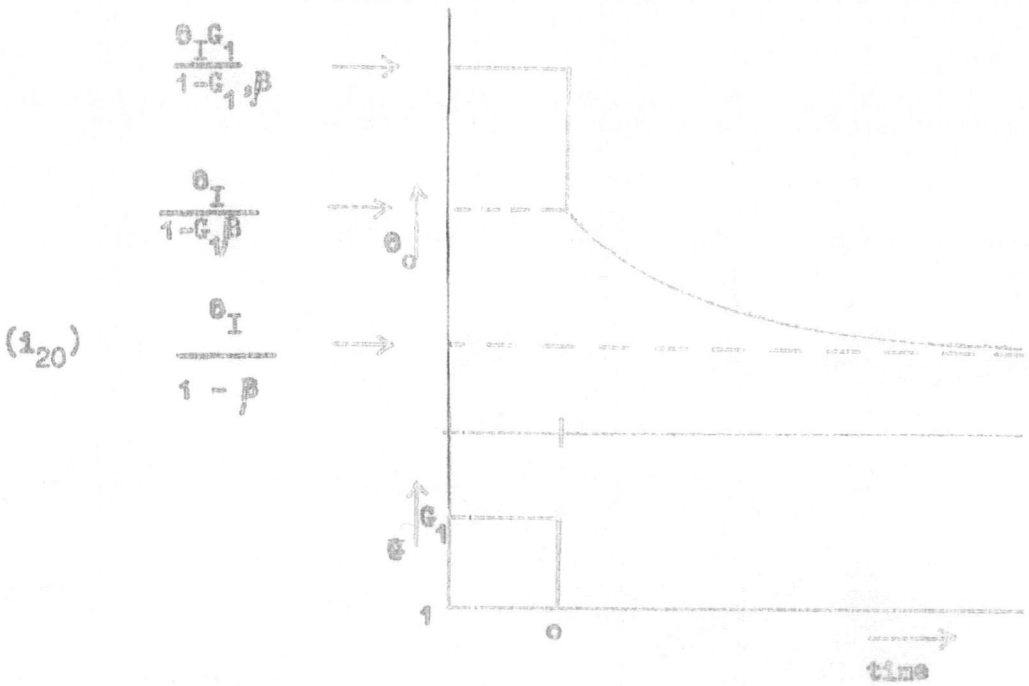

Fig. 8.10

$$\theta_o = \theta_I \frac{1}{1 - \beta(1 - \epsilon^{-t/\tau})} \qquad \ldots\ldots 8.3$$

Initially ($t = 0$), $\beta(1 - \epsilon^{-t/\tau}) = 0$ so that there is no feedback and $\theta_o = \theta_I$. Thus θ_I may be identified as the gap current in the absence of the postulated feedback mechanism. As t increases, the feedback loop provides an increasing input to the adder and θ_o gradually rises to a stable value of $\frac{\theta_I}{1-\beta}$ as t tends to infinity.

The resultant rise is shown in figure 8.9. Curve b shows the timing of the step waveform applied to the input (θ_I) and curve a shows the output which results (θ_o). This curve closely resembles the initial portion of figures 8.1 and 8.2. Thus, the initial rise of i_{20} on switching on the filament may be interpreted as a necessary consequence of the positive feedback mechanism cited to explain the instabilities of i_2, provided the phenomena giving rise to this mechanism are still present when ionization in the gap is absent.

The recovery of i_{20} following a period when ionization had occurred

When the u.h.f. field is removed, gas amplification by collision ionization may be expected to fall to zero. Thus, in terms of the simple circuit of figure 8.7, this may be regarded as a decreasing step applied to the amplifier gain, G, from G_1 to unity. When this occurs the loop time constant element will act as a storage element to retain the value of θ fed to the attenuator.

Assuming that steady conditions have been reached before the application of this step, this value of θ will be the maximum output, $\theta_{o(max)}$ which was eventually established when the u.h.f. field was

applied (figure 8.8 ~~xxxxx~~ c). Thus the feedback loop presents an input to the adder of $\beta\ \theta_{o(max)}$; so that the output, θ_o, which since $G = 1$ is the output from the adder, is $\left\{\theta_I + \beta\ \theta_{o(max)}\right\}$. Thus on application of the step function to G, θ_o falls instantaneously from (Appendix 2, equation A2.2)

$$\theta_{o(max)} = \frac{\theta_I G_1}{1-\beta G_1}$$

to

$$\theta_I + \beta\ \theta_{o(max)} = \frac{\theta_I}{1-G_1\beta}$$

As the time constant element recovers, the input to the attenuator decreases with time. The value of θ fed back thus decreases with time so that θ_o shows a progressive decrease. This will occur until the steady value,

$$\theta_o = \frac{\theta_I}{1-\beta}$$

is reached. Thus θ_o shows a time variation plotted in figure 8.10.

This curve corresponds closely to figure 8.3 representing the recovery of i_{20} after ionization has occurred in the gap. This suggests that the observed 'recovery' of i_{20} may be regarded as the recovery of the feedback loop controlling the instabilities of i_2. It would therefore appear that this again is a necessary consequence of the positive feedback hypothesis. Thus if there is some feedback mechanism containing a long time constant (of the order of minutes), and this appears to be necessary for an explanation of the instabilities of i_2, the observed variations in i_{20} described in figures 8.1, 8.2 and 8.3 are a necessary consequence.

8.5 Conclusions

The experimental fact that all the long time constant phenomena have time constants of the same order, suggests a common mechanism. The preceeding two sections show that, in principle, all these phenomena can be explained in terms of a single equivalent circuit with a positive feedback loop containing a time constant of a few minutes. In the next chapter a detailed argument is presented for considering the charging of insulating films over the electrode surfaces as the most likely mechanism by which this feedback is effected. There the loop time constant is seen to be the relaxation time of the film which is shown to control the time scale of each of these long time constant phenomena.

Further it will be seen that if $\beta = 0$, i.e. in the absence of feedback or in the absence of this film, none of these effects occur. Thus on this hypothesis, if one of these effects occur all are to be expected and if one is absent all the others may be expected to be absent. This is broadly true experimentally. In particular, if the initial rise of i_{20} is not observed, the instabilities of i_2 are likewise absent. However it is likely that the film is never completely absent, i.e. β may be small but never zero, so that certain effects may be observed, at small amplitude, even if the i_{20} rise was not evident to its usual extent. Hence in certain cases a slight rise of i_{20} after ionization is observed even in the apparent absence of the initial i_{20} rise and the instabilities of i_2. It may thus be concluded that β may vary widely from experiment to experiment, with corresponding

variation in long time constant effects. In the following chapter it is shown that these variations in β correspond to variations in film thickness.

It is important to point out that the circuit of figure 8.7 is not necessarily a rigorous equivalent circuit for the gap. Thus this analogue must not be pushed too far. Nevertheless, this circuit serves to illustrate the basic principles involved and to link the various observed effects by a single hypothesis of positive feedback.

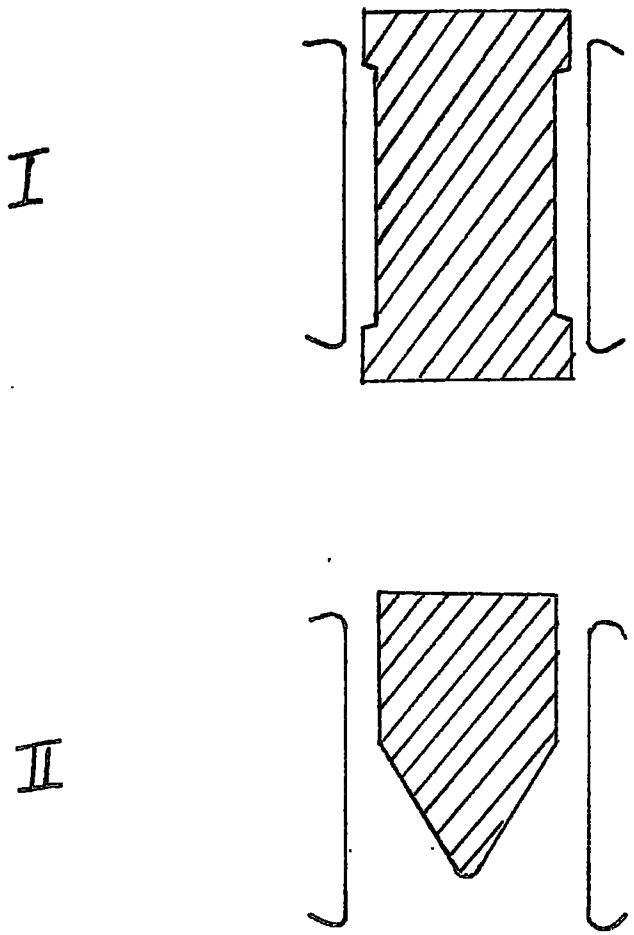

Fig. 9.1: The shape of the di-electric wedge. I is the plan and II the elevation as the wedge falls through the gap.

CHAPTER 9

POSSIBLE MECHANISMS OF POSITIVE FEEDBACK

It has already been suggested that the long time constant appears to be associated with the interelectrode gap itself, where possible mechanisms may involve the electrode surfaces as well as the gas. The longest time constant in the gas may be expected to be associated with some chemical change or with the production of metastables. However, no metastables have been found in hydrogen (at least in sufficient quantities to explain the observed effects) and the production of atomic hydrogen (Corrigan and Von Engel, 1958) would cause a change in gap current opposite to that observed. The time for such secondary products to diffuse out of the gap is expected to be of the order of milliseconds, and is thus too short to explain the observed time constants. It is therefore concluded that it is unlikely that any phenomenon in the gas is responsible for these effects.

To check this conclusion experimentally, a di-electric wedge was dropped through the gap to displace the slice of gas between the electrodes during the progress of each of the long time constant phenomena. The wedge was so shaped as not to make contact with the electrode surfaces in its passage through the gap (figure 9.1). However, no effect on the progress of any of the time functions could be found to suggest that the gas was playing an important role.

It is therefore thought likely that surface phenomena, rather than conditions in the gas itself, are responsible for the slow changes in the observed gap current. A mechanism whereby the drift

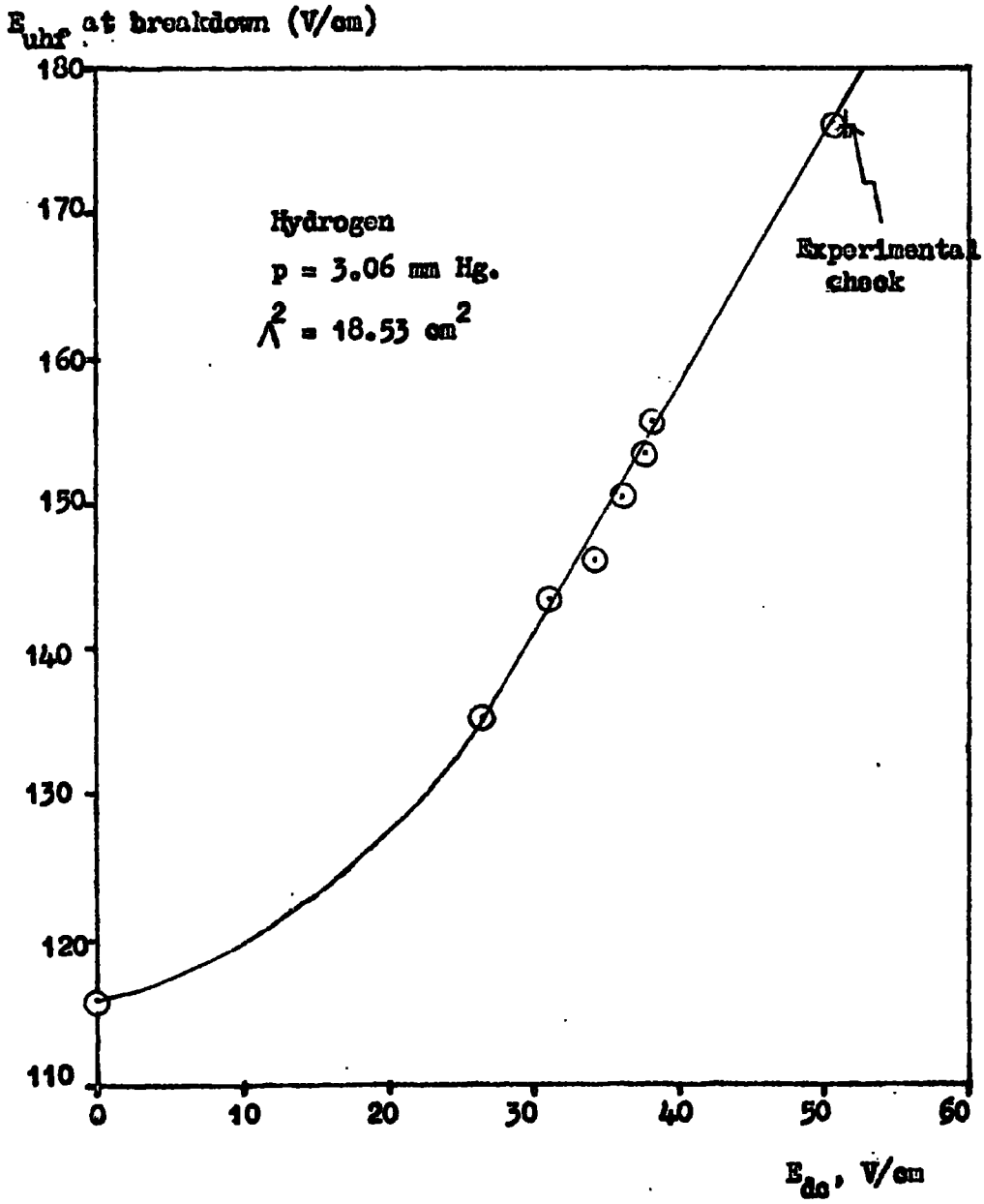
E_{uhf} at breakdown (V/cm)
180
170
160
150
140
130
120
110
0
10
20
30
40
50
60
E_{dc}, V/cm
Hydrogen
p = 3.06 mm Hg.
λ^2 = 18.53 cm^2
Experimental check

Fig. 9.2

field is progressively removed as a consequence of the charging of surface films by the unidirectional gap current, i_2, is presented in the succeeding sections.

9.1 The Effect of the Progressive Reduction of the Drift Field, E_{dc}

Varnerin and Brown (1950) have investigated the way in which a small unidirectional field alters the u.h.f. breakdown stress of a gap. By solving the appropriate differential equation, they have deduced that the breakdown condition for this case, is similar to that for the pure u.h.f. case, provided that the diffusion length, Λ, is replaced by a modified diffusion length, Λ_m, given by:

$$\frac{1}{\Lambda_m^2} = \frac{1}{\Lambda^2} + \left(\frac{E_{dc}}{2D/\mu}\right)^2 \qquad \ldots\ldots 9.1$$

From this equation Λ_m may be calculated for a given set of conditions. Using this in place of Λ, the value of breakdown stress may be obtained from the $p\Lambda$, $E\Lambda$ plots for pure u.h.f. breakdown. This has been done for hydrogen at a pressure of 3.06 mm Hg in a gap for which $\frac{1}{\Lambda^2} = 18.53$, and is shown in figure 9.2. There the values of μ/D were taken from Varnerin and Brown's results and the $E\Lambda$ - $p\Lambda$ plot used was that published by Brown ('Basic Data on Plasma Physics', Wiley 1959, p. 150). An experimental check point is shown, indicating that there is agreement between the breakdown stress calculated from the theory of Varnerin and Brown and the breakdown stresses obtained experimentally in the present apparatus.

This method was used to calculate the expected breakdown stress for cases where instabilities leading to breakdown occurred. For the

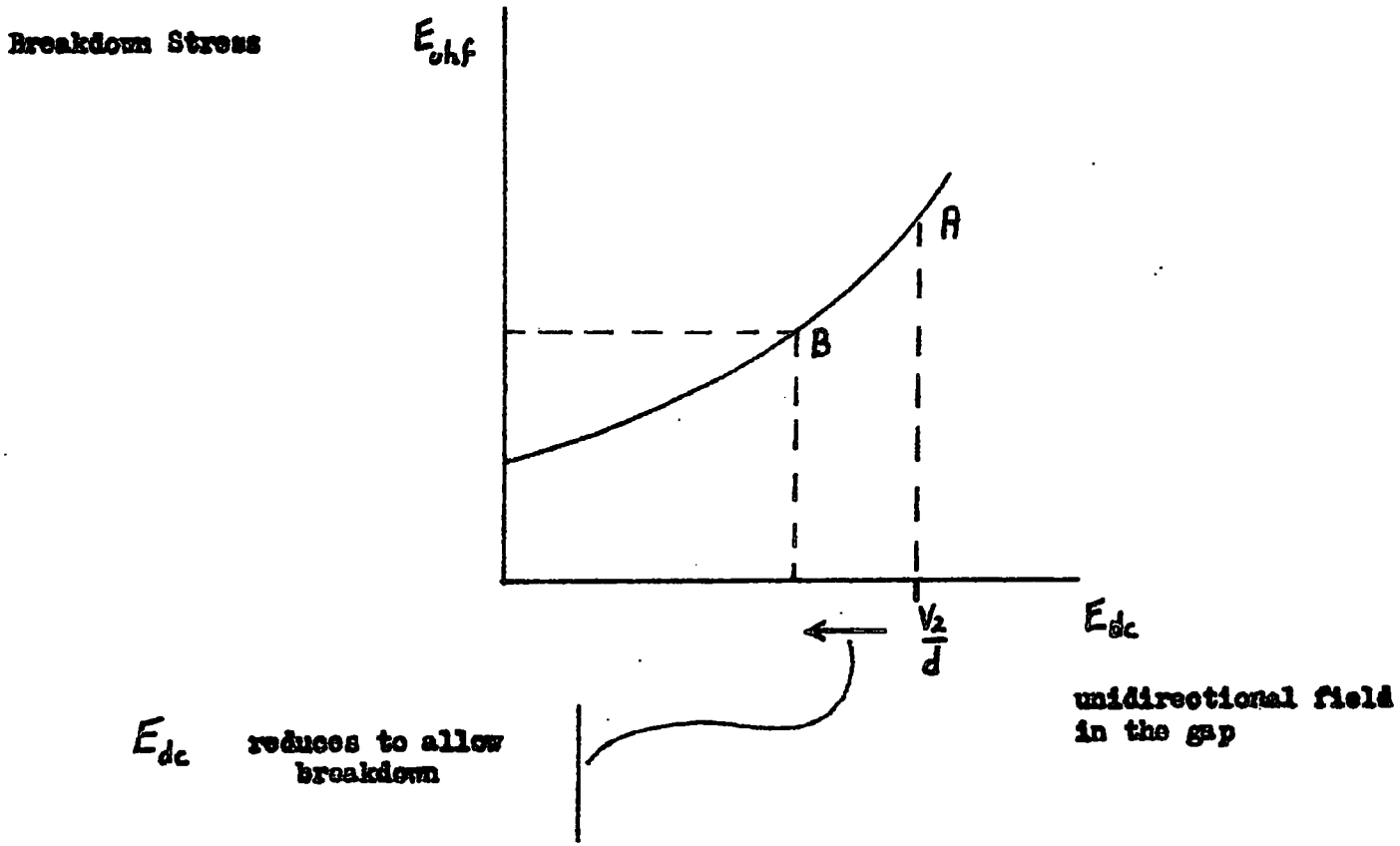
Breakdown Stress
E_{ohf}
A
B
$\frac{V_2}{d}$
E_{dc}
unidirectional field in the gap
E_{dc} reduces to allow breakdown

Fig. 9.3

particular case of figure 8.6, the applied E_{dc} was 32 V/cm, so that the expected breakdown stress may be calculated as 208 V/cm. However, figure 8.6 shows that instabilities resulting in breakdown occur above 149 V/cm. This is above the pure u.h.f. stress of 146.7 V/cm but much below that expected with the value of E_{dc} applied. In the absence of any change in the gas itself it is therefore concluded that some mechanism by which the unidirectional field is removed must operate to allow breakdown to occur.

Say that the applied voltage across the gap, V_2, corresponds to a point A on the Breakdown stress curve of figure 9.3, and the applied u.h.f. field to a point B. Under these conditions the u.h.f. field is too small to give breakdown. The field V_2/d must therefore be progressively removed so that E_{dc} runs to a value corresponding to point B and then breakdown occurs.

It now remains to explain the rise of amplification, prior to breakdown, on this hypothesis of unidirectional field removal. The observed amplification will be dependent on the extent of ionization in the gap and the partition of the electrons thus formed to the two electrodes. In what follows any change in the partition of electrons will be neglected. The observed electron amplification will then depend on the net rate at which an electron has an ionizing collision, ψ, and the time during which such an electron is in the gap, t_L. Thus,

$$A = f(\psi, t_L) \qquad \ldots\ldots 9.2$$

In the present case, E_{uhf} remains constant and is sufficiently large compared to E_{dc}, to say that E_{dc} contributes a negligible amount

to the electron energy. Thus, the electron energy and hence ψ may be regarded as constants during variations in E_{dc}.

Using the modified diffusion length defined by equation 9.1, the mean electron lifetime, t_L, at breakdown with a unidirectional field, E_{dc}, is:-

$$\frac{1}{D}\left\{\frac{1}{\Lambda^2}+\left(\frac{E_{dc}}{2D/\mu}\right)^2\right\}^{-1} \qquad \ldots\ldots 9.3$$

This applies to conditions just before breakdown in the absence of an injected electron stream. When amplification is high the electrons are generated predominantly in the body of the gas so that the injection of electrons may be regarded as a negligible perturbation of the system considered by Varnerin and Brown. Further their treatment applies to individual electrons, before the build up of space charge, which are the conditions expected in the present case.

Equation 9.3 shows that the electron lifetime may be expected to increase as the unidirectional field is reduced. Thus if it is postulated that E_{dc} is progressively reduced during the amplification changes of figures 8.4 and 8.5, a progressive increase in t_L is to be expected. Hence the electrons would be available for a longer time to ionize at the same rate so that the amplification would increase, as expressed by equation 9.2.

Substituting for t_L from equation 9.3 in equation 9.2 gives:-

$$A = f\left(\psi, \frac{1}{D}\left\{\frac{1}{\Lambda^2}+\left(\frac{E_{dc}}{2D/\mu}\right)^2\right\}^{-1}\right) \qquad \ldots\ldots 9.4$$

which expresses the way in which A varies as E_{dc} is progressively reduced.

To make quantitative estimates of the rise of amplification it is necessary to specify the form of the function of equation 9.4. As already stated the strict treatment of electron flow at high amplification has been found to be intractable. The following approximate treatment is therefore adopted.

If a current, i_e, is emitted into the gap from the emitting electrode, the number of these emitted electrons in the gap at any given time is $i_e t_L$. During the lifetime of these electrons, t_L, they will each create ψt_L new electrons. These in turn, each generate ψt_L other electrons during their lifetime and so on. Hence an electron cloud is built up in the gap over a period of time to give the total number of electrons, N, in the gap when the steady state is reached as:

$$i_e t_L + i_e t_L \cdot \psi t_L \cdot + i_e t_L \cdot (\psi t_L)^2 + \ldots.$$

summed to infinity.

Each of these electrons has a lifetime of t_L so that the rate of loss of electron from the gap is $\frac{N}{t_L}$ which may be evaluated by summing the above series to give,

$$\frac{i_e}{1-\psi t_L}$$

It is then possible to obtain an approximate expression for the gap transmission coefficient, defined by $T_g = \frac{i}{i_e^2}$, if it is assumed that the partition of these N electrons to the two electrodes is independent of E_{dc}. Then if γ is the fraction of N reaching the collecting electrode,

$$i_2 \approx \gamma \left\{ \frac{1}{1 - \psi t_L} \right\} \cdot i_e$$

and

$$T_g = \frac{i_2}{i_e} \approx \gamma \left\{ \frac{1}{1 - \psi t_L} \right\} \qquad \ldots\ldots 9.5$$

If the flow of electrons from the holes is assumed independent of gap conditions, i_e is constant, so that, remembering $i_e \propto i_{20}$,

$$A = \frac{i_2}{i_{20}} \propto \frac{i_2}{i_e} = T_g \qquad \ldots\ldots 9.6$$

The function of equation 9.4 may then be evaluated from equations 9.5 and 9.6 to give,

$$A \approx A_o \left[1 - \frac{\psi}{D} \left\{ \frac{1}{\Lambda^2} + \left(\frac{E_{dc}}{2D\mu} \right)^2 \right\}^{-1} \right]^{-1} \qquad \ldots\ldots 9.7$$

where, A_o is the constant of proportionality of equation 9.6. Equation 9.7 may be rewritten in the form

$$\frac{A}{A_o} \approx \frac{\frac{1}{\Lambda^2} + \lambda^2}{\frac{1}{\Lambda^2} + \nu^2} \qquad \ldots\ldots 9.8$$

where,

$$\lambda = \frac{\mu E_{dc}}{2D} \quad \text{and} \quad \nu^2 = \lambda^2 - \frac{\psi}{D} .$$

It is now possible to make a quantitative estimate of the change in E_{dc} required to account for the slow rise of amplification of figure 8.4. If E_{dc_1} is the initial field and E_{dc_2} is that remaining after equilibrium has been reached, equation 9.8 shows that,

$$\left(\frac{E_{dc}}{2D/\mu} \right)^2 \approx \frac{\frac{1}{\Lambda^2} \left\{ 1 - \frac{A_o}{A_2} \right\} - \frac{\psi}{D}}{\left\{ \frac{A_o}{A_2} - 1 \right\}} \qquad \ldots\ldots 9.9$$

where $A_o = A_1 \left[\frac{\frac{1}{\Lambda^2} + \nu_1^2}{\frac{1}{\Lambda^2} + \lambda_1^2} \right]$

and the suffixes 1 and 2 refer respectively to the values of these quantities initially and when equilibrium has been reached. If it is assumed that E_{dc1} is the applied unidirectional field of 32 V/cm the value of E_{dc2} may be calculated as 20 V/cm. This reduction of the drift field by 12 V/cm would suggest that such an hypothesis of progressive field removal could be tenable quantitatively.

Preliminary experimental measurements of amplification as a function of drift field have been made by Nicholls (1960) (figure 4.1) where a decrease of amplification with increasing drift field is evident at high amplifications. However, as the above theory suggests, the drift field present during experiments of this type is in doubt, so that direct measurement of the change in drift field for a given amplification change must be viewed with caution. However, measurements of this type do give support to the theory.

9.2 Surface Phenomena

It has already been suggested that surface phenomena are the most likely cause of the slow changes in gap current. These changes may be explained in terms of a slow partial removal of the drift field, if the electrode surfaces are covered by partially conducting dielectric films.

Thus it will be postulated that there are two dielectric films, distributed evenly ever each electrode. In the work that follows no properties will be assumed for the films other than to assume them to be leaky dielectrics, capable of representation by a parallel combination of a large capacitance, C_F, and large resistance, R_F. It will also

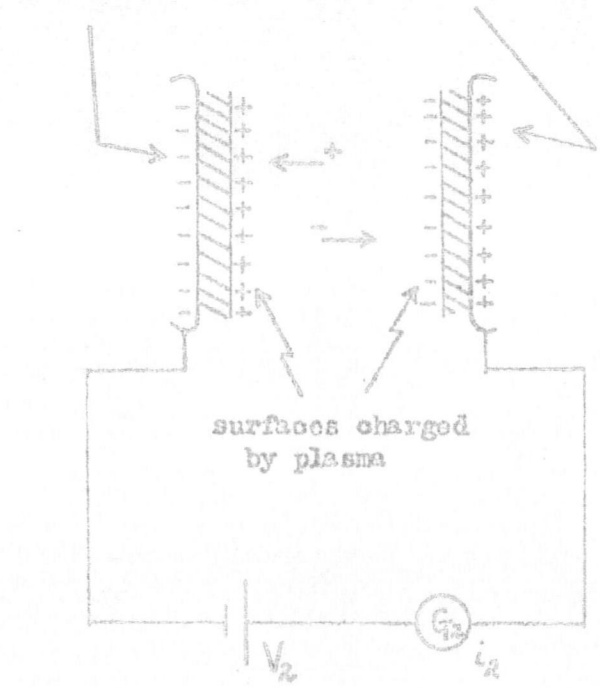

Fig. 9.4 The charging of surface films by ionization in the gap. The capacitance charges initially on the electrodes due to their self- are omitted.

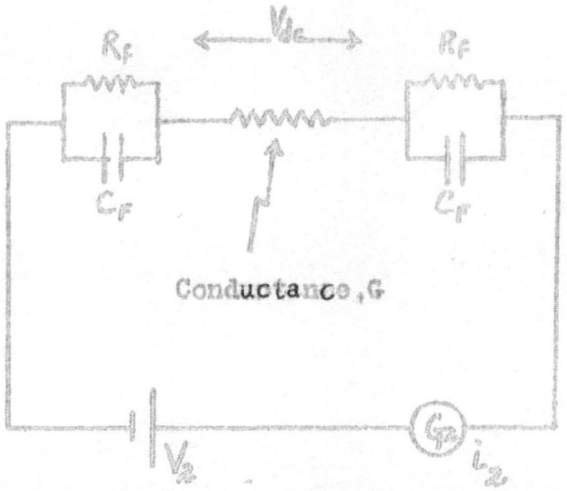

Fig. 9.5

be assumed that the electrodes are continuous i.e. that the presence of holes may be neglected.

When ionization occurs in such a gap with a small drift field applied, positive ions go preferentially to the cathode and electrons to the anode. Hence there is a net flow of charges onto the electrode surfaces which can only be neutralized by conduction through these surfaces. If the film resistance is assumed high the flow of such currents is severely limited so that there is a build up of charge on the surface of the film (figure 9.4). This charge is built up so as to progressively increase the unidirectional voltage dropped across the film. Since the overal unidirectional voltage, V_2, remains constant the gap voltage, V_{dc}, and thus $E_{dc}\left(=V_{dc}/d\right)$ are progressively decreased. It is therefore concluded that the drift field in such a gap may be expected to be progressively reduced by the flow of unidirectional gap current.

This current flow will, on the principle of continuity, be that in the external circuit i.e. i_2. Part of this current flows through the film leakage resistance, R_F, and the rest (that forming the surface charge) charges the film capacitance, C_F. Thus for low frequencies the gap may be represented by the equivalent circuit of figure 9.5. Here G represents the gap and is shown as a passive conductance to express the fact that a conduction path can be maintained by ionization under u.h.f. fields in the absence of a drift field. The gap capacitance is small and has therefore been neglected.

The voltage dropped across the two films in series will be called the polarization voltage, V_p. The rate of change of V_p will be the rate of charging of the leaky capacitors, C_F, by the current i_2, so that,

$$\frac{dV_p}{dt} = \frac{2}{C_F}\left(i_2 - \frac{V_p}{R_F} \right) \qquad \ldots\ldots 9.10$$

This equation may be solved for V_p by using the transform $V_p = V_p' \cdot \epsilon^{-\frac{2t}{\tau F}}$, and putting $V_p = 0$ at $t = 0$, to give,

$$V_p = \frac{2}{C_F} \cdot \epsilon^{-\frac{2t}{\tau_F}} \cdot \int_0^t i_2 \cdot \epsilon^{\frac{2t}{\tau_F}} \cdot dt. \qquad \ldots\ldots 9.11$$

where $\tau_F = C_F R_F$, the time constant by which a surface charge leaks through the film and will be referred to as the relaxation time. It is of interest to note here that the relaxation time is a characteristic of the film material only; for if C_F and R_F are expressed as functions of the permittivity, ϵ_F, the resistivity, σ_F, and the geometry of the film, it may be shown that $\tau_F = \epsilon_F \cdot \sigma_F$. The measurement of τ_F is thus significant in the determination of the film material.

The voltage across the gap, V_{dc}, at a time, t, after ionization began is therefore,

$$V_{dc} = V_2 - \frac{2}{C_F} \cdot \epsilon^{-\frac{2t}{\tau_F}} \cdot \int_0^t i_2 \cdot \epsilon^{\frac{2t}{\tau_F}} \cdot dt. \qquad \ldots\ldots 9.12$$

Here, V_2 is the initial voltage across the gap and factors of 2 in the

final term allows for the fact that there are two equal films. This equation expresses the way in which the drift field, V_{dc}/d, is expected to be progressively reduced by the flow of unidirectional current.

This current, i_2, is controlled by the discharge itself and is the result of the application of this drift field $\left(V_{dc}/_{d}\right)$ to the discharge. The flow of current across the gap is dependent on the electron flow pattern in the gap, which is essentially a balance between drift and diffusion rates. This problem has been analysed in detail in Chapter 6, but quantitative evaluations of the electron flow pattern for amplification greater than unity have been found to be intractable. It is therefore necessary to confine discussion to the case when the amplification is high, and to take the approximate results of the previous section, where changes in the partition of electrons are neglected. The amplification and thus the gap current, is there shown to increase as the drift field decreases. The effect of gap conditions on the flow of charge carriers in the gap may thus be expressed in the relation, $i_2 = i_2 (E_{uhf}, V_{dc})$ or referring to figure 9.5 by $G = G (E_{uhf}, V_{dc})$.

A possible feedback mechanism which could explain the amplification rise of figures 8.4 and 8.5 may now be seen to be as follows. Following the loop round, a change in u.h.f. field will increase i_2. This causes an increase in V_p and thus a decrease in V_{dc}, with a time constant defined by both film characteristics and the current flow in the gap (as defined by equation 9.12). This decrease in drift field

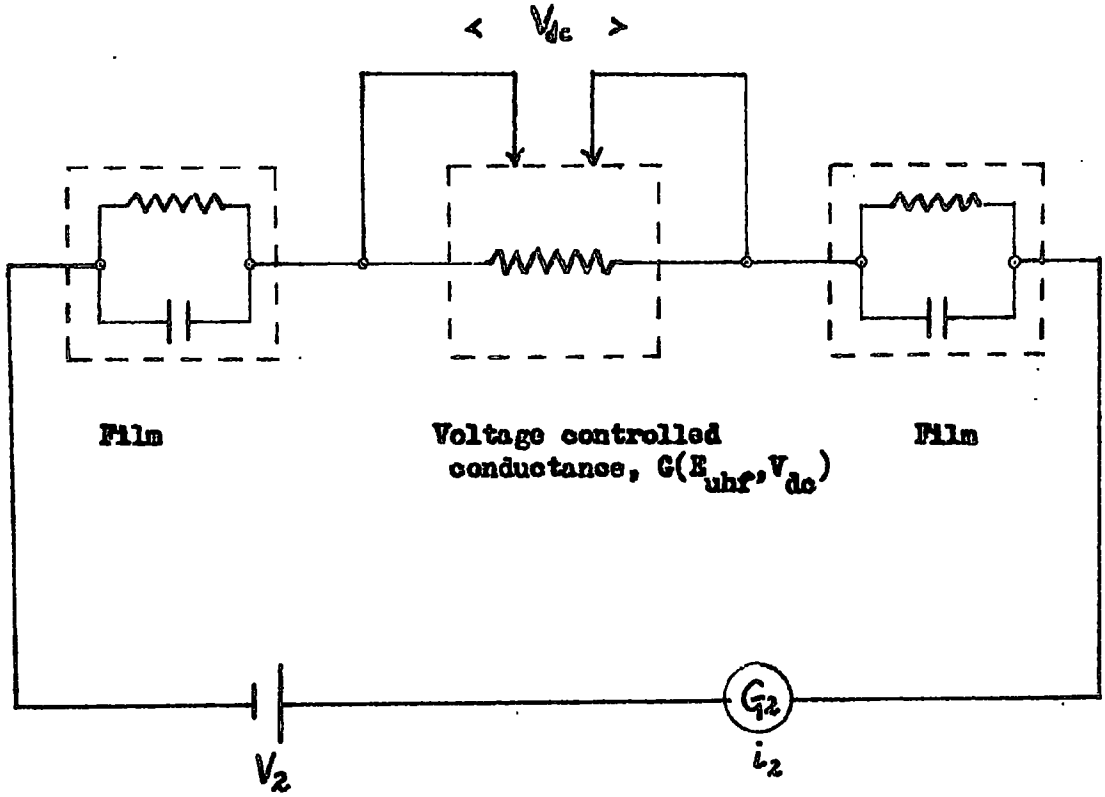
< V_{dc} >
Film
Voltage controlled conductance, $G(E_{uhf}, V_{dc})$
Film
V_2
G_{12}
i_2

Fig. 9.6

$\left(V_{dc}/d\right)$ results in an increase of electron lifetime in the gap and thus a rise in amplification as indicated by equation 9.8. This implies an increase in gap current closing the positive feedback loop.

The equivalent circuit of figure 9.5 may be extended to show this feedback loop. Figure 9.5 already includes the mechanism by which V_{dc} is varied by i_2. It therefore remains to include the effect of this charge of V_{dc} on the electron flow pattern in the gap. This may be included by replacing the gap conductance, G, by a voltage controlled conductance, $G\ (E_{uhf},\ V_{dc})$ as shown in figure 9.6. The gap conductance represents the $i_2 - V_{dc}$ characteristics of the gap which may be derived from equation 9.8 as

$$i_2 \approx i_{20} A_o \frac{\frac{1}{\Lambda^2} + \lambda^2}{\frac{1}{\Lambda^2} + \nu^2} \qquad \ldots\ldots\ 9.13$$

N.P.
//Since the surfaces are charged by the flow of gap current it is to be expected that the time constants associated with the removal of drift field will be dependent on electron flow in the gap. Thus the time constant is expected to be dependent on gap conditions e.g. gas, pressure etc. In particular, for a given drift field the gap current, i_2, has been shown experimentally (Chapter 4) to increase with u.h.f. field applied. Thus the polarization voltage is expected to build up more rapidly at higher u.h.f. fields so that the time constant associated with the removal of the drift field will decrease. This has been confirmed experimentally.

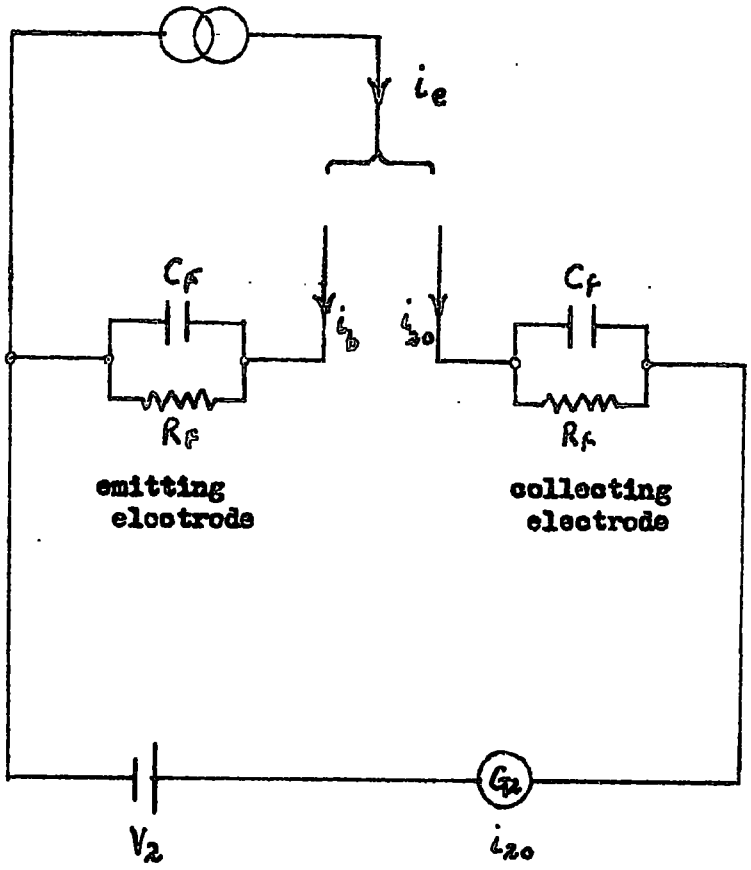
i_e
C_f
i_b
i_{20}
C_f
R_f
R_f
emitting electrode
collecting electrode
V_2
G_2
i_{20}

Fig. 9.7

The hypothesis of drift field removal by the charging of insulating surface films, would therefore explain the instabilities observed in the amplification. It remains to obtain independent evidence for surface polarization. Experiments designed to attempt this are described in the next chapter. In the meantime the drift of the initial gap current, i_{20}, will be considered in terms of the above hypothesis.

9.3 A possible Explanation of the Observed Drifts in the Initial Gap Current, i_{20}.

The feedback mechanism of the previous section is applicable to cases when ionization and thus amplification is high. The present section will deal with the case when the probability of ionization is so small that the injected current gives rise to current flows consisting mainly of electrons.

The electron flow under such conditions has been analysed in detail in Chapters 5 and 6. There it is shown that of the current injected, i_e, the majority diffuses back to the emitting electrode to give a back diffusion current of i_B. The remainder, a fraction T_g, crosses the gap and forms the current, i_{20}. It may be shown that the gap transmission coefficient, T_g, and thus i_{20}, increase with the drift field in the gap. $\left(V_{dc}/d\right)$.

The currents, i_{20} and i_B, consisting mainly of electrons, flow to the collecting and emitting electrodes respectively (figure 9.7) so that the films on both these electrodes become negatively charged. The voltage, V_c, dropped across the collecting electrode film will be so

directed as to reduce the gap voltage and that across the emitting electrode/film, V_e, to increase the gap voltage. Thus,

$$V_{dc} = V_2 + V_e - V_c \qquad \ldots\ldots 9.14$$

It may be shown (Chapter 5) that $T_g \approx \frac{1}{10}$, thus the current, i_B, is much larger than i_{20}, so that V_c is small compared to V_e and equation 9.14 shows that the flow of these currents result in an increase in V_{dc}. Thus on switching on the filament i_e is established and the gap voltage (and thus the drift field) progressively increased by the predominant charging of the emitting electrode surface by the current, i_B.

When ionization is small and a drift field only acts, the expression for T_g (equation 6.25) may be further approximated to give

$$T_g \approx \frac{\epsilon^{\alpha d}}{\epsilon^{\alpha d} + \frac{d}{2b}\,\epsilon^{-\lambda b}} \qquad \ldots\ldots 9.15$$

where, α is Townsend's first ionization coefficient. This shows that the slow rise in drift field results in a slow increase in T_g and thus a progressive increase of i_{20}. Hence the initial rise of i_{20} shown in figures 8.1 and 8.2.

The increase in i_{20} of figure 8.2 corresponds to an increase of T_g by a factor of 1.47. From equation 9.15 it may be shown that this corresponds to a change in E_{dc} from the applied field of 32 V/cm to approximately 70 V/cm, when T_g changes from .085 to .125. Thus it may be concluded that the initial rise of figure 8.2 may be explained by the progressive increase of E_{dc} resulting from the gradual build up

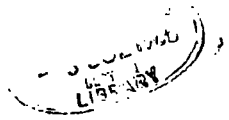

of a polarization voltage of approximately 38 volts.

When the steady state is reached all the current flows through the film resistances so that $V_e = i_B R_F$ and $V_c = i_2 R_F$. Thus remembering that $T_g = \frac{i_{20}}{i_e}$, equation 9.14 gives the gap voltage in the steady state as,

$$V_{dc} = V_2 + R_F\, i_{20_{eq}} \left(\frac{1}{T_{g_{eq}}} - 2\right) \qquad \ldots\ldots 9.16$$

where, $i_{20_{eq}}$ and $T_{g_{eq}}$ are the steady values corresponding to a field in the gap of $V_{dc}/_{d}$. A value of the film resistance, R_F, may be calculated from this equation. For the case of figure 8.2 R_F is found to be approximately $10^{10}\Omega$.

Equation 9.16 shows that the value of V_{dc} is controlled by the film resistance. From this equation it may be shown that, at low amplifications the higher this resistance, the more the polarization voltage and thus the larger the value of E_{dc} at equilibrium. Hence, (equation 9.15) $i_{20_{eq}}$ may be expected to increase with increasing film resistance. The varying extent of the i_{20} rise, observed experimentally, may therefore be accounted for by variation in R_F from experiment to experiment. This is expected to imply a variation in film thickness.

Further, the instabilities in amplification depend on the resistance of the film being high. Hence the resistance of the film links the instabilities of amplification with the initial drift of i_{20}. Thus in the absence of a rise of i_{20}, R_F must be small and thus little or no instabilities of amplification would be expected. This link has been observed experimentally in that instabilities most often occur after a large rise of i_{20}.

It should be noted that the feedback mechanism here is somewhat different from that at high amplification. When ionization is small the current, i_{20}, is related to the unidirectional field by the gap transmission coefficient of equation 9.15. This shows that i_{20} decreases (and i_B increases) with decreasing unidirectional field, E_{dc}. This is the reverse to that which occurs at high amplification, where i_2 increases with E_{dc}. However, there is still an overal positive feedback as a consequence of the predominance of i_B.

CHAPTER 10

EXPERIMENTAL DETECTION OF SURFACE POLARIZATION

In the previous chapter it has been suggested that insulating surface films exist on the electrodes which can be charged by the flow of unidirectional gap current. In the present chapter methods will be described by which the resultant polarization voltage may be measured experimentally, and various predictions from this hypothesis verified.

In the work to be described the filament is inoperative and there is no injected current. (The flow of gap current is caused by running a u.h.f. discharge in the gap). Apart from this, the apparatus is as described previously (Chapters 2 and 3).

If the films are initially uncharged and a voltage V_2 is applied to the gap, the resultant field in the gap, E_{dc}, will be the geometrical field V_2/d. The u.h.f. breakdown stress is therefore expected to be that corresponding to this field (V_2/d). However, if the gap is broken down, some unidirectional current will flow and the surface films will charge up to some polarization voltage, V_p. Thus the gap voltage, V_{dc}, will be reduced to $(V_2 - V_p)$. On terminating the discharge the residual drift field is $(V_2 - V_p)/d$ so that subsequent u.h.f. breakdown stresses are correspondingly modified.

Thus a gap with insulating films over the electrodes is expected to have two types of breakdown stress. The initial breakdown stress corresponds to zero polarization voltage and subsequent or secondary breakdown stresses are dependent on the polarization voltages.

Determination of a secondary breakdown stress may be used to measure the polarization voltage, V_p. It has been pointed out in the previous chapter, that it is possible to derive the breakdown stress with a superimposed drift field from breakdown data for the pure u.h.f. case using the modified diffusion length given by equation 9.1. Similarly for a given pressure and breakdown stress, the modified diffusion length may be derived from the $E\Lambda$, $p\Lambda$ plot for pure u.h.f. breakdown. Using this value of the modified diffusion length, it is possible to calculate the drift field from equation 9.1, and thus V_p from the relation

$$E_{dc} = \frac{V - V_p}{d}$$

These methods were applied to deduce the polarization voltage from a series of measurements of u.h.f. breakdown fields. Experimental results described in the present chapter will be confined to similar conditions to those present in the preceeding chapters so that an indication of the presence of surface polarization here is evidence for the presence of such polarization in the previous work.

10.1 Measurement of the relaxation time

If a film is charged and the charging current ended, the charge slowly leaks through the internal resistance of the film, R_F, with a time constant of the relaxation time of the film. Thus the relaxation time of the film, $\tau_F = C_F R_F$, can be determined by measuring the u.h.f. breakdown stress after successive time intervals and using these to calculate the potential drop across the film and so its variation with time.

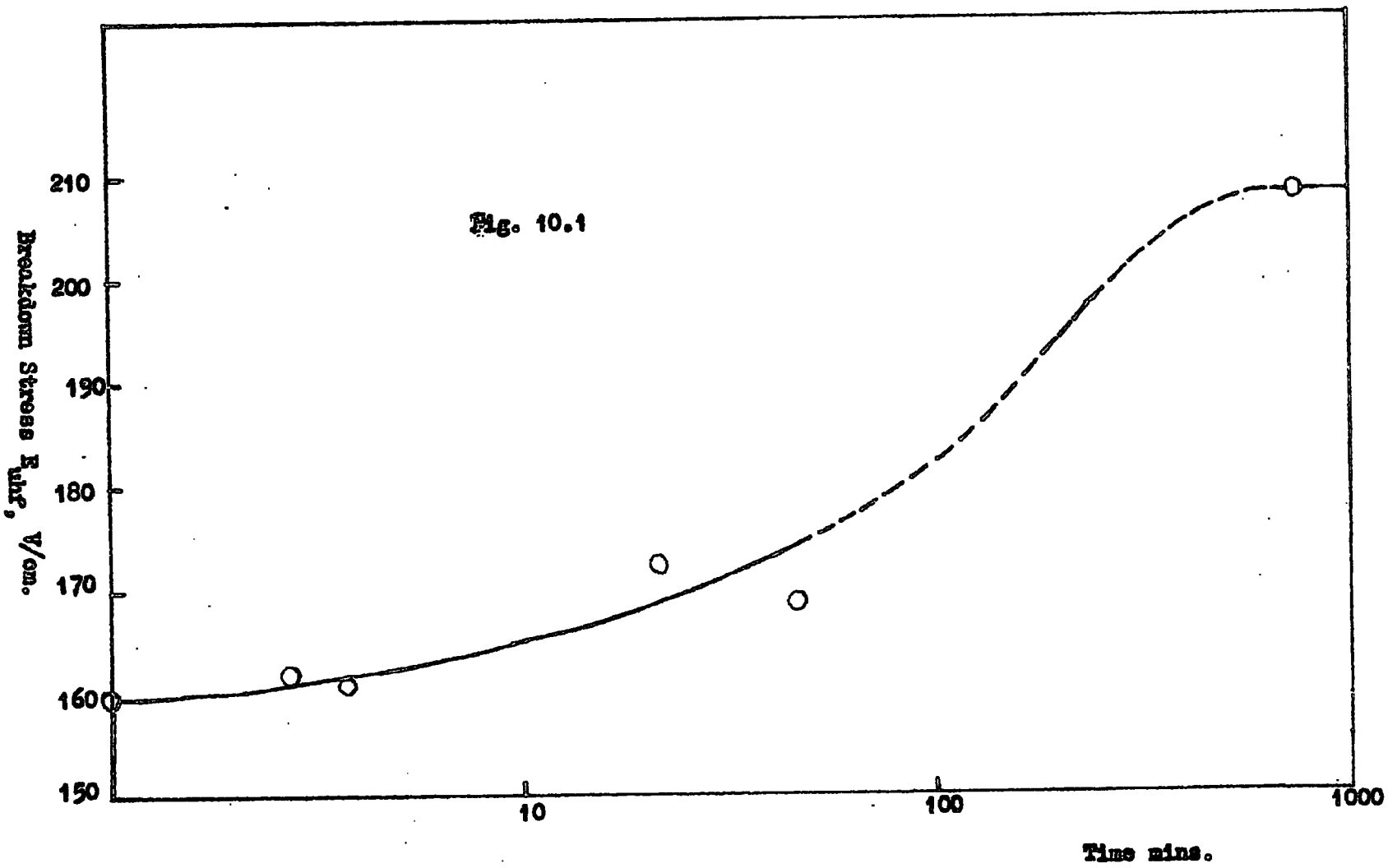
Fig. 10.1
Breakdown Stress E_{bd}, V/cm.
210
200
190
180
170
160
150
10
100
1000
Time mins.

A typical plot of u.h.f. breakdown stress as a function of the time after the termination of a previous discharge is shown in figure 10.1. When this time is short the secondary breakdown stress is seen, in this case, to be close to that for the pure u.h.f. case, indicating that the resultant drift field is nearly zero. As the time increases the film gradually discharges and the drift field approaches its geometrical value of V_2/d. In this case the relaxation time is seen from figure 10.1 to be approximately 3 hours.

The initial breakdown stress referred to above is that for zero polarization voltage and thus corresponds to that approached when the time between successive discharges is large (i.e. 209V/cm on figure 10.1). This is found to agree with the breakdown stress expected when the polarization voltage is zero, i.e. the breakdown stress corresponding to a drift field of V_2/d. Figure 10.1 serves to demonstrate that the initial and secondary breakdown stresses are clearly distinguishable experimentally.

The secondary breakdown stress measured immediately after a discharge was found to vary widely from film to film. The range of values was found to extend from that corresponding to zero drift field up to that with $E_{dc} = V_2/d$ when no polarization was detectable.

When the drift field, E_{dc}, is so small (< 5 volts/cm) that it scarcely competes with diffusion as an electron removal mechanism, the u.h.f. breakdown stress is indistinguishable from that when $E_{dc} = 0$. The indication of a breakdown stress corresponding to pure u.h.f.

breakdown does, therefore not necessarily mean that $E_{dc} = 0$, but that $E_{dc} < 5$ volts/cm.

It is expected that E_{dc} cannot be reduced to zero by the charging of surface films, since some charge will leak through the film resistance which must be replaced by a unidirectional current flow across the gap. This necessitates some remaining drift field to just unbalance the discharge sufficiently to supply this unidirectional current. Further it follows that the higher the film resistance, the less unidirectional leakage current flow and the less residual unidirectional field across the gap. This implies that the higher the polarization voltage, the higher the film resistance. From observation on the secondary breakdown stress it is thus possible to get some idea of the film resistance. Likewise the variation in this stress from experiment to experiment may be attributed to variation in film resistance. This agrees with the conclusion in section 9.3 that similar variations of the instability and drift of gap current result from variations in film resistance.

10.2 Cyclic application of E_{dc}

If after charging the film, the discharge is terminated and V_2 is reduced to zero, the polarization voltage, V_p will be left across the film and will give rise to a field of $E_{dc} = -V_p/d$ in the gap. If $V_p \approx V_2$, the breakdown stress should then equal the initial stress with the film discharge and V_2 applied across the gap.

Experiments carried out in this way confirm this view. Figure 10.2 shows time plots of the sequence of operations used and results obtained.

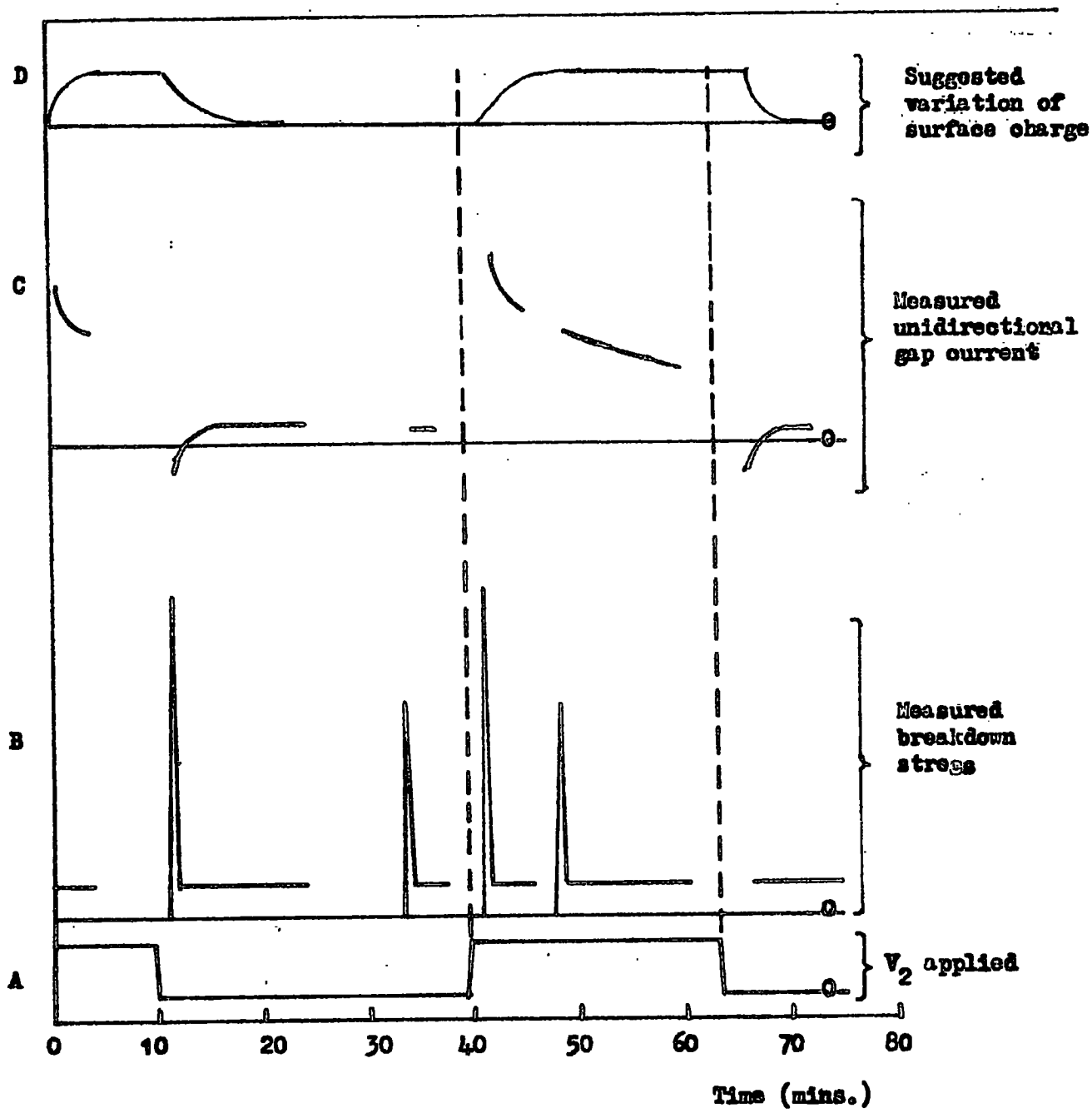

Fig. 10.2 Vertical scales arbitrary

Curve A shows how the applied unidirectional gap voltage, V_2, is varied, and Curve B shows the u.h.f. field to give breakdown and subsequently to maintain the discharge. The gapsin this curve correspond to termination of the discharge and the peaks are the breakdown values. Curve C shows the observed unidirectional current flow, i_2, which represents the film charging current, while Curve D gives a diagrammatic representation of the suggested charge variation on the electrode surfaces.

Starting on the left of figure 10.2 ($t = 0$), the film is charging as a consequence of the field E_{dc}, applied to the maintained discharge. Curve C shows the charging current. After 5 mins. the discharge is terminated and at 10 mins. V_2 is reduced to zero, so that a unidirectional field of $-V_p/d$ is left across the gap. The next breakdown stress corresponds as predicted to a drift field of V_2/d since $V_p \approx V_2$. Curve C shows the film discharging as the polarization is reduced by the flow of gap current in the reverse direction to normal since the field is opposite to normal. A subsequent breakdown measurement (33 mins.) thus corresponds to the pure u.h.f. case. This suggests that a discharge in the gap in the absence of an applied unidirectional field can remove surface polarization and reduce V_p/d to less than 5 volts/cm.

At 40 mins., V_2 is reapplied and the breakdown stress corresponds to V_2/d. For this value of E_{dc} the breakdown stress is more critically dependent on the drift field; thus V_p/d is zero to within less than 0.1 volt/cm. Thus it may be concluded that a discharge in the absence of

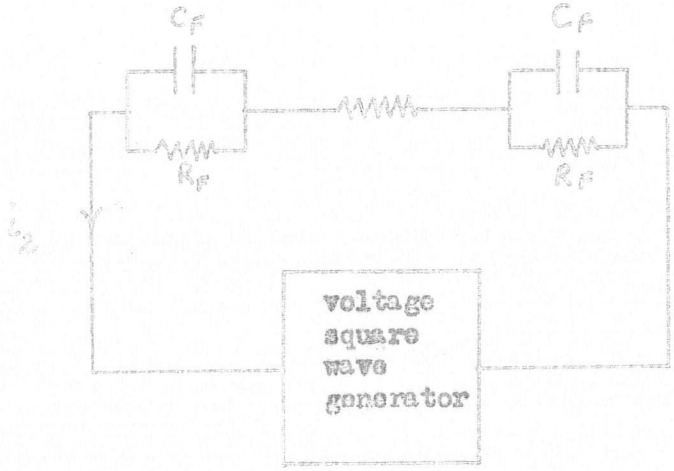

a.

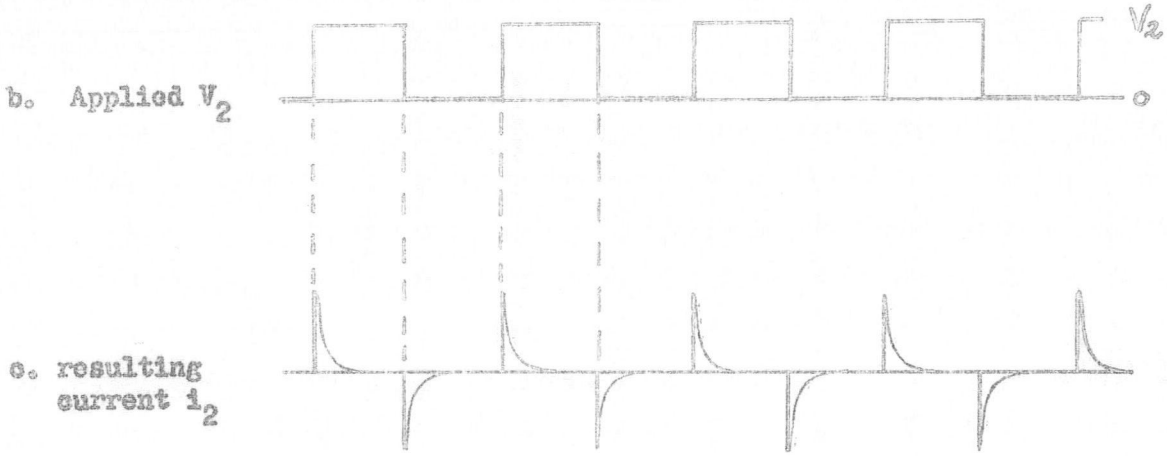

b. Applied V_2

c. resulting current i_2

Fig. 10.3

a drift field removes the surface polarization. This is as expected since a pure u.h.f. discharge between similar electrodes is essentially a symmetrical system, with no net flow of charge carriers across its boundaries and thus no net flow of charging current.

After this breakdown (42 mins.) the film is recharged by the current i_2 (Curve C) so that a subsequent discharge is that for the pure u.h.f. case. At 64 mins., V_2 is again removed and the conditions at the beginning of this sequence are re-established. This sequence may be continued indefinitely with similar results.

It was shown in the previous chapter how the gap could be represented by the equivalent circuit of figure 9.5. In the present experiment the battery supplying V_2 has effectively been replaced by a square wave generator, figure 10.3a. Thus the current waveform should be similar to the differential form of these applied square waves (figure 10.3b). The similarity of this waveform with that of Curve C is immediately apparent.

10.3 Calculation of film constants

From information gained from these experiments it is possible to derive values for the internal resistance of the film, R_F, its capacitance, C_F, and an approximate value of the film thickness, d_F. As before it is assumed that there are precisely similar uniform films completely covering the opposing faces of the electrodes.

In the previous chapter an expression was derived for the polarization voltage, V_p, in terms of the film capacitance and the unidirectional gap current, i_2, (equation 9.12) as

$$V_p = \frac{2}{C_F} \cdot \epsilon^{-\frac{2t}{\tau_F}} \int_0^t i_2 \cdot \epsilon^{\frac{2t}{\tau_F}} \cdot dt \qquad \ldots\ldots 10.1$$

In the above experiments, V_p is measured from breakdown measurements, i_2 as a function of time while the film is charging and the relaxation time, τ_F, from measurements similar to these of figure 10.1. It is therefore possible to evaluate C_F from equation 10.1.

Since the film may be expected to be very thin the width of the charge layer may be expected to be of the order of film thickness, d_F. Thus a value of d_F calculated from C_F by assuming the film to be equivalent to a parallel plate capacitor, must be regarded as an effective thickness. The true thickness is probably a few Ångström units greater than this. Nevertheless such calculations provide a useful indication of film thickness, but require some assumption as to the relative permittivity of the film material, ϵ_F. Further, the relaxation time is $C_F R_F$ so that it may be used to calculate the resistance of the film and its resistivity, σ_F, since the effective dimensions of the film are known.

In the particular case of experiments described in this chapter, the properties of the film assumed present, were as follows.

$$C_F = 3500 \text{ pF}$$

$$\epsilon_F/d_F = 1.8 \times 10^7 m^{-1}$$

Assuming $\epsilon_F \approx 1$, $d_F \approx 500$ Å

$$R_F \approx 10^{12} \Omega$$

$$\sigma_F \approx 10^{18} \Omega.\text{cm}.$$

It is thus concluded that in this typical case, the experimental observations are explicable with a film 500 Å thick, with a resistivity of $10^{18}\Omega.cm$.

Values of R_F are found to vary widely from film to film, probably corresponding to variations in thickness. The values of R_F obtained here may be compared with those calculated from the initial rise of i_{20} (Chapter 9 section 9.3). Thus in the particular case of the rise of i_{20} shown in figure 8.2, R_F has been shown to be $1.4 \times 10^{10}\Omega$. This value and that above are within the range of R_F observed experimentally. This illustrates the range of R_F which may be observed from experiment to experiment. Reasonable agreement has been found between the values of R_F calculated from the initial rise of i_{20}, and by the present method, confirming the hypothesis of the presence of a film.

10.4 Use of the ellipsoid field meter

An alternative measurement of the field in the gap and thus the polarization voltage, may be made using the ellipsoid field meter already described. This instrument may be calibrated in terms of known unidirectional fields and subsequently used for direct measurement of the field resulting from the polarization voltage, V_p.

Calibration is carried out by discharging the film and applying known unidirectional voltages across the gap when the field is the geometrical field V_2/d. The film may be discharged by allowing sufficient time for the charge to leak through the internal resistance of the film. Alternatively, when the relaxation time is too long for this to be

convenient, a u.h.f. discharge may be run without an applied unidirectional gap voltage, when the film should be discharged as a consequence of the symmetry of a pure u.h.f. discharge as described previously.

The method of measurement is to run a discharge in the presence of an applied drift field, terminate the discharge and remove the applied voltage. Any drift field remaining is then due to surface polarization only, and may be measured with the field meter.

As a consequence of the square law nature of this instrument, it is relatively insensitive at small values of field strength. This may be overcome to a large extent by using a thinner fibre, which reduces the torsional control and thus increases the sensitivity. However, the frequency of oscillation and thus the calibration, then becomes critically dependent on the amount of damping and thus on the gas pressure. An alternative solution, which has been applied in many experiments, is to use the fact that a small change in field strength is more easily detectable at higher field values. Thus the field in the gap is reinforced by effectively increasing the gap voltage before measurements are made.

Fields measured with the ellipsoid fieldmeter agree completely with those obtained by breakdown stress measurements. This is true independently of the way in which the film is discharged for calibration purposes. Thus there is complete confirmation of the previous work, and, therefore, considerable evidence for surface polarization.

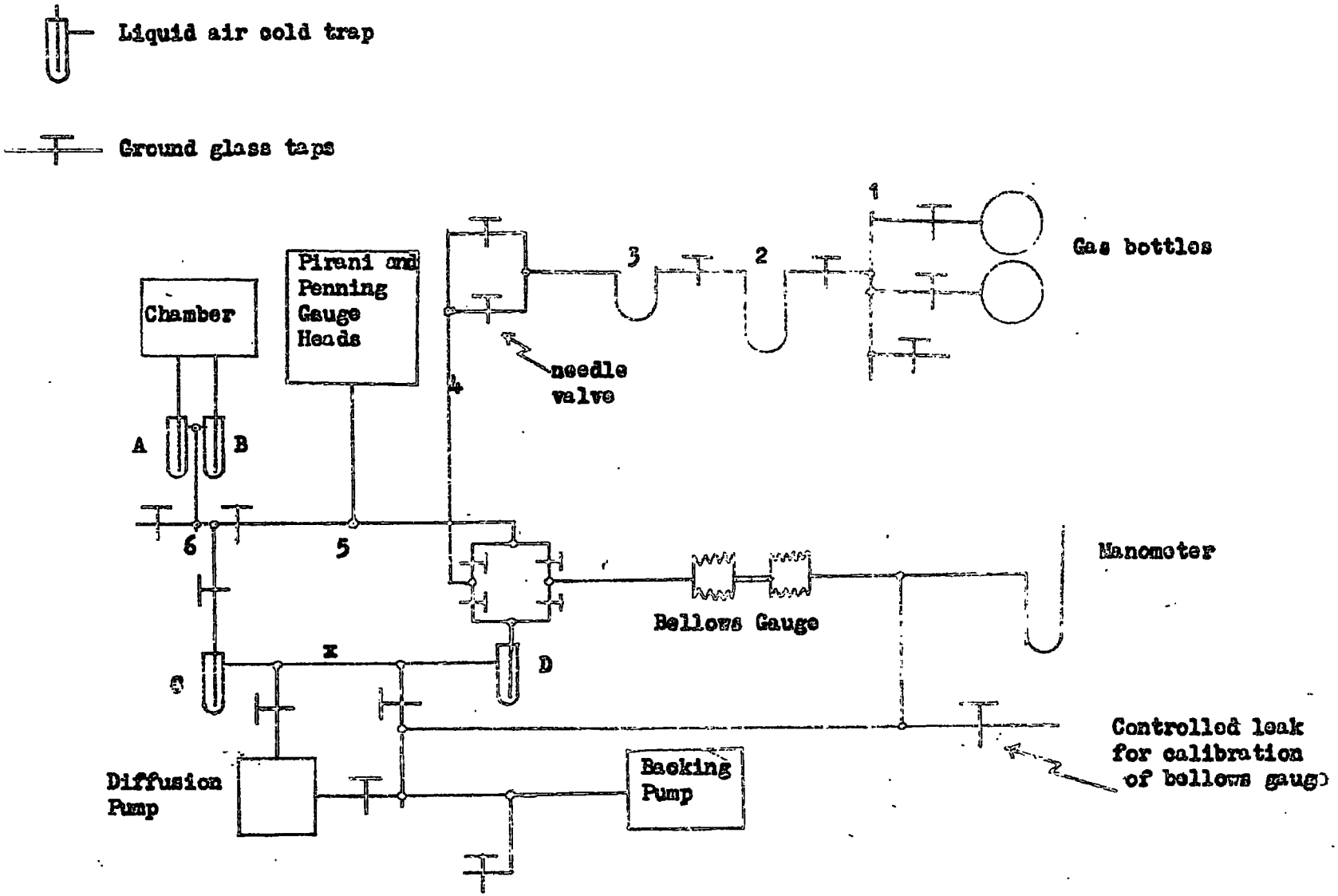
Liquid air cold trap
Ground glass taps
Chamber
Pirani and Penning Gauge Heads
needle valve
Gas bottles
Manometer
Bellows Gauge
Controlled leak for calibration of bellows gauge
Diffusion Pump
Backing Pump
A
B
C
D
x
1
2
3
4
5
6

Fig. 11.1

CHAPTER 11

THE FORMATION AND REMOVAL OF SURFACE FILMS

Evidence having been found for the presence of surface films, the present chapter will deal with attempts to remove them and avoid their formation.

In the experiments described so far, Apiezon greasewas used in the taps, Apeizon oil in the Diffusion pump and Amyl Acetate had been used for deposition of the oxide coating on the filament and cleaning the electrodes. It was felt that these substances, present as impurities in the system, might be responsible for the present of an insulating surface film. To reduce the partial pressures of these impurities a more efficient system of cold traps was therefore considered desirable. Since at this point in the work the apparatus was moved to a new laboratory, the opportunity was taken to redesign the vacuum system completely. This system is shown in figure 11.1 and was used throughout the work that follows.

The basic principles used in the design of the new system were as follows.

1. The chamber was isolated from the pumping system by a cold trap (c in figure 11.1). This was to prevent back-flow of impurities i.e. oil vapours etc. into the chamber.
2. A system of cold traps (A and B) was placed close to the chamber to trap any impurities that were released from surfaces during an experiment.
3. The pumping line was shortened, so that the diffusion pump was as

close as possible to the chamber. This allowed more rapid pumping so that the chamber could be isolated from the pumping system by a stop-cock sooner, and thus there is less time during which the flow of vapours from the pump might contaminate the chamber.

4. The gas pipetting and the pressure measuring systems were isolated from the chamber by cold traps (A and B) to prevent exchange of vapour impurities between these sections. To further facilitate this, separate pumping lines were used to the gas pipetting and the pressure measuring systems (via D) and the chamber (via C). Each of these lines contained a cold trap to minimise enchange of vapours via the pumping system. In particular the system was arranged to prevent Acetate vapour from the electrodes in the chamber from contaminating the whole system.

5. Provision was made to introduce gas into the chamber at a previously determined pressure. To facilitate this a 6 stage pipetting system was used and a needle valve installed to provide delicate control of the filling operation. The needle valve was bypassed by an ordinary tap to facilitate pumping of the system on the far side of the valve. In the event of accidentally filling the chamber to too high a pressure, the gas in the chamber could be expanded into section X, and a second attempt at filling could then be made. If lower pressures are required than are measureable on the gauge, these may be measured in expansion 4 or 5 and then further expanded into the chamber.

In the experiments that follow Silicone Oil type 704 was used in the diffusion pump and Silicone grease in the taps. No filament was installed.

Following the installation of this vacuum system a series of experiments were undertaken to test the efficiency of the system with respect to film build up. The method used to detect films was by the following series of operations based on the results of Chapter 10:-

a) Any residual polarization of the film was removed by running a pure u.h.f. discharge.

b) A unidirectional voltage, V_2, was applied to the gap and the u.h.f. breakdown stress measured. This corresponded to a drift field of $\frac{V_2}{d}$ volts/cm. During the discharge which followed, the films, if present, were changed to some voltage, V_p.

c) This discharge was terminated, leaving a field of $\frac{V_2 - V_p}{d}$ in the gap, which was determined by measurements of the secondary u.h.f. breakdown stress.

The difference of the breakdown stresses measured in steps b and c, then indicated V_p. If the film is thin it may be expected that V_p be small. Thus $V_2 - V_p \approx V_2$ and the measurement of V_p is made in a region where the u.h.f. breakdown stress is critically dependent on V_{dc}. Thus regarding the indication of a polarization voltage (i.e. a difference in the two breakdown stress measurements) as indicating the presence of a film, this method is a sensitive indicator of the presence of films.

A series of experiments was undertaken in which the electrodes were cleaned, quickly put into the chamber and pumping commenced. On filling

with hydrogen or argon to a given pressure (about 5 mm.Hg.) tests were made for films using the above technique. These suggested that there was less surface polarization if traps A and B were applied in addition to trap C during pumping. If pumping was finished after only a short time, the chamber filled and tests made rapidly, the polarization detected was found to be very small.

A further decrease in the polarization voltage was found to occur if the electrodes were cleaned with jewellers rouge only, rather than with amyl acetate. In later experiments rouge was used exclusively for cleaning purposes.

To conclude, surface polarization may be reduced if (i) traps A and B are applied early in the pumping stages (ii) the pumping time is reduced to a minimum and (iii) jewellers rouge is used for cleaning the electrodes.

It would therefore appear possible to reduce the initially detected polarization to an acceptable level using these techniques, but complete removal does not appear possible. Further there is some evidence for an increase of polarization with time on leaving the system to stand. This is, however, only a small effect.

Davies (private communication) has shown that silicone grease rapidly forms a layer over metal surfaces by condensation from vapour contaminating the system. The above results are compatible with the idea that some film may be built up in this way. However, the results are by no means conclusive. For instance slow oxidation of the electrodes caused by the presence of oxygen as an impurity might cause this increase of polarization on leaving the apparatus to stand. Further, there is no

reason to assume that one mechanism only exists.

11.1 Cleaning Electrodes by Bombardment with hydrogen ions

Llewellyn Jones and Davies (1951 a and b) have shown that the variations of d.c. sparking potential after prolonged bombardment of an oxide film with hydrogen ions, is compatible with the idea that this film is slowly removed by this bombardment. Thus if the present film were one of oxide, it might well be removed by running a hydrogen discharge in the gap. It is interesting to note that Llewellyn Jones and Davies (1951a) used silicon greased taps but mercury diffusion pumps isolated by liquid air traps. The impurities in their system may therefore be expected to differ from those in the present system by the presence of pump oil vapour. However, the diffusion pump is well isolated from the chamber by traps A, B and C. (Figure 11.1).

Following Llewellyn Jones and Davies an attempt was made to clear the residual polarization by running a discharge in hydrogen. A unidirectional field of 500 volts/cm was applied together with a u.h.f. field. The discharge was run for a few weeks and periodic tests of surface polarization were made. These revealed that surface polarization was increasing with time and eventually almost all the unidirectional voltage was dropped across the films. Further running of the discharge did not affect this condition. Further experiments using a 50 c.p.s. alternating voltage in place of the unidirectional voltage across the gap, when electrons and ions alternately bombard each electrode, gave similar results. These observations suggest that the film was being built up rather than being removed.

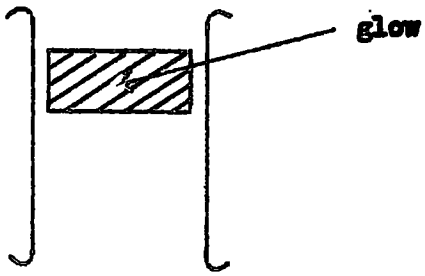

a. Pure u.h.f.

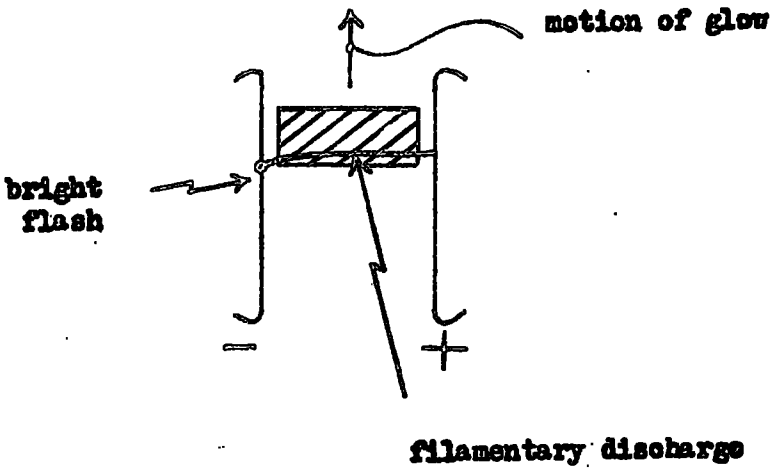

b. Combined u.h.f. and unidirectional fields.

Fig. 11.2

Up to this point in the investigation no film or tarnish had been observed on the electrode surfaces. However, after running the discharges described above there was considerable tarnishing of the electrodes and films, exhibiting interference fringes, were clearly visible.

11.1.1 The form of discharge observed

With such films, the form of discharge observed in the gap, with combined unidirectional and u.h.f. fields was of interest. A pure u.h.f. discharge at higher power than would give breakdown is observed as a cylindrical glow, between, but not touching, the electrodes (figure 11.2a). It does not fill the full width of the gap and is usually asymmetrically positioned. This position fluctuates over the electrode surfaces, remaining in any one place for only a short time.

On applying a high unidirectional field to this, the glow itself is unaltered. However, with fields above about 100 volts/cm, there are occasional bright flashes on the cathode surface followed by a filamentary discharge across the gap originating from the point of the flash (figure 11.2b). Immediately following this, the glow moves away from the region where the bright flash occurred. These filamentary discharges occur at random times

and the bright flash can occur anywhere on the electrode surface, but only on the cathode.

The mechanism of this discharge has not been investigated in detail. However, the bright flashes on the electrode might be the result of the film breaking down under the high unidirectional field resulting from surface charge on the film. It is suggested in section 11.3, that the relaxation time is compatible with a film of silica. For such a material the breakdown stress would be about 10^6 V/cm. This would correspond to a voltage across a film 3×10^{-5} cms thick of 30 volts. It is therefore to be expected that the film might break down if the applied unidirectional gap voltage was greater than some 60 volts. In practise bright flashes on the surface are only observed if the voltage is greater than thisvalue, suggesting that these represent points at which the film has broken-down.

The cathode was pitted after this experiment suggesting that considerable energy is released during this breakdown. A yellow deposit was afterwards found on the walls of the chamber, close to the gap, suggesting that some brass had been removed from the cathode. In their work on pulsed microwave discharges in resonators (λ = 10 cms), Prowse and Jasinski found similar bright spots on their electrode surfaces which showed the spectrum of the electrode material. Their electrodes were also found to be pitted.

A possible explanation of why these flashes only occur on the cathode might be that the incidence of positive ions plays some part in initiating the breakdown of the film, e.g. by the secondary emission of electrons.

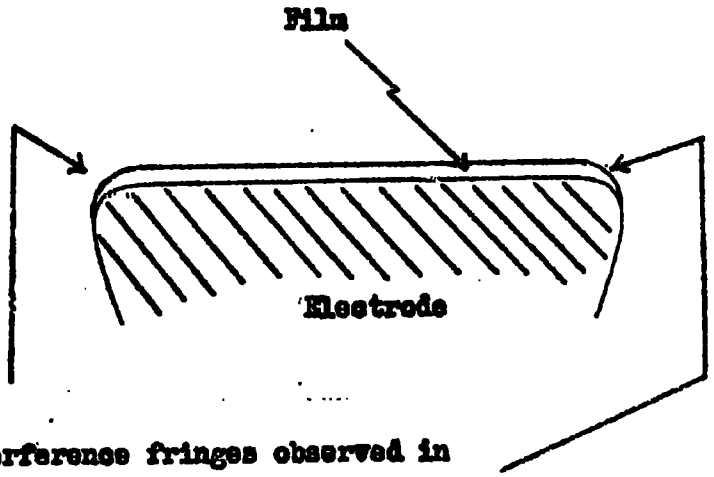

Interference fringes observed in these regions.

Fig. 11.3

It is to be expected that the surface charge is drained around the point at which the film broke down. Thus in the vicinity of this point the breakdown stress will correspond to that with an additional unidirectional field. Hence a movement of the glow to a region where the electrons have a longer time to ionize and the glow is easier to maintain, might be expected to follow the film breakdown. This would explain the observed movement of the glow.

11.1.2. Films observed after discharges in hydrogen

The typical film observed after running a discharge with an alternative unidirectional/50 c.p.s. alternating field superimposed on the u.h.f., for a few weeks will be discussed in detail.

Over the emitting electrode surface (cathode) there was an apparently uniform film exhibiting interference fringes around the edges of the electrodes. Over the surface bounding the discharge, the film was unaffected by cleaning with dry tissue or acetone whereas the back of the electrodes, which showed some tarnish, could easily be cleaned with acetone. Thus there appears to be some fundamental difference between the film over the electrode surface and the tarnish behind the electrode. The existence of interference fringes round the curving surface of the electrode may thus be interpreted as a region where the film over the electrode surface reduces in thickness. Thus the film appears to be confined to the region of the electrode bounding the discharge of which figure 11.3 shows a cross-section. From observation of the fringes, the film thickness is of the order of 10^4 Å.

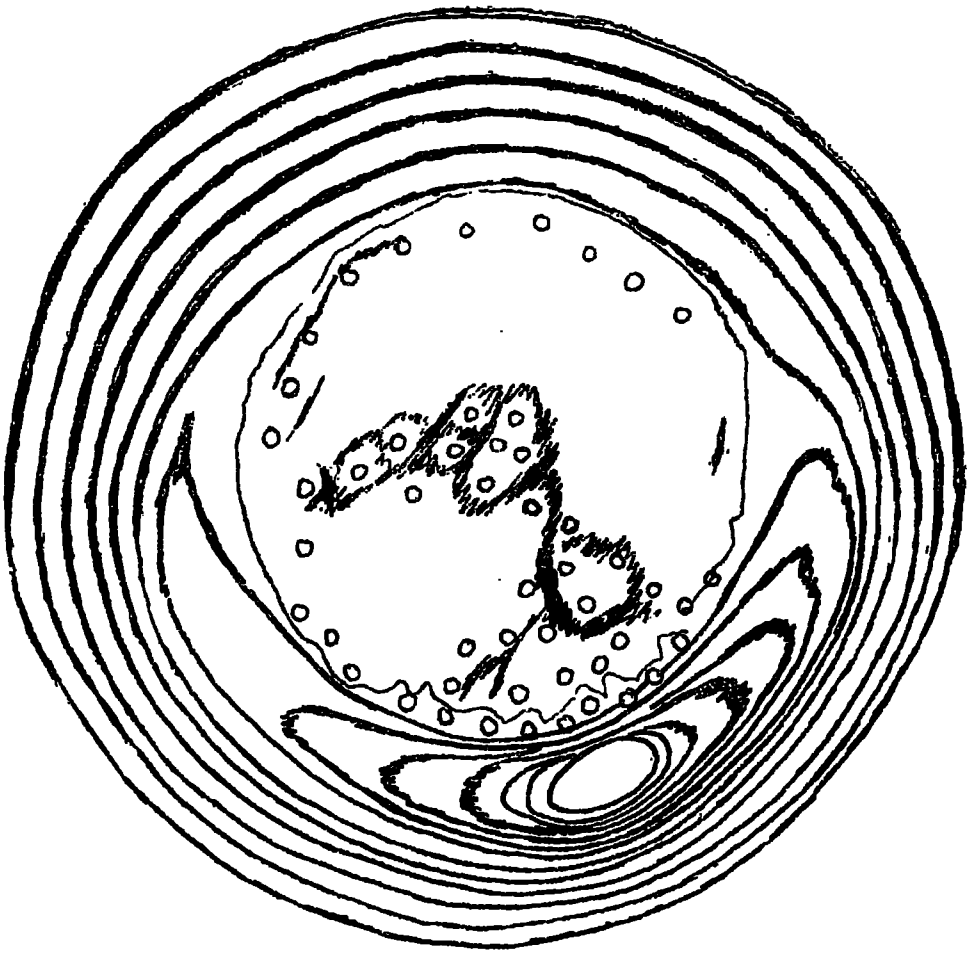

Fig. 11.4

Over the collecting electrode (anode) the film appeared to be less uniform. Around the curved edges of the electrodes interference fringes were again obsèrvable in day-light. A sketch of the fringes observed under sodium light is shown in figure 11.4. No fringes were observed in the central region which appeared to be clean, but some darker and lighter regions were observed around the holes, as is suggested in figure 11.4. As with the emitting electrode the film appeared to be confined to the surface bounding the discharge. On both electrodes, no interference fringes were found on the electrode assembly except over the region bounding the discharge.

The following conclusions may be drawn,

a) Since the film is confined to surfaces bounding the discharge, it is probable that the discharge itself was responsible for the formation of the films.

b) The fact that the film on the cathode is, in general, thicker than that on the anode, suggests that some positively charged ion is involved.

It is interesting to note that result a) is at variance with the corresponding results of Llewellyn Jones and Davies.

11.2 Bombardment with Argon Ions

In analysing the processes of film formation by a discharge, it is of interest to have some knowledge of the part played by the gas itself.

Thus the above experiments were repeated using argon at about 5 mm pressure. Such experiments are also of interest since Farnsworth and his colleagues (1955) have suggested a method of cleaning surfaces employing argon ion bombardment.

Here again a film was built up confined to the surface bounding the discharge, but of quite a different nature from that formed by a hydrogen discharge. It appeared white when seen by the naked eye and exhibited no interference fringes. When viewed under the microscope, illuminated with light parallel to the electrode surface and using a magnification of 600, the 'film' was seen to have a granular structure. These 'particles' were apparently distributed evenly over both electrodes.

On the cathode, the particles appeared just less than 1μ across. Large aggregates of these particles, piled to a depth of 2-4 particles, were common. These were of no definite shape, but ranged from lines to circular structures. The background particles were of constant density right up to the boundary of these aggregates.

On the anode, the particles were again about 1μ diameter in the centre of the electrode, but decreased to half this diameter at the edges. A few small aggregates were observed but these were rare, consisting of not more than ten individual particles (i.e. much smaller than observed on the cathode).

The density of particles was difficult to determine due to lack of resolution. However, they appeared to be just sufficiently dense to

cover the electrode surface and in places there appeared to be more than one layer of particles.

The fact that this film differs considerably from that formed in the presence of hydrogen, suggests that the gas plays some part in the process. It would be interesting to find the way in which these films differ chemically. However, there is in general too little material to perform any definite tests. Nevertheless, an X-ray powder photograph was taken using some of the film built up in argon. Unfortunately, the result showed an amorphous structure and no elements could be detected.

11.3 Relaxation time

On the face of it, the material of the film could be recognised by measuring the relaxation time and comparing it with values measured on materials in bulk or calculated from the product of the resistivity and permittivity of the materials. However, it is not certain that the properties of the material in bulk are applicable to very thin films. For instance, if the film thickness is less than the mean free path of electrons in the material (of the order of 100 $\mathring{A}$) an abnormally low resistance with corresponding decrease in resistivity from the value from measurements on the material in bulk, might be expected. Thus it is likely that the relaxation time, τ_F, decreases with film thickness when this thickness is less than about 10^3 $\mathring{A}$. However, for films of thickness greater than 10^3 $\mathring{A}$, the measurement of τ_F is expected to provide a useful indication of the material of the film.

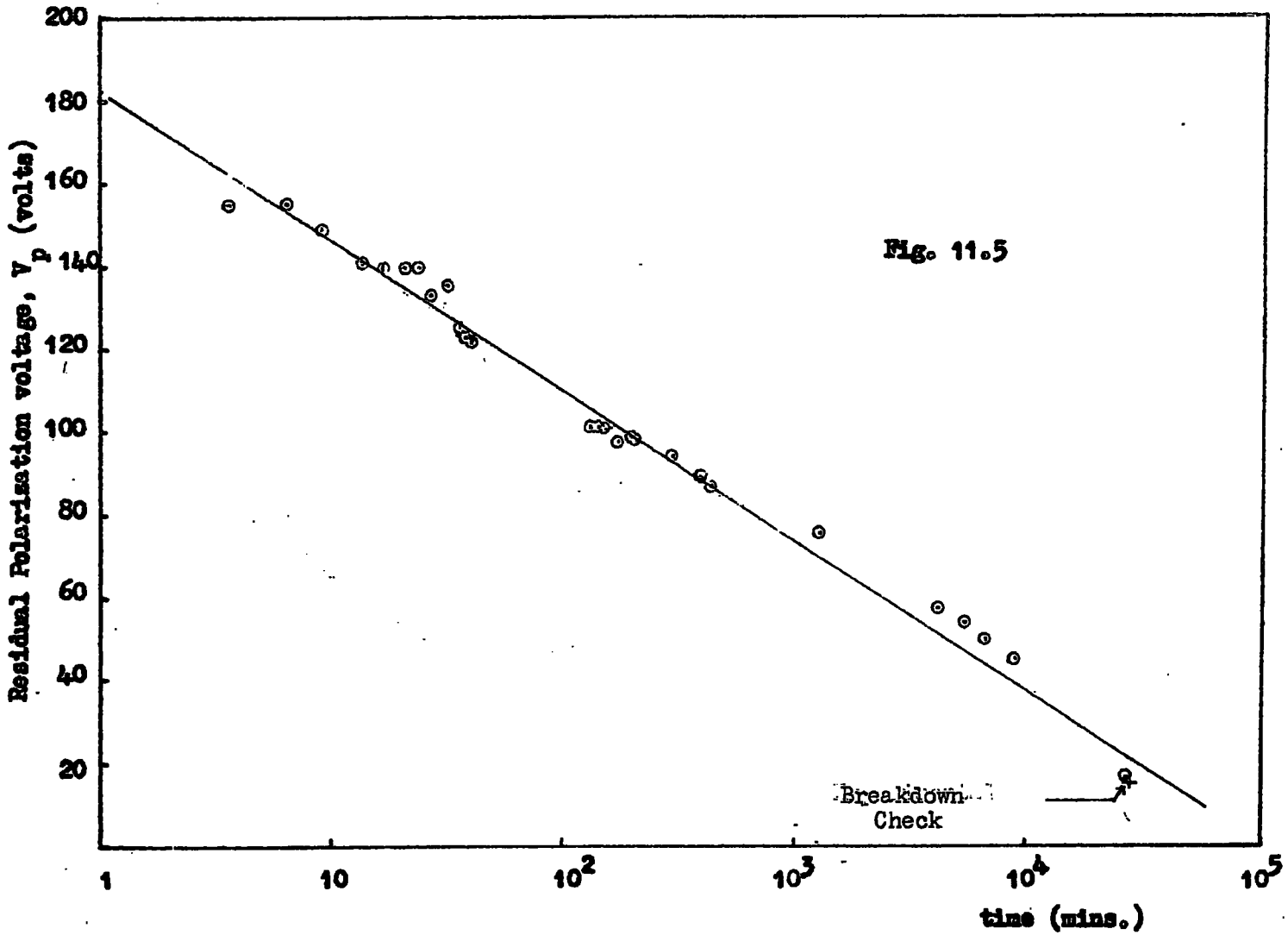
Residual Polarisation voltage, V_p (volts)
200
180
160
140
120
100
80
60
40
20
1
10
10^2
10^3
10^4
10^5
time (mins.)
Breakdown
Check

Fig. 11.5

The ellipsoid field meter is a satisfactory device for the measurement of relaxation times. The film may be charged by running a u.h.f. discharge in the presence of an applied unidirectional gap voltage. Direct measurement of the field resulting from the polarization voltage may then be made as a function of time after termination of the discharge and removal of the applied gap voltage.

The ellipsoid in no way interferes with the charge on the surfaces, so that the voltage across the films may be measured while retaining a high insulation of the surface. It is thus possible to measure the decrease in voltage as the surface charge leaks away through its own internal resistance. In this way a direct measurement of the relaxation time constant of a film is feasible, provided that the rate of change of voltage is sufficiently small to enable an adequate number of ellipsoid swings to be observed.

The relaxation time of the film deposited by prolonged discharge in hydrogen (section 11.1.2) was measured using this technique. A plot of polarization voltage against time is shown in figure 11.5, which indicates a relaxation time of about 2×10^3 mins (about 2 days). Comparing this with the time constant of 200 mins observed in the case (Chapter 10) when Apiezon grease and oil was used in the system, suggests that there are different film materials in the two cases. This indicates that the grease or oil played some part in the formation of the film.

The film with Apiezon grease and oil was only some 500 Å thick which is of the order of the expected mean free path of an electron, so that a low value of τ_F might be expected. Measurement of τ_F with a film built up as the above, which did not exhibit interference fringes and thus was expected to be thinner, but was sufficiently thick to give considerable polarization, gave relaxation times of similar order to those indicated in figure 11.5. On the other hand for very thin films exhibiting only a small amount of polarization a much smaller value of τ_F did occur. To conclude, it would appear that τ_F and thus the film material in the present experiments differs from that when Apiezon grease and oil were used.

Comparison of the value of τ_F for the film built up by prolonged discharge in hydrogen, and relaxation times calculated from properties of various materials in bulk suggests that this film consists of silica for which the expected relaxation time is 5×10^3 mins (fused silica). Comparison of the relaxation times of films built up by discharges in argon and hydrogen suggest that the materials are different in the two cases. However, this difference might be the result of differences in the structure rather than in the chemical composition of the film.

Experiments of this type can thus be used to investigate the nature of films built up under differing conditions. In particular, the nature of the present film might be investigated by measuring the relaxation time of films built up by discharges when the different impurities in the system are present in varying amounts. In this way those impurities contributing to the formation of the film might be traced. This type of experiment has been only partially attempted in

the above work. A detailed investigation would provide an interesting experiment for the future.

11.4 Monitoring Film Thickness (in Argon)

The effective resistance of the film is $\frac{V_p}{i_2}$, so that assuming a constant resistivity, the relative thickness of a film may be easily obtained from simultaneous measurements of V_p and i_2. Prior to an investigation of the rate of increase of this relative thickness as the film is built up by the discharge, the V_p - i_2 characteristics of various films built up in argon were measured to establish the way in which the measured relative thickness $\frac{V_p}{i_2}$, can vary with V_p.

A series of experiments was therefore carried out in which i_2 and V_p were measured, for various values of applied gap voltage V_2. The experimental procedure was as follows:

a) The film was discharged by use of a pure u.h.f. discharge in the gap, and observation made of the unidirectional current, i_2, which flowed during the process and tended to zero as the process was completed.

b) A unidirectional voltage, V_2 was applied to the gap and the u.h.f. breakdown stress measured. Values of breakdown stress thus obtained were used to plot a calibrated curve of breakdown stress against V_2. This was then used to determine the gap voltage, V_{dc}, for subsequent experiments.

c) After this breakdown, $\frac{1}{2}$ min was allowed for the film to charge up and so approach the steady condition. The current i_2 was then measured.

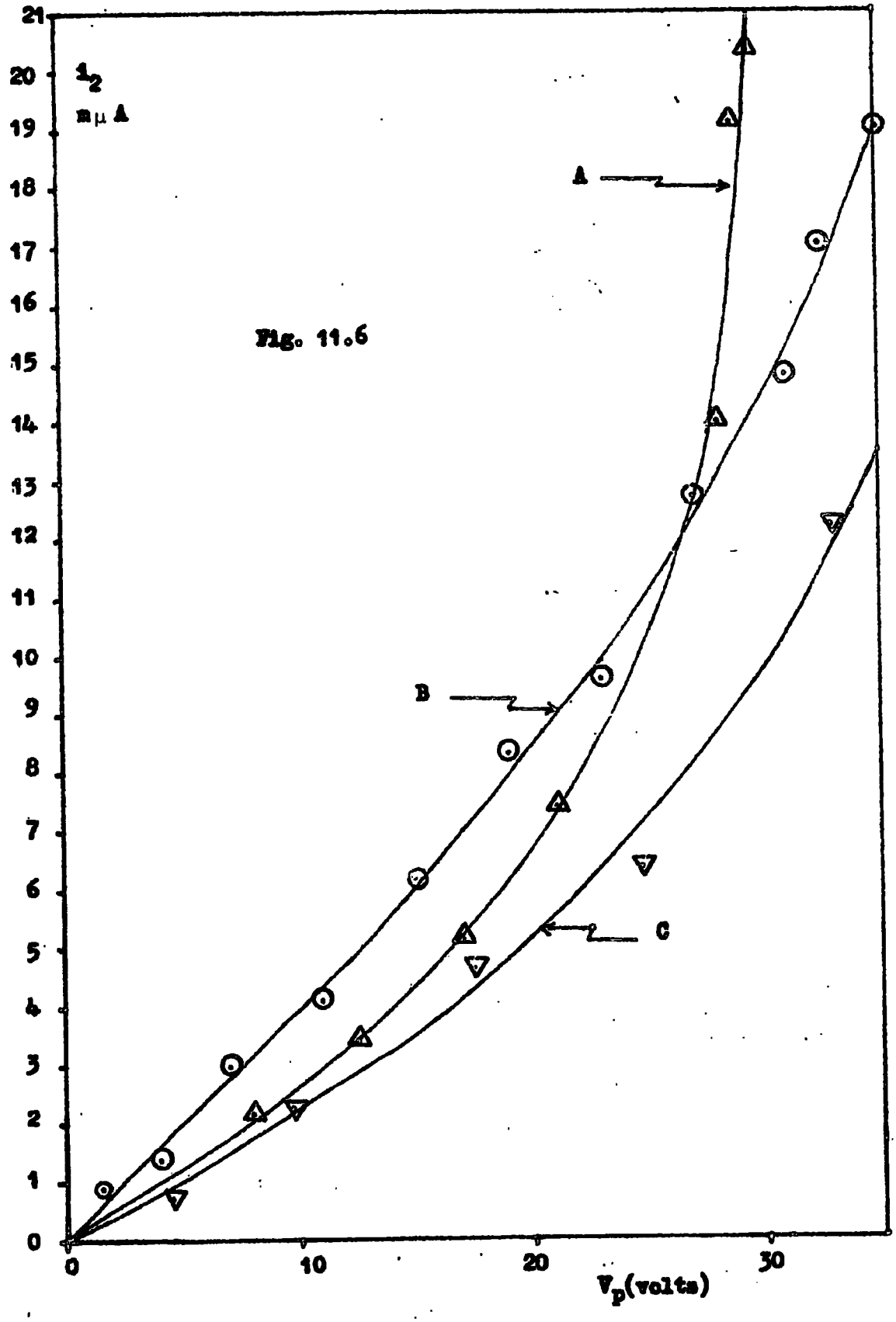
i_2
mμA
A
B
C
Fig. 11.6
V_p(volts)
0
10
20
30
1
2
3
4
5
6
7
8
9
10
11
12
13
14
15
16
17
18
19
20
21

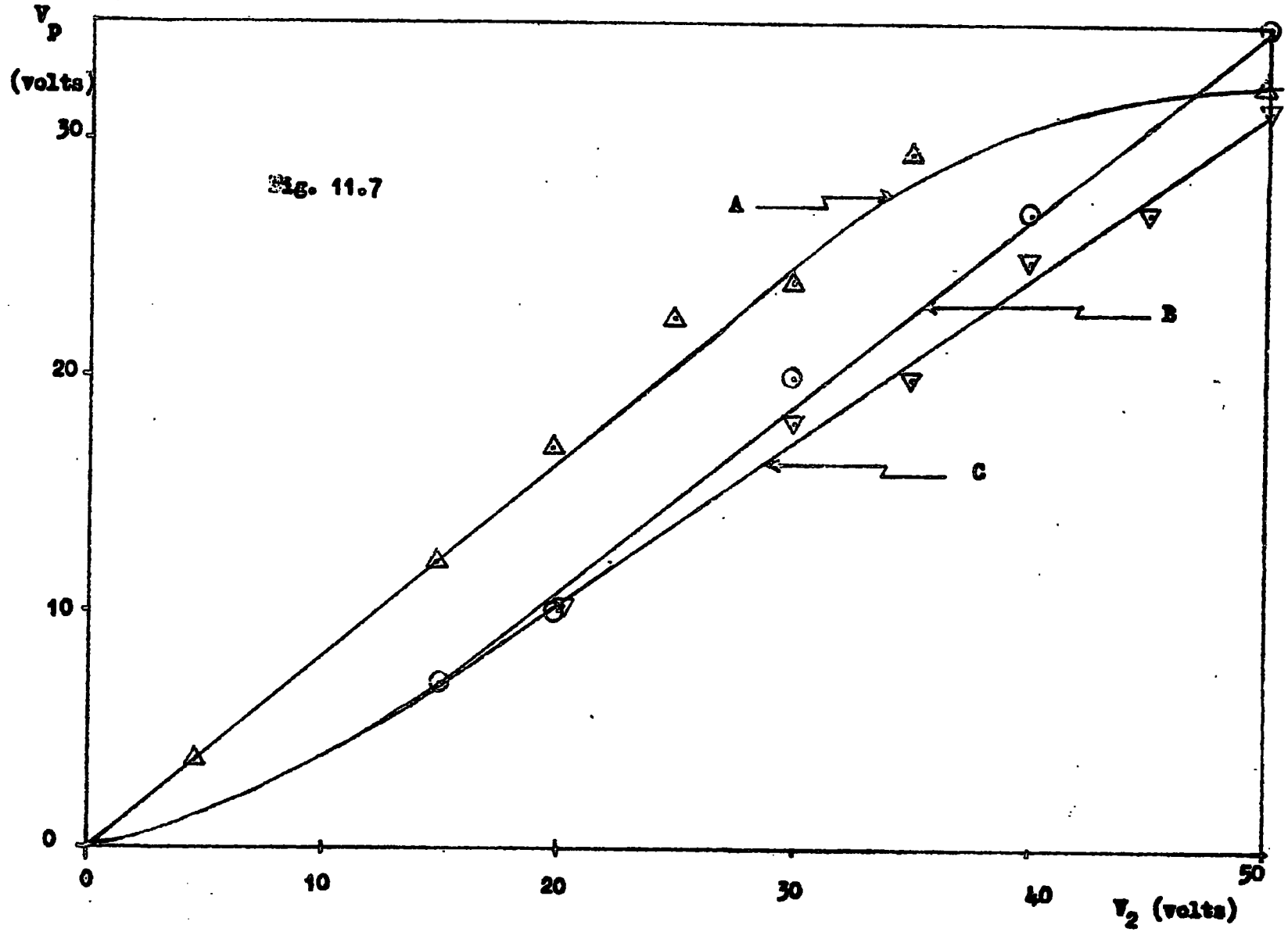

Fig. 11.7

d) Immediately after this measurement, V_p was measured by terminating the discharge, reducing V_2 to zero, and then determining the breakdown stress. From the calibrated curve derived from results (b) the value of V_p corresponding to this stress was read off directly. (This method was found to be most accurate since $V_p \approx V_2$).

Curve B of figure 11.6 is a typical plot of i_2 against V_p for a given film. Curve C, is the film resulting from B after running a discharge for 35 mins with full power u.h.f. field and V_2 = 40 volts. As expected this film (C) has a higher effective resistance than the original film (B), which may be interpreted as an increase in thickness. The corresponding plots of V_p against V_2 are shown in figure 11.7.

One interesting case which often occurred has properties typified by curves A of figures 11.6 and 11.7. Figure 11.6 shows that above a polarization voltage of some 30 volts the current, i_2, rises steeply. If the applied voltage, V_2, (figure 11.7) is raised above the value to give $V_p \approx 30$ volts, little further increase in V_p occurs. This is as expected if the film itself had broken down at a value of V_p of 30 volts. The rapid rise of current before this (figure 11.6) suggests the onset of some ionization phenomena in the film itself. The fact that curves B and C do not show this tendency to a maximum value of V_p and a 'runaway' of i_2, suggests that these films are thicker than A and thus require a greater value of V_p to break them down. Experiments to test this have not yet been attempted, but would provide interesting data on the mechanism represented by curve A.

If this were true, this would provide a simple means of investiga-

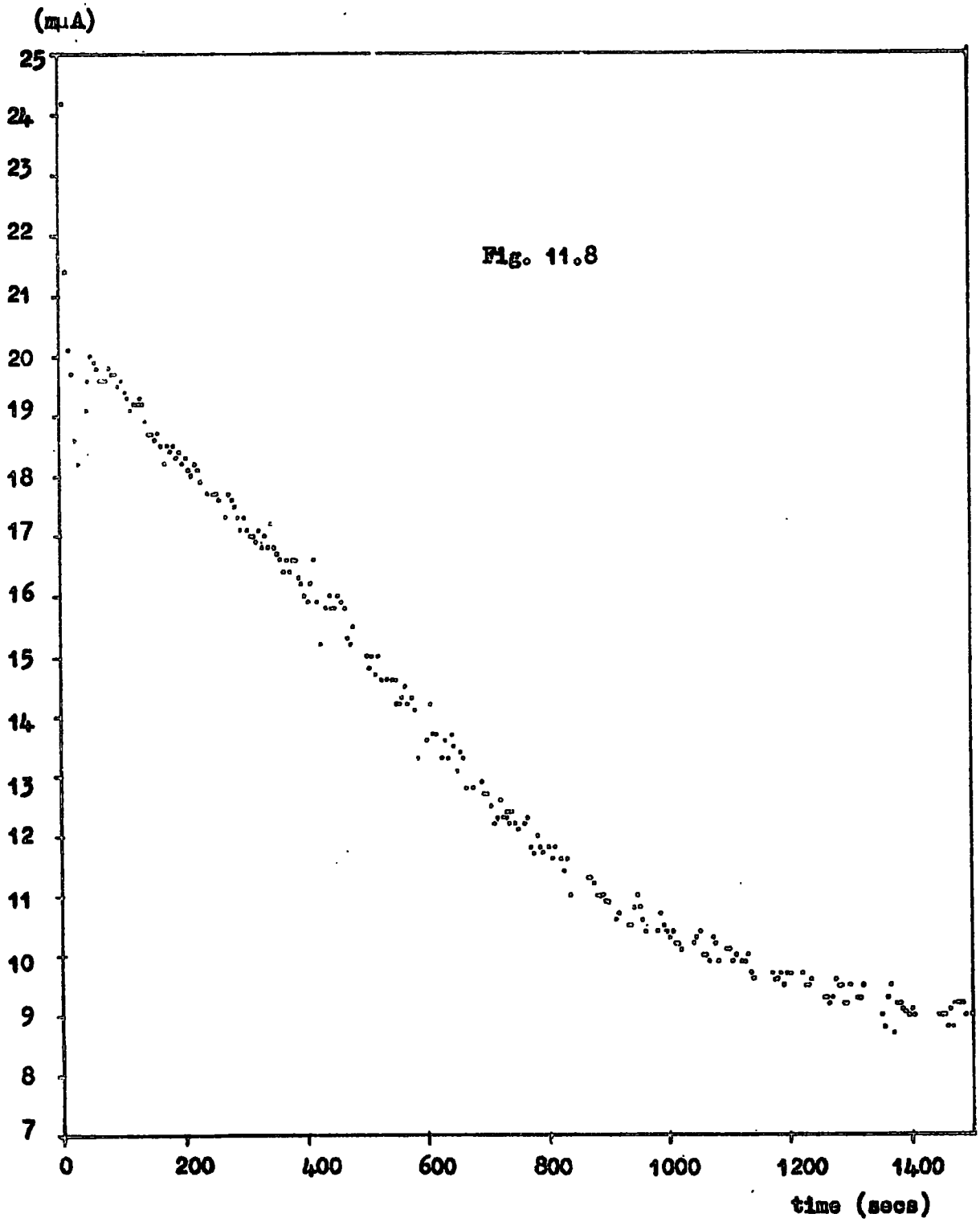
Gap current, i_2
(mμA)
25
24
23
22
21
20
19
18
17
16
15
14
13
12
11
10
9
8
7
0
200
400
600
800
1000
1200
1400
time (secs)

Fig. 11.8

ting the breakdown of thin di-electric films. Having completed such work, measurements of the film breakdown stress might provide a very accurate means of measuring film thickness.

11.4.1 Measurement of the rate of formation of a film by a discharge in Argon

In these experiments the film was allowed to build up under a u.h.f. discharge with an applied unidirection gap voltage of 40V(V_2). During this process the thickness of the film was monitored by periodic measurements of i_2 and V_p, the latter by periodic remeasurements of the u.h.f. breakdown stress.

In the particular experiment described below V_p remained at 35.9 volts to within the accuracy to which it could be measured ($\approx$2%). On the other hand i_2 showed a progressive decrease with time, as shown in figure 11.8.

On switching on the discharge, with the films initially discharged, i_2 rose to a high value and then drifted back over the first 20 secs. This can be interpreted as the charging of the film by i_2. As the film is charged the voltage across the discharge decreases and hence i_2 decreases towards its steady value. Once the film has been charged, the whole of the gap current must flow through the film leakage resistance. Since V_p is essentially constant, this implies that i_2 can only change if the film resistance changes. Thus the decrease of i_2 with time must correspond to an increasing film resistance. Assuming the resistivity is constant this may be interpreted as an increase of film thickness, d_F. Thus remembering $d_F \propto \frac{V_p}{i_2}$ and V_p is a constant, figure 11.8 may be

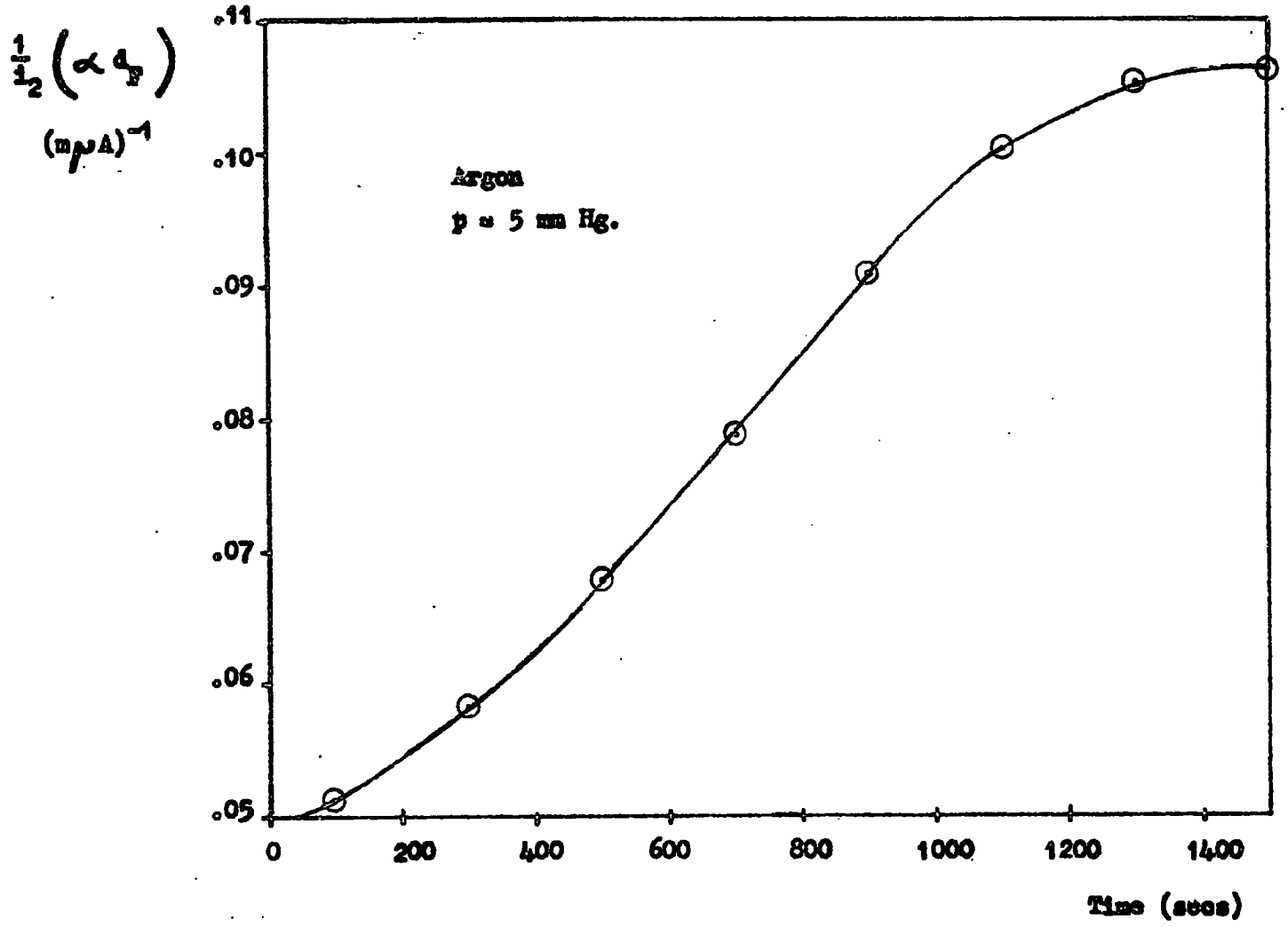
$\frac{1}{i_2}\left(\alpha q_F\right)$
$(m\mu A)^{-1}$
.11
.10
.09
.08
.07
.06
.05
Argon
p = 5 mm Hg.
0
200
400
600
800
1000
1200
1400
Time (secs)

Fig. 11.9

replotted as $\frac{1}{i_2}$ against time (figure 11.9) which is essentially a plot of the relative film thickness against time. This suggests that there is a slow build up of the film to twice the thickness in about 10 mins.

This rate of build up corresponds to an increase of about 0.5 x 10^{-4} cm in film thickness, and 10^{-4} cm^3 in film volume, during 10 mins. Assuming that one molecule has a volume of 10^{-22} cms^3, this would suggest that 10^{18} molecules must be deposited in ten minutes. On the other hand, if the impurity responsible for this film occurred in the gap at a pressure of 10^{-5} mm.Hg., the gap would only contain some 10^{10} molecules. This suggests that the whole of the material diffuses into the gap during this ten minutes.

Taking the diffusion coefficient as being about .1 in c.g.s. units, the rate of flow of vapour into the gap can be estimated at 10^9 molecules/sec. Thus the time required to build up the above film would be of the order of 10^9 secs. This rate of flow is clearly insufficient to explain the observed rate of build up.

It is unlikely that the impurities exist to any higher pressure, unless present in the gas introduced into the chamber. Cold traps would be expected to trap any organic vapours which might be present and it is unlikely that any substance not trapped would be responsible for the films.

There is the possibility that the observed rate of build up is ficticious. If the resistivity were to increase steeply with film thickness in the region in which this experiment were performed, it might be possible to explain this rapid increase in film resistance with a much smaller increase in film thickness. As discussed in the previous

section some variation of this form may be expected for films of approximately 10^{-6} cm. thick. It is therefore likely that what is observed is the deposition of a thin layer on a film of about 10^{-5} cm. thick to give a greatly increased film resistance. Thus this does not rule out impurities as a source of film material.

The dip of figure 11.8, which occurs at about 30 secs. does not always occur, and at present there is insufficient information for an explanation to be attempted. Consideration of the decrease in the rate of build up of the film at 1300 secs. likewise requires further information before a definite explanation can be presented. However, possible explanations might be that the film is flaking off the electrodes as rapidly as it is put on, or that there is a depletion of vapour round the gap, or that there is some change in resistivity. There is further evidence for the first of these in that a white deposit slowly forms on the bottom of the chamber. Further such a flaking off of the film would explain the observation that the resistance of a film decreases on standing. Thus film C could be reduced to film B by leaving overnight.

The fact that such observations as those described above might be explained in terms of some electron bombardment conductivity, emphasises the need to repeat these experiments with films of known thickness and to obtain independent measurements of the resistivity. Fundamentally such experiments are necessary for complete justification of this form of measurement of film thickness. Nevertheless Becker (1904) and Ansbacher and Ehrenberg (1951) have shown that bombardment with electrons of energy of those present in the above experiments, is unlikely to produce a marked effect. Nevertheless to clarify the mechanism of the above measurements

further controlled experiments using known impurities are desirable.

11.5 Conclusions

There appears to be considerable evidence that the film is built up by the discharge. This is indicated by the predominance of the film over surfaces bounding the discharge and by the increase in resistance of a film after subjection to the presence of a discharge.

In general, the film is built up on both electrodes, but there is a tendency for there to be a thicker film on the cathode, suggesting that some positively charged ion is responsible for the build up of the film. The fact that it is built up on both electrodes is to be expected in a system where the electron energy is supplied predominantly by a u.h.f. field. Under such conditions a considerable flow of positive ions to the anode may be expected and thus a film is built up on the anode as well as on the cathode.

Possible origins of the film

Since the films are often visible and sometimes cause a deposit at the bottom of the enclosure, they cannot consist of adsorbed gas but must be of material solid at ordinary temperatures. Thus it is likely that the ions which eventually cause the build up, are derived from large impurity molecules.

It is to be expected that these impurity molecules are co-valent. Thus they can only be ionized by the breaking of a co-valent bond so that a corresponding negative ion is to be expected. However, experimental observation of the films suggest that this negative ion plays

no major part in the formation of films.

A possible source of these impurities is the silicones employed in the pump oil and tap grease. As already mentioned Llewellyn Jones and Davies did not use silicone pump oil and they apparently did not have film formation. Another source could be glass decomposition products sputtered from the walls of the enclosure, but if this is so it is difficult to see why Llewellyn Jones and Davies did not have film formation.

Silicones

Silicone greases and oils consist of polymers containing the siloxane radical:-

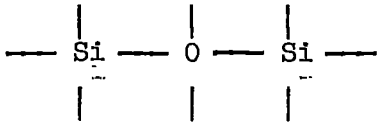

Dibeler, Mohler and Reese (1953) have made mass spectrograph studies of the ions formed by electron bombardment of hexamethyl disiloxane,

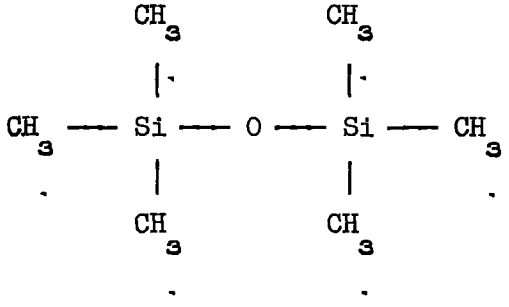

and octamethyl trisiloxane,

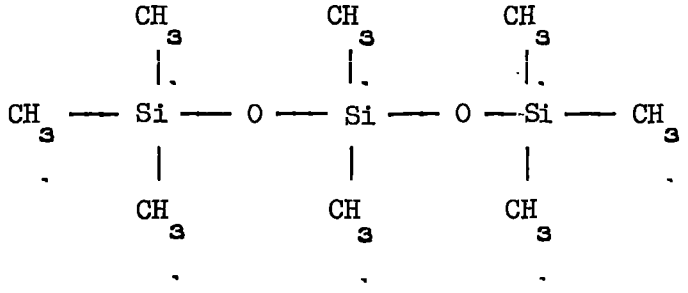

Table 11.1 Mass spectra of hexamethyl disiloxane $(CH_3)_6 Si_2O$

$\frac{m}{e}$	Ion	Relative intensity at 70 volts nominal electron energy	Appearance Potential eV
66	$(CH_3)_4 Si_2 O^{++}$	12.4	25
73	$(CH_3)_2 Si^{+}$	11.8	15
147	$(CH_3)_5 Si_2 O^{+}$	100	9.6
162	$(CH_3)_6 Si_2 O^{+}$	.03	-

Table 11.2 Mass spectra of octamethyl trisiloxane $(CH_3)_8 Si_3 O_2$

$\frac{m}{e}$	Ion	Relative intensity	Appearance potential eV
63.7	$(CH_3)_5 Si_2 O_2^{+++}$	0.35	-
7.3	$(CH_3)_2 Si^{+}$	42.9	12
103	$(CH_3)_6 Si_3 O_2^{++}$	12.8	22, 13.6
221	$(CH_3)_7 Si_2 O_2^{+}$	100	9.6
236	$(CH_3)_8 Si_2 O_2^{+}$	.02	-

The relative intensities of the ions and the ionizing potentials (appearance potentials) are shown in tables 11.1 and 11.2.

For both these compounds the most probable ion is that formed by the loss of a methyl radicle, CH_3, with an ionization potential of 9.6 eV.

Since these siloxanes contain the basic radicals likely to occur in silicone grease it would appear reasonable to assume that silicone grease vapour may be ionized in a plasma in a similar way to these siloxanes. The ionizing potential would thus appear to be of the order of 10 eV. This is below the minimum ionization potentials of both hydrogen, 13.59 eV, and argon, 15.75 eV, ($H \rightarrow H^+$ and $A \rightarrow A^+$ respectively). It is thus to be expected that the probability of ionization of the grease molecule is greater than that for a gas molecule since many more electrons will have an energy greater than 10 eV than will have an energy greater than 13 or 15 eV.

The vapour pressure of silicone is approximately 10^{-5} mm.Hg. It is shown in section 11.4 that the rate of build up of the film suggested in this section (11.4) could not be accounted for with such a small vapour pressure of impurity. Nevertheless, the doubt attributed to the interpretation of these results in the previous section, suggest that silicone grease need not be ruled out on these grounds.

Glass decomposition products

Bill and Evett (1959) have obtained evidence that pyrex glass chemically sputters in the presence of gaseous ions, liberating impurities into the system. They have suggested that these decomposition

products can account for insulating films over metal electrodes, which polarize in the way described above. Farnsworth (1958) has suggested a process of electrode cleaning employing bombardment of the surface with argon ions. Bill and Evett have suggested that the varying effectiveness of this method, may be accounted for by the decomposition of glass during bombardment and bake out.

It would therefore appear likely that the present films are built up by glass decomposition products. Bill and Evett have found little sputtering of the glass by bombardment with neon ions. Thus it would be interesting to see whether such films are built up in neon. If they are it would appear that glass decomposition is not responsible for the impurity involved.

The material of the film

The material of the film itself has not been investigated chemically. It is, however, of interest to see how the dependency of the nature of the film on the gas used might be explained.

If the ions were formed by breaking of a co-valent bond; on neutralization by an electron on the electrode surface they would form radicals with free bonds. It is well known that such radicals are unstable and thus they would be expected to undergo some chemical change. Possible forms of change would be:

a) Combination with other similar radicals to form polymerisation products. This would appear to be unlikely in view of the small number of impurity ions striking the surface.

b) Combination with incident ions of the gas of the discharge. Hydrogen might form such bonds but not argon in view of its inert nature.

c) Some rearrangement to give an unsaturated molecule.

d) Decomposition into two or more molecules.

In the case of hydrogen, there will be a large flux of hydrogen ions to the surface, so that hydrogenation of the impurity radical is a likely process. In the case of argon no such process can occur so that rearrangement or decomposition would be expected. The participation of the gas in this way would account for the differences in the type of film observed in the presence of the two gases.

Conclusions

There is firm evidence for the build up of films by a u.h.f. discharge. It does not appear that these films can be accounted for in terms of the electrode material or the nominal gas. Two possible sources of impurities are from silicones in the tap grease and diffusion pump oil or from the chemical decomposition of glass. In section 11.3 it was suggested that the film resulting from a prolonged discharge in hydrogen was silica and that the material when silicones were used differed from that when Apiezon grease and oil were used. This would suggest that glass, present in both cases, was not predominantly responsible. It is therefore thought that silicones are the most likely sources of film material, although glass may also be a contributory factor.

The methods of investigation developed here, are applicable to a more systematic study. Experiments of particular interest would include

a comparison of films built up in various gas (particularly neon) and measurement of the electrical properties of thin films.

CHAPTER 12

CONCLUSIONS

Measurements of amplification of an electron stream crossing a region of u.h.f. field, have indicated the importance of diffusion in the transport mechanism. As the u.h.f. field is increased, the drift field has a slowly decreasing control over electron flow. Thus as breakdown is approached the discharge is largely diffusion controlled and is expected to exhibit similar properties. Two forms of discharge have been identified theoretically, one occurring at low amplifications when the drift field largely controls the flow and the predominant electron source is the emitting electrode; the other at high amplifications when diffusion largely controls the electron flow and the predominant source of electrons is collision ionization in the gas.

A theory of electron flow by a combination of drift and diffusion has been worked out for low amplifications. Calculations from this theory suggest that the ionization rates in present case are larger than those determined from discharges in unidirectional fields.

At higher gas amplification instabilities were observed in the unidirectional gap current, which have been traced to the presence of partially insulating surface films over the electrodes. It has been shown experimentally that a unidirectional field cannot be maintained at its applied value when surface films are present. Further, experimental evidence suggests that this film is built up by the presence of a discharge, probably from heavy impurity materials in

the gap.

These conclusions suggest that in the basic experiment, in which amplifications are measured in combined u.h.f. and drift fields, there is considerable doubt as to the value of the drift field. For a given applied gap voltage, V_2, and a given gap current, i_2, once the film is charged the polarization voltage is $2i_2R_F$ and the drift field is $\frac{(V_2-2i_2R_F)}{d}$. Thus measured values of R_F might be used to evaluate the drift field in any experiment. However, since the film is thought to be built up by the discharge so that R_F is increased, the value of R_F in any case is also in doubt.

It has been suggested that Silicone vapours are largely responsible for the build up of the film. If this is so, formation of films could be prevented by using a high-purity vacuum system, in which all such impurity vapours were eliminated. However, such a system would still be contaminated with glass decomposition products, especially as the glass would have to be baked out, a process which Bill and Evert claim to accelerate the decomposition of glass. Further it appears likely that such decomposition products would form films over the electrodes even in the absence of a discharge. It, therefore, appears likely that it is not possible to remove the surface films completely. Nevertheless it has been shown that even with the present vacuum system, it is possible to reduce polarization to an acceptable level. However, amplification measurements may be made in the presence of films provided the uncertainty in the value of R_F is reduced. This may be achieved by reduction of the impurity level so that the rate of build up of the

film is reduced, or by the deliberate introduction of films of resistance large compared to that which will be built up. The value of R_F may be measured by the methods already described and the drift field at any instant calculated.

When instabilities in gap current arise there is a progressive increase in amplification with time which has been found to be the result of a progressive decrease in the drift field due to charging of the films. Thus effectively, plots of amplification against time are to be regarded as plots of amplification against drift field on some non-linear scale. Knowing C_F and R_F, which can be measured by the methods developed, the drift field at any instant may be calculated from equation 9.12, so that measurements of amplification as a function of drift field at constant u.h.f. field are obtained.

Thus it is concluded that measurements of amplification and thus the ionization rate are possible in the presence of surface polarization, by applying a correction for the potential drop resulting from the unidirectional current flow through the film. Further measurements of amplification would therefore appear profitable, even if surface polarization cannot be completely removed.

APPENDIX 1

The design of a Light-Sensitive Bistable Circuit

A transistor bistable circuit of the type shown in figure A1.1 has been treated by Wolfendale, 1957, who showed that the two stable states were both controlled by T1, one with T1 taking maximum current (bottomed) and one with T1 taking negligible current (cut off). When T1 is a phototransistor, the treatment of Wolfendale requires modification to include the effect of light incident on the base of T1.

Light incident on the base will, if the quanta of energy are in excess of the band gap energy, produce hole-electron pairs. Since the minority carriers will be swept over the collector base potential barrier on diffusing to it, these will be extracted by the collector from the base region. Thus the incidence of light gives rise to an effective forward current injected into the base. A similar process occurs as a result of the thermal production of hole-electron pairs giving rise to a collector leakage current in the ordinary transistor. The effect of admitting light may thus be considered as adding a further component to the collector leakage current, I_{co}.

It may be shown (Wolfendale) that the loop gain of this circuit at low frequency is approximately $\frac{R_2}{R_3}$. The condition that stable states exist is that the loop gain may be reduced to less than unity. However, for triggering action it is necessary that the gain rises above unity so that R_2 must be greater than R_3.

In the stable state in which T1 is bottomed, the gain is reduced to below unity by the following action. The bottomed condition may be regarded as a forward bias of the base-collector diode, so that a

Fig. A 1.1

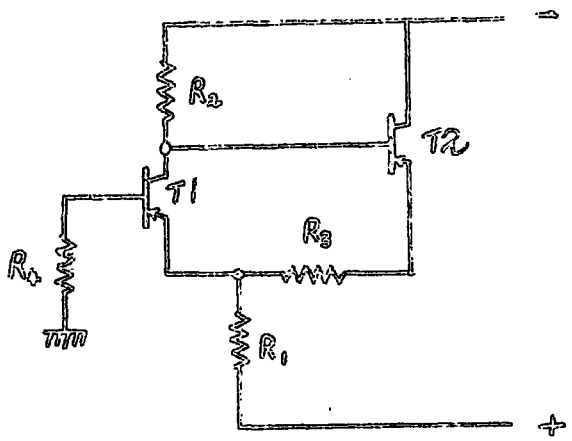

Fig. A 1.2

Circuit conditions with T1 bottomed

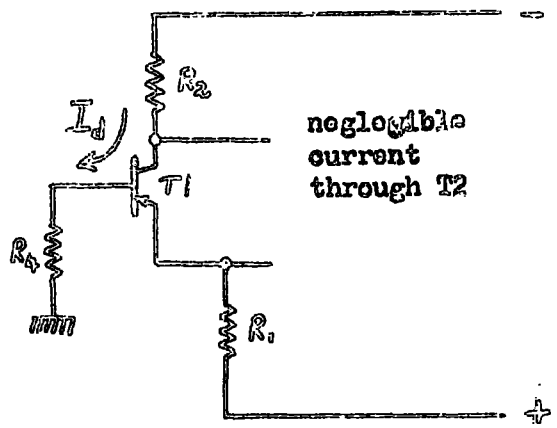

Fig. A 1.3

Circuit conditions with T1 cut off

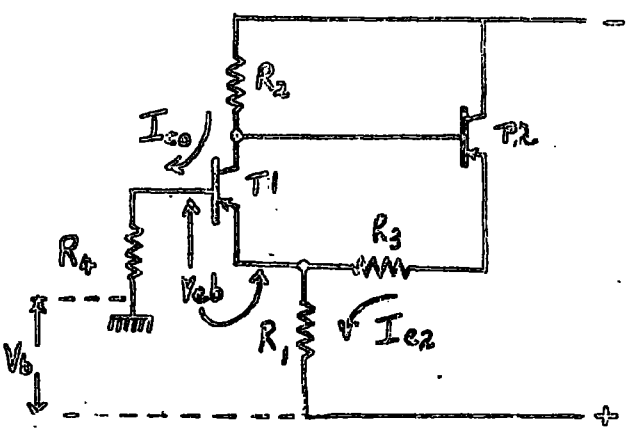

current I_d flows between collector and base. This diode effectively shunts R_2 with R_4 (figure A1.2) so that the value of the collector load of T1 (R_2) is effectively reduced. Provided this current flow is sufficient to reduce the effective collector resistor so that the loop gain drops to below unity, this state is stable. Any flow of collector leakage current, I_{co}, would mearly increase I_d and thus decrease the loop gain further. Hence the incidence of light onto T1 when in this state, would have no tendency to trigger the circuit and would in fact increase the stability of the state. Thus provided the circuit parameters controlling the stability of this state are chosen neglecting the collector leakage current, there is no tendency for the circuit to be triggered from this state by either light or temperature variations.

The stability of the state when T1 is cut off however, may be shown to be dependent on the collector leakage current. When T1 is cut off, the emitter-base diode may be regarded as being back-biased sufficiently for there to be negligible current flow across it, so that only the collector leakage current flows in the base circuit (figure A1.3).

Summing potentials in the emitter-base circuit of figure A1.3:

$$R_1 I_{e_2} = V_b + I_{co} R_4 + V_{eb}$$

If V_{ebo} is the emitter-base voltage required to back bias the emitter-base diode sufficiently to reduce the loop gain to unity, the condition that this state be stable is that the diode be biased further back than

this by the flow of the emitter current of T2 through R_1 i.e.

$$R_1 I_{e_2} > V_b + I_{co} R_4 + V_{ebo}$$

or
$$I_{co} < \frac{1}{R_4} \left\{ I_{e_2} R_1 - V_b - V_{ebo} \right\}$$

If,
$$I_{co} > \frac{1}{R_4} \left\{ I_{e_2} R_1 - V_b - V_{ebo} \right\}$$

the loop gain becomes greater than unity and the circuit switches to the states with T1 bottomed. This increase in I_{co} may be arranged to be the result of illuminating T1, when the circuit may be triggered from the state with T1 cut off to that with T1 bottomed.

If I_{co} is the value of the collector leakage current in the absence of illumination and $I_{co} + \Delta I_{co}$ is that with sufficient illumination to just trigger the circuit, ΔI_{co} is the trigger sensitivity and is given by

$$\Delta I_{co} = \frac{1}{R_4} \left\{ I_{2} R_1 - V_b - V_{ebo} \right\} - I_{co}.$$

It may be seen from this equation that the level of illumination at which the circuit triggers may be varied by adjustment of $\frac{I_2 R_1}{R_4}$. In a practical circuit this may be achieved by a variable resistor in series with either R_1 or R_4.

Any light signal will be composed of a background illumination (noise) superimposed upon the signal itself. Should the general background illumination give variations in excess of ΔI_{co}, the circuit will be triggered by background alone. Thus it is necessary that the trigger sensitivity, ΔI_{co}, satisfies the condition:

$$\Delta I_{co} > \frac{1}{R_4} \left\{ I_2 R_1 - (V_b + V_{ebo}) - I_{co} R_4 \right\} + \Delta I'_{co}$$

when the background illumination fluctuates so that I_{co} varies in the range from I_{co} to $I_{co} + \Delta I'_{co}$.

It should be noted that changes in temperature also contribute to $\Delta I'_{co}$. Thus it is necessary to include in $\Delta I'_{co}$ not only maximum background fluctuates but also maximum temperature fluctuations. This limits the sensitivity of the circuit to small changesin illumination.

Thus, it may be concluded, that when T1 is cut off this circuit is triggered by light pulses of increasing illumination, whereas in the bottomed condition the state of the circuit may be made insensitive to illumination or temperature fluctuations.

APPENDIX 2

The Analysis of a System with Positive Feedback

Consider a simple loop containing an amplifier, with a gain, G, and an attenuator which feeds a fraction, β, of the output back to be added to the input without phase change round the loop (positive feedback). Assume some time constant, τ, in this feedback loop, which may, for simplicity, be represented as a series resistor and shunt capacitor. The complete circuit is shown in figure 8.7.

Let the operational parameter of this circuit be θ. It will be assumed that θ is applied to the loop time constant element as a voltage. Thus for positive going step inputs, the transfer function of the loop time constant element will be $(1 - \epsilon^{-t/\tau})$.

Thus, it may be shown that if a step function of amplitude, θ_I, is put into the loop at the input, the output will be a time function given by:

$$\theta_o = \theta_I \frac{G}{(1 - \beta.G(1 - \epsilon^{-t/\tau}))} \qquad \ldots\ldots \text{A2.1}$$

with a maximum value $(t \to \infty)$ of

$$\theta_{o(max)} = \theta_I \frac{G}{1 - \beta G} \qquad \ldots\ldots \text{A2.2}$$

From this equation two conditions of the loop may be recognized. If $\beta G(1 - \epsilon^{-t/\tau}) < 1$, θ_o will have a finite value, but if $\beta G(1 - \epsilon^{-t/\tau}) = 1$ θ_o becomes infinite. In this latter case, once the loop is set up the output voltage is independent of the input voltage.

Consider the case when a step increase from unity to G_1 is applied to the gain of the amplifier, G, where $\beta G_1 > 1$. Then before the applica-

tion of the step, G = 1 so that $\beta G < 1$ and there is a steady output given by:

$$\theta_o = \theta_I \frac{1}{1 - \beta} \qquad \ldots\ldots \text{A2.3}$$

On increasing G to a value G_1, $\beta G_1 > 1$. However, since t is small, $(1 - \epsilon^{-t/\tau})$ is small so that $\beta G_1 (1 - \epsilon^{-t/\tau}) < 1$ and equation A2.1 shows that the output is controlled by the input initially.

Thus on applying the step function to G, t = 0 so that $\beta G_1 (1 - \epsilon^{-t/\tau}) = 0$ and there is no change in the value of θ presented by the feedback loop to the adder. Since G = 1 initially, the output, θ_o, is then the input to the amplifier, $\frac{\theta_I}{1 - \beta}$, (from equation A2.3) amplified by a factor G_1 i.e.

$$\theta_o(\text{initial}) = \frac{\theta_I}{1 - \beta} \cdot G_1 \qquad \ldots\ldots \text{A2.4}$$

This rise in θ_o will occur instantaneously.

Subsequently, $\beta G_1 (1 - \epsilon^{-t/\tau})$ will increase with time allowing increased feedback so that θ_o slowly rises. Eventually $G_1 \beta (1 - \epsilon^{-t/\tau})$ approaching unity and θ_o then runs to infinity. The time required to reach the condition when $\theta_o \to \infty$ after the application of the step, may be found by equating $G_1 \beta (1 - \epsilon^{-t/\tau})$ to unity, to give a time

$$\tau \, \ell n \left\{ \frac{1}{G_1 \beta - 1} \right\}$$

This shows that as G_1 increases, the time to reach this condition decreases.

Thus, the time variation of θ_o for the case of $G_1 \beta > 1$ may be derived, for an increasing step applied to G_1, from equation A2.1, as the curve of figure 8.8b.

Repeating the above procedure with $\beta G_1 < 1$, gives the response of the stable system to a step increase of G. In this case the maximum value of θ_I will be finite. On applying the step function to G there will be the same instantaneous rise as described above, followed by a gradual rise of θ_o, as defined by equation A2.1. This gradually approaches a maximum value of the input amplified by a factor of $\frac{G_1}{1 - \beta G_1}$ (equation A2.2). This is plotted in figure 8.8c.

REFERENCES

Ansbacher, F., Ehrenberg, W., 1951, Proc. Phys. Soc., 64, 362.

Becker, A., 1904, Ann. Phys. Lpz., 13, 394.

Bills, D.G., Evett, A.A., 1959, American J. App. Phys., 30, 564.

Biondi, M.A., 1951, Rev. Sci. Instr., 22, 500.

De Boer, J.H., 1935, 'Electron Emission and Adsorbtion Phenomena', Cambridge: University Press.

Bradbury, N.E., Nielson, R.A., 1936, Phys. Rev., 49, 388.

Brown, S.C., Biondi, M.A., 1949, Phys. Rev., 75, 1700.

Bruce, F.H., 1947, J.I.E.E., Pt. II, 94, 129.

Compton, K.T., 1923a, Phys. Rev., 22, 333.

1923b, Phys. Rev., 22, 432.

Compton, K.T., Langmuir, I., 1930, Rev. Mod. Phys., 2, 123.

Corrigan, S.J.B., Von Engel, A., 1958, Proc. Roy. Soc. London, 245, A, 335.

Crompton, R.W., Hall, B.I.H., Macklin, W.C., 1957, Aust. J. Phys., 10, 366.

Dibeler, V.H., Mohler, F.L., Reese, R.M., 1953, J. Chem. Phys., 21, 180.

Druyvesteyn, M.J., 1930, Physica, 10, 61.

Duncan, R.A., 1957, Aust. J. Phys., 10, 54.

Farnsworth, H.E., Schlier, R.E., George, T.H., Burger, R.M., 1955, American J. App. Phys., 26, 252.

1958, " " " " , 29, 1150.

Gill, E.W.B., Donaldson, R.H., 1931, Phil. Mag., 12, 719.

Githens, S., 1940, Phys. Rev., 57, 822.

Gutton, C., Gutton, H., 1928, Comptes Rondu, 186, 303.

Hall, B.I.H., 1955, Aust. J. Phys., 8, 468.

Herlin, M.A., Brown, S.C., 1948a, Phys. Rev., 74, 291.

1948b, Phys. Rev., 74, 902.

Huxley, L.G.H., 1940, Phil. Mag., 30, 396.

Jackson, W., 1944, 'High frequency transmission lines', Methuen.

Llewellyn Jones, F., Davies, D.E., 1951a, Proc. Phys. Soc. B, 64, 397.

1951b, Proc. Phys. Soc. B, 64, 519.

Llewellyn Jones, F., Morgan, G.D., 1951, Proc. Phys. Soc. B, 64, 560.

Llewellyn Jones, F., Parker, A.B., 1950, Nature, 165, 960.

1952, Proc. Roy. Soc. A, 213, 185.

MacDonald, A., Brown, S.C., 1949, Phys. Rev., 76, 1692.

Margenau, H., 1946, Phys. Rev., 69, 508.

Maxwell, J.C., 1904, 'Electricity and Magnetism', Vol. II, Oxford.

Nicholls, M.J., 1960, Ph.D. Thesis, Durham University.

Pidduck, F.B., 1925, "Treatise on Electricity', Cambridge.

Prowse, W.A., Clark, J., 1958, Proc. Phys. Soc., 72, 625.

Rose, D.J., Brown, S.C., 1952, J. Appl. Phys., 23, 1028.

Thompson, J., 1937, Phys. Rev., 23, 1.

Thornton, W.M., Thompson, W.G., 1932, J.I.E.E., 71, 1.

Townsend, J.S., 1900, Nature, Lond., 62, 340.

1903, Phil. Mag., 6, 358.

1915, 'Electricity in Gases', Oxford: Clarendon Press.

1925, 'Motion of Electrons in Gases', Oxford.

1947, 'Electrons in Gases', Hutchinsons.

Varnerin, L.J., Brown, S.C., 1950, Phys. Rev., 79, 946.

Wolfendale, E., 1957, Electronic Eng., 29, 83.

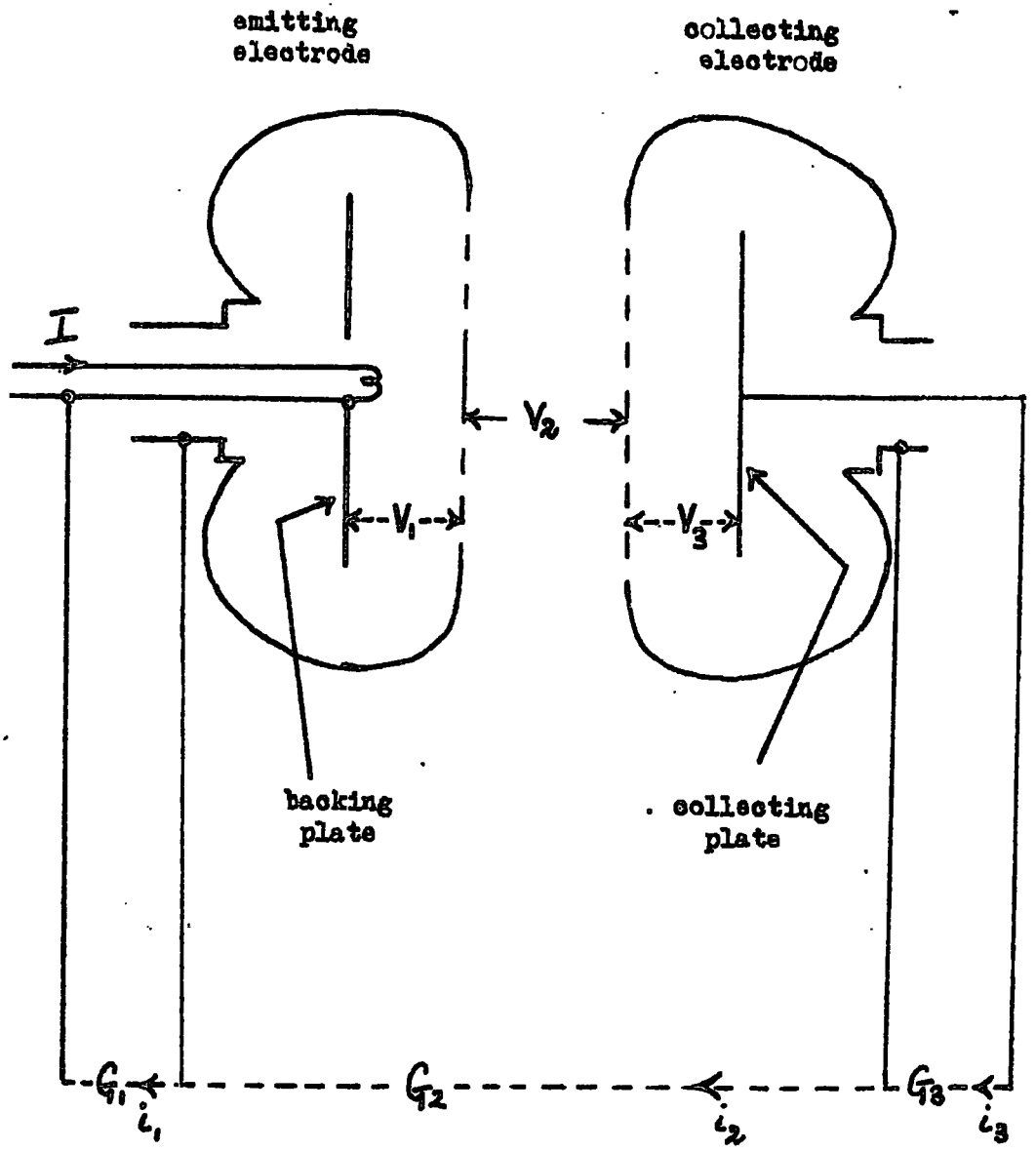

Fig. 2.1: Diagram of the electrodes and current-measuring system.

An Experimental Study of the Development of Gaseous Ionization at Ultra High Frequencies

by R.E. Long

Abstract

The work is concerned with the study of ionization and related processes occurring during the transition to breakdown at ultra high frequencies. Electrons are injected into a parallel plate gap through holes in one electrode and drift towards the other under a small unidirectional field. A stronger ultra high frequency field is superimposed upon this drift field to give collision ionization in the gap. Measurements of the number of electrons crossing the gap show that as the high frequency field increases the gap current decreases initially and then rises as breakdown is approached. A theory is presented to explain the initial drop quantitatively in terms of a back diffusion current to the emitting electrode. An extention of this theory to the subsequent rise show that the electron density initially increases exponentially across the gap but as breakdown is approached this changes to a sinusoidal form. A quantitative treatment of the first case is presented.

Provision is made to modulate the emitted electron stream with the object of measuring transit times. Preliminary measurements have demonstrated the feasibility of the method. It is shown that, as a consequence of diffusion, the time measured in such experiments is that for the propagation of the pulse of electrons rather than the time it would take individual electrons to drift across the gap.

Instabilities and drift of gap current have been traced to the presence of partially insulating films on the electrodes. It is shown experimentally that in combined drift and ultra high frequency fields, the drift field may be progressively reduced by the charging of these films. Methods for measuring film constants and calculating the resultant drift fields are given. Firm evidence is presented that such films are built up by discharges from impurities in the gap.